

VIABILITY OF THE WATER DUMP FLOODS TECHNIQUE IN GOT

Ms. Apirudee Anansupak

**A Thesis Submitted in Partial Fulfillment of the Requirements
for the Degree of Master of Engineering Program in Petroleum Engineering
Department of Mining and Petroleum Engineering
Faculty of Engineering
Chulalongkorn University
Academic Year 2011**

Copyright of Chulalongkorn University

บทคัดย่อและแฟ้มข้อมูลฉบับเต็มของวิทยานิพนธ์ตั้งแต่ปีการศึกษา 2554 ที่ให้บริการในคลังปัญญาจุฬาฯ (CUIR)

เป็นแฟ้มข้อมูลของนิสิตเจ้าของวิทยานิพนธ์ที่ส่งผ่านทางบัณฑิตวิทยาลัย

The abstract and full text of theses from the academic year 2011 in Chulalongkorn University Intellectual Repository (CUIR)

are the thesis authors' files submitted through the Graduate School.



ความสามารถในการอัดน้ำแทนที่แบบถ่ายเทในอ่าวไทย

นางสาว อภิญญา อนันต์สุภัค

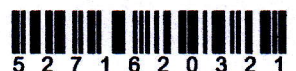
วิทยานิพนธ์นี้เป็นส่วนหนึ่งของการศึกษาตามหลักสูตรปริญญาวิทยาศาสตรมหาบัณฑิต

สาขาวิชาวิศวกรรมปิโตรเลียม ภาควิชาวิศวกรรมเหมืองแร่และปิโตรเลียม

คณะวิศวกรรมศาสตร์ จุฬาลงกรณ์มหาวิทยาลัย

ปีการศึกษา 2554


ลิขสิทธิ์ของจุฬาลงกรณ์มหาวิทยาลัย




5 2 7 1 6 2 0 3 2 1


Thesis Title VIABILITY OF THE WATER DUMP FLOODS
TECHNIQUE IN GOT
By Ms. Apirudee Anansupak
Field of Study Petroleum Engineering
Thesis Advisor Assistant Professor Suwat Athichanagorn, Ph.D.
Thesis Co-advisor Mauricio Villegas, Ph.D.

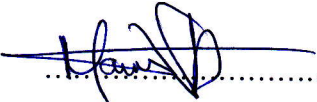
Accepted by the Faculty of Engineering, Chulalongkorn University in
Partial Fulfillment of the Requirements for the Master's Degree



.....Dean of the Faculty of Engineering
(Associate Professor Boonsom Lerdhirunwong, Dr.Ing.)


THESIS COMMITTEE


.....Chairman
(Associate Professor Sarithdej Pathanasetpong)


.....Thesis Advisor
(Assistant Professor Suwat Athichanagorn, Ph.D.)


.....Thesis Co-advisor
(Mauricio Villegas, Ph.D.)


.....Examiner
(Assistant Professor Jirawat Chewaroungroj, Ph.D.)


.....External Examiner
(Thotsaphon Chaianansutcharit, Ph.D.)

อภิฤดี อนันต์สุภัท : ความสามารถในการอัดน้ำแทนที่แบบถ่ายเทในอ่าวไทย (VIABILITY OF THE WATER DUMP FLOODS TECHNIQUE IN GOT) อ. ที่ปริกษาวิทยานพนธ์หลัก: ผศ. ดร. สุวัฒน์ อธิชนากร, อ.ที่ปริกษาวิทยานพนธ์ร่วม: ดร. เมาริชิโอ วิลิคัส, 112 หน้า.

ลักษณะของแอ่งปัดดาณีในอ่าวไทยเป็นแหล่งกักเก็บขนาดเล็กและมีรอยเลื่อนและการเรียงตัวเป็นชั้นๆในแนวคิ่ง ปริมาณน้ำมันและก๊าซธรรมชาติสำรองในแต่ละหลุมนั้นไม่มาก จึงมีการลงทุนพัฒนาหลุมด้วยงบประมาณไม่สูงมากนัก การเพิ่มงบประมาณการลงทุนเพิ่มเติมอย่างการติดตั้งท่อส่งน้ำ สำหรับการทำการอัดแทนที่ด้วยน้ำหรือการติดตั้งปั๊มนั้นเป็นเรื่องยากในการประเมิน การอัดน้ำแทนที่แบบถ่ายเทนั้นเป็นเทคโนโลยีที่ได้รับการพิสูจน์แล้วว่าสามารถเพิ่มปริมาณการผลิตน้ำมันในแหล่งกักเก็บน้ำมันขนาดเล็ก ในงานศึกษานี้เราได้ใช้แบบจำลองแหล่งกักเก็บด้วยการจำกัดการวิเคราะห์เชิงตัวเลขในแบบต่างๆเพื่อประเมินประสิทธิภาพการแทนที่แบบถ่ายเทในอ่าวไทย ในการศึกษานี้ได้ทำการประเมินประสิทธิภาพตามแผนการต่อไปนี้ (1) การเปรียบเทียบการผลิตผ่านหลุมผลิตสามหลุมภายใต้การไหลจากแรงขับก๊าซกับการอัดน้ำแทนที่แบบถ่ายเทผ่านการอัดน้ำจากหลุมริม และ หลุมกลาง (2) การเปรียบเทียบประสิทธิภาพการผลิตจากการอัดน้ำแทนที่แบบถ่ายเทด้วยการปรับขนาดแหล่งน้ำใต้ดิน (3) ประเมินผลกระทบจากดัชนีการผลิตด้วยความสามารถในการผลิตน้ำมันจากการอัดน้ำแทนที่แบบถ่ายเท (4) ประเมินผลกระทบจากดัชนีการอัดน้ำแทนที่ด้วยความสามารถในการผลิตน้ำมันจากการอัดน้ำแทนที่แบบถ่ายเท (5) ความสามารถของการอัดน้ำแทนที่แบบถ่ายเทที่ความลึก 4000, 6000 และ 8000 ฟุต ใต้ระดับน้ำทะเล (6) ความสามารถของการอัดน้ำแทนที่แบบถ่ายเทจากแหล่งกักเก็บน้ำที่อยู่ในตำแหน่งต่ำกว่า (7) สร้างแบบจำลองเพิ่มสำหรับการเปลี่ยนแปลงในคุณสมบัติของของเหลว (8) ศึกษาแบบจำลองเพื่อหาช่วงเวลาที่เหมาะสมที่สุดของการอัดน้ำแทนที่แบบถ่ายเท

ในการศึกษาพบว่า การอัดน้ำแทนที่แบบถ่ายเทสามารถเพิ่มประสิทธิภาพการผลิตได้มากถึง 12 เปอร์เซ็นต์ ซึ่งขึ้นกับการเลือกวางหลุมอัดน้ำและขนาดของแหล่งน้ำใต้ดิน จากผลการศึกษาแนะนำว่า ตำแหน่งของหลุมอัดน้ำที่ดีที่สุดคือหลุมผลิตด้านริม จากการศึกษาแนะนำว่าสัดส่วนของแหล่งน้ำใต้ดินต่อน้ำมันประมาณ 43 เท่านั้นจะได้ประสิทธิภาพการผลิตสูงสุด นอกจากนี้จากการทำแบบจำลองชี้ให้เห็นว่า ประสิทธิภาพการผลิตของทุกเวลาที่ต่างกันในการอัดน้ำแทนที่แบบถ่ายเทนั้นมากกว่าการผลิตแบบไม่มีการอัดน้ำแทนที่แบบถ่ายเท.

ภาควิชา วิศวกรรมเหมืองแร่และปิโตรเลียม

สาขาวิชา วิศวกรรมปิโตรเลียม

ปีการศึกษา 2554

ลายมือชื่อนิสิต..... *อภิฤดี อนันต์สุภัท*

ลายมือชื่ออ.ที่ปริกษาวิทยานพนธ์หลัก..... *John Ohm*

ลายมือชื่ออ.ที่ปริกษาวิทยานพนธ์ร่วม..... *[Signature]*

5271620321: MAJOR PETROLEUM ENGINEERING
KEYWORDS: /WATER DUMP FLOODS

APIRUDEE ANANSUPAK. VIABILITY OF THE WATER DUMP FLOODS
TECHNIQUE IN GOT. ADVISOR: ASST. PROF. SUWAT ATHICHANAGORN,
Ph.D., CO-ADVISOR: MAURICIO VILLEGAS, Ph.D., 112 pp.

The Pattani Basin, Gulf of Thailand, is characterized by small, faulted, and vertically stacked fluvial reservoirs. The oil and gas reserves per well are small and are developed through low cost wells. Any additional investments, such as water injection pipelines and pumps are hard to justify. Water dump flood is proved technology, and it could be a viable IOR technique for small oil reservoirs. This study evaluates dump flooding in the Pattani Basin, Gulf of Thailand via finite difference numerical simulation and aims to identify parameters such the ratio of aquifer to reservoir size that yield successful dump flooding projects. This study evaluated the following scenarios: (1) comparing three wells producing under solution-gas drive mechanism against water dump flood from an edge well and a water dump flood from a center well, (2) comparing the performance of water dump flood as a function of the aquifer size, (3) evaluating the impact of well productivity index (PI) on the oil recovery for the water dump flood, (4) evaluating the impact of well injectivity index (II) on the oil recovery for the water dump flood, (5) studying viability and performance of water dump flood at reservoir depths of 4000, 6000, and 8000 ft TVDSS, (6) studying viability and performance of an underlying aquifer dump flooding, (7). Simulating more cases by changing oil gravity, and (8) performing simulation runs to study the optimal depletion point to begin the water dump flooding.

The study found that dump flooding can increase the recovery factor up to 12 percent depending on the choice of well location and aquifer to reservoir size. The results of the study suggest that the best well locations are edge wells. The study suggests that there is an optimal aquifer to reservoir ratio around 43 RBL/RBL that maximizes oil recovery factor. Finally, the oil recovery efficiency for all different times to start water dump flood is higher than no water dump flood.

Department: Mining and Petroleum Engineering

Field of Study: Petroleum Engineering

Academic Year: 2011

Student's Signature: 

Advisor's Signature: 

Co-advisor's Signature: 

Acknowledgements

I would like to express my sincere gratitude to my thesis advisor, Asst. Prof. Suwat Athichanagorn for his guidance and support throughout the course of this research.

I would like to express my big thanks to my thesis co-advisor, Dr. Mauricio Villegas for his great suggestion, assistance, and motivation along this research.

I would like to also thank all faculty members in the Department of Mining and Petroleum Engineering who have offered petroleum knowledge, technical advice, and invaluable consultation.

I would like to thank Chevron Offshore Thailand for allowing me to take part of the company's training program and supplying computational resources and financial support towards the master degree program at Department of Mining and Petroleum Engineering. I would like to express my gratitude to Chevron's earth scientists and petroleum engineers for their suggestion and supplementation of geological and well data.

Finally, I would like to express my sincere gratitude to my family for their constant support and to all of my friends for their encouragement and friendship.

Contents

	Page
Abstract (Thai)	iv
Abstract (English)	v
Acknowledgement	vii
Contents	vii
List of Tables	ix
List of Figures	x
Nomenclatures	xvii
CHAPTER	
I. INTRODUCTION.....	1
1.1 Introduction and problem statement.....	1
1.2 Objectives.....	2
II. LITERATURE REVIEW.....	3
III. THEORY AND CONCEPT.....	7
3.1 Injectivity.....	8
3.2 Productivity.....	11
3.3 Overall recovery efficiency.....	11
3.3.1 Displacement efficiency.....	11
3.3.2 Sweep efficiency.....	12
3.4 Optimum time to waterflood.....	13
IV. RESERVOIR MODEL CONSTRUCTION.....	14
4.1 Reservoir model.....	14
4.2 Rock and fluid properties.....	15
4.2.1 Rock properties.....	16
4.2.2 Fluid properties.....	17
4.3 SCAL (Special core analysis).....	18
4.4 Wellbore.....	19
4.5 Vertical flow performance.....	21

CHAPTER	Page
4.6 Sensitivity parameters	21
V. WATER DUMP FLOOD RESULT	22
5.1 Impact of injector location	22
5.2 Impact of aquifer volume	28
5.2.1 Effect of decreased in aquifer size	28
5.2.2 Effect of increasing in aquifer size	31
5.2.3 Effect of well location	34
5.3 Effect of well productivity index	35
5.4 Effect of well injectivity index	40
5.5 Effect of depth-related properties	44
5.5.1 Reservoir depth of 6000 ft TVDSS (Case II)	46
5.5.2 Reservoir depth of 8000 ft TVDSS (Case III)	49
5.5.3 Comparison of water dump flood performance at different reservoir depths	52
5.6 Viability of water dump flood of underlying aquifer	53
5.6.1 Performance of water dump flood from underlying aquifer	56
5.6.2 Performances of water dump flood of an overlaying and underlying aquifer dump flooding via an edge well injector	59
5.7 Impact of API gravity	60
5.8 Effect of time to start water dump flood	63
VI. CONCLUSIONS AND RECOMMENDATIONS	67
6.1 Conclusions	67
6.2 Recommendations	68
REFERENCES	69
APPENDICES	71
VITAE	107

List of Tables

	Page
Table 4- 1: Varied parameter values for Base case.....	16
Table 4- 2: Fluid properties and pore volume for base case.....	17
Table 4- 3: Fixed parameter value for all scenarios.....	17
Table 4- 4: Production constrain and economic limit.....	21
Table 5- 1: Oil recovery factors for different well locations.....	27
Table 5- 2: Oil recovery factors for different aquifer sizes.....	30
Table 5- 3: Oil recovery via an edge injector for increasing aquifer size.....	34
Table 5- 4: Oil recovery factors for different productivity indices.....	39
Table 5- 5: Oil recovery factors for different injectivity indices.....	43
Table 5- 6: Parameters for various depth scenarios.....	44
Table 5- 7: Fluid properties and pore volume for various scenarios.....	45
Table 5- 8: Oil Recovery factors of water dump flood at depth of 6000 ft for different injector locations.....	48
Table 5- 9: Oil recovery factors of water dump flood at depth of 8000 ft for different injector locations.....	51
Table 5- 10: Oil recovery factors of water dump flood at different depth.....	52
Table 5- 11: Variable parameter values for underlying aquifer model.....	54
Table 5- 12: Fluid properties and pore volume for various scenarios.....	55
Table 5- 13: Oil recovery factors of an underlying aquifer for different injector locations.....	58
Table 5- 14: Oil recovery factors for an overlaying and underlying aquifer dump flooding via an edge well injector.....	60
Table 5- 15: Fluid properties and pore volumes for various °API scenarios @ 4000 ft.....	60
Table 5- 16: Oil recovery factors of water dump flood via an edge well injector for oil with different API gravities.....	62
Table 5- 17: Oil recovery factors for different times to start water dump flood via an edge well injector.....	65
Table B- 1: Oil Recovery through a center injector with decreased in aquifer sizes.....	104
Table B- 2: Oil Recovery through a center injector with increase in aquifer sizes.....	106

List of Figures

	Page
Figure 1- 1: Schematic of a dump flood using an overlaying aquifer to support production from an oil reservoir.	1
Figure 3- 1: A sketch of pressure distribution of water dump flood reservoir model.....	7
Figure 3- 2: Water injectivity variations in a radial system.	10
Figure 4- 1: Structural model of oil reservoir and overlaying aquifer.	15
Figure 4- 2: Side view of Structural model of oil reservoir and overlaying aquifer.	15
Figure 4- 3: Water/oil relative permeability curve	18
Figure 4- 4: Gas/oil relative permeability curves.	19
Figure 4- 5: Wellbore schematic.....	20
Figure 5- 1: Oil production rates for different injector locations	23
Figure 5- 2: Water production trends for different injector locations	24
Figure 5- 3: Gas production rates for different injector locations	24
Figure 5- 4: Average reservoir pressures for different injector locations	25
Figure 5- 5: Contour map of water saturation for base case @ day 900	26
Figure 5- 6: Contour map of water saturation for dump flooding via an edge well injector @ day 900.....	26
Figure 5- 7: Contour map of water saturation for dump flooding via a center well injector @ day 900.....	27
Figure 5- 8: Oil production rates for different aquifer sizes	29
Figure 5- 9: Contour map of water saturation for dump flooding via an edge well injector with aquifer/reservoir volume of 2.14 rbl/rbl @ day 900	29
Figure 5- 10: Contour map of water saturation for dump flooding via an edge well injector with aquifer/reservoir volume of 0.214 rbl/rbl @ day 900	30
Figure 5- 11: Oil production rates for different aquifer sizes	31
Figure 5- 12: Water production trend for different aquifer sizes.....	32
Figure 5- 13: Contour map of water saturation for dump flooding via an edge well injector with aquifer/reservoir volume of 8.56 RBL/RBL @ day 900.....	32
Figure 5- 14: Contour map of water saturation for dump flooding via an edge well injector with aquifer/reservoir volume of 85.6 RBL/RBL @ day 900.....	33

Figure 5- 15: Oil recovery factors as a function of aquifer to reservoir size and injector location	35
Figure 5- 16: Variation of productivity index as a function of time	36
Figure 5- 17: Oil production rates for different productivity indices	37
Figure 5- 18: Water cross flow rates for different productivity indices	37
Figure 5- 19: Contour map of water saturation for dump flooding via an edge well injector for PI of 14.14 stb/day/psi @ day 900.....	38
Figure 5- 20: Contour map of water saturation for dump flooding via an edge well injector for PI of 2.828 stb/day/psi @ day 900.....	38
Figure 5- 21: Oil recovery factors for different productivity indices	39
Figure 5- 22: Variation of injectivity index as a function of time	40
Figure 5- 23: Oil production rates for different injectivity indices.....	41
Figure 5- 24: Water cross flow rates for different injectivity indices.....	41
Figure 5- 25: Contour map of water saturation for dump flooding via an edge well injector for II of 33.0 stb/day/psi @ day 900.....	42
Figure 5- 26: Contour map of water saturation for dump flooding via an edge well injector for II of 3.30 stb/day/psi @ day 900.....	43
Figure 5- 27: Oil production rates of water dump flood at depth of 6000 ft for different injector locations	46
Figure 5- 28: Contour map of water saturation at depth of 6000 ft for base case @ day 900 .	47
Figure 5- 29: Contour map of water saturation of water dump flood at depth of 6000 ft for edge well injector @ day 900.....	47
Figure 5- 30: Contour map of water saturation of water dump flood at depth of 6000 ft for center well injector @ day 900.....	48
Figure 5- 31: Oil production rates of water dump flood at depth of 8000 ft for different injector locations	49
Figure 5- 32: Contour map of water saturation at depth of 8000 ft for base case @ day 900 .	50
Figure 5- 33: Contour map of water saturation of water dump flood at depth of 8000 ft for edge well injector @ day 900.....	50
Figure 5- 34: Contour map of water saturation of water dump flood at depth of 8000 ft for center well injector @ day 900.....	51
Figure 5- 35: Oil recovery factors for reservoir at depth of 4000, 6000 and 8000 ft	53
Figure 5- 36: Structural model of underlying aquifer.....	54
Figure 5- 37: Oil production rates of an underlying aquifer for different injector locations...56	56

Figure 5- 38: Contour map of underlying aquifer for base case @ day 900.....	57
Figure 5- 39: Contour map of water saturation of underlying aquifer dump flooding via an edge well injector @ day 900.....	57
Figure 5- 40: Contour map of water saturation of underlying aquifer dump flooding via a center well injector @ day 900.....	58
Figure 5- 41: Oil production rates for an overlaying and underlying aquifer dump flooding via an edge well injector.....	59
Figure 5- 42: Water production rates for an overlaying and underlying aquifer dump flooding via an edge well injector (water cross flow into reservoir).....	60
Figure 5- 43: Oil production rates of water dump flood via an edge well injector for oil with different API gravities.....	61
Figure 5- 44: Contour map of water saturation for water dump flood via an edge well injector for 30 °API oil.....	62
Figure 5- 45: Contour map of water saturation for water dump flood via an edge well injector at day 15 @ day 900.....	64
Figure 5- 46: Contour map of water saturation for water dump flood via an edge well injector at day 240 @ day 900.....	64
Figure 5- 47: Contour map of water saturation for water dump flood via an edge well injector at day 600 @ day 900.....	65
Figure 5- 48: Oil recovery factors for different times to start water dump flood via an edge well injector.....	66
Figure A- 1: Contour map of water saturation for base case @ day 900.....	73
Figure A- 2: Contour map of water saturation for dump flooding via an edge well injector @ day 900.....	73
Figure A- 3: Contour map of water saturation for dump flooding via a center well injector @ day 900.....	73
Figure A- 4: Contour map of water saturation for dump flooding via an edge well injector with aquifer/reservoir volume 0.214rbl/rbl @ day 900.....	74
Figure A- 5: Contour map of water saturation for dump flooding via an edge well injector with aquifer/reservoir volume 0.43rbl/rbl @ day 900.....	74
Figure A- 6: Contour map of water saturation for dump flooding via an edge well injector with aquifer/reservoir volume 0.54rbl/rbl @ day 900.....	75
Figure A- 7: Contour map of water saturation for dump flooding via an edge well injector with aquifer/reservoir volume 0.71rbl/rbl @ day 900.....	75

Figure A- 8: Contour map of water saturation for dump flooding via an edge well injector with aquifer/reservoir volume 1.07rbl/rbl @ day 900.....	76
Figure A- 9: Contour map of water saturation for dump flooding via an edge well injector with aquifer/reservoir volume 2.14rbl/rbl @ day 900.....	76
Figure A- 10: Contour map of water saturation for dump flooding via an edge well injector with aquifer/reservoir volume 4.28rbl/rbl @ day 900.....	77
Figure A- 11: Contour map of water saturation for dump flooding via an edge well injector with aquifer/reservoir volume 6.42rbl/rbl @ day 900.....	77
Figure A- 12: Contour map of water saturation for dump flooding via an edge well injector with aquifer/reservoir volume 8.56rbl/rbl @ day 900.....	78
Figure A- 13: Contour map of water saturation for dump flooding via an edge well injector with aquifer/reservoir volume 10.7rbl/rbl @ day 900.....	78
Figure A- 14: Contour map of water saturation for dump flooding via an edge well injector with aquifer/reservoir volume 21.4rbl/rbl @ day 900.....	79
Figure A- 15: Contour map of water saturation for dump flooding via an edge well injector with aquifer/reservoir volume 42.8rbl/rbl @ day 900.....	79
Figure A- 16: Contour map of water saturation for dump flooding via an edge well injector with aquifer/reservoir volume 64.2rbl/rbl @ day 900.....	80
Figure A- 17: Contour map of water saturation for dump flooding via an edge well injector with aquifer/reservoir volume 85.6rbl/rbl @ day 900.....	80
Figure A- 18: Contour map of water saturation for dump flooding via an edge well injector with aquifer/reservoir volume 107rbl/rbl @ day 900.....	81
Figure A- 19: Contour map of water saturation for dump flooding via an edge well injector with aquifer/reservoir volume 214rbl/rbl @ day 900.....	81
Figure A- 20: Contour map of water saturation for dump flooding via an edge well injector with aquifer/reservoir volume 321rbl/rbl @ day 900.....	82
Figure A- 21: Contour map of water saturation for dump flooding via an edge well injector for PI 28.28stb/day/psi @ day 900	82
Figure A- 22: Contour map of water saturation for dump flooding via an edge well injector for PI 14.14stb/day/psi @ day 900	83
Figure A- 23: Contour map of water saturation for dump flooding via an edge well injector for PI 2.828stb/day/psi @ day 900	83
Figure A- 24: Contour map of water saturation for dump flooding via an edge well injector for II 330stb/day/psi @ day 900	84

Figure A- 25: Contour map of water saturation for dump flooding via an edge well injector for II 165stb/day/psi @ day 900	84
Figure A- 26: Contour map of water saturation for dump flooding via an edge well injector for II 33stb/day/psi @ day 900	85
Figure A- 27: Contour map of water saturation for dump flooding via an edge well injector for II 16.5stb/day/psi @ day 900	85
Figure A- 28: Contour map of water saturation for dump flooding via an edge well injector for II 3.3stb/day/psi @ day 900	86
Figure A- 29: Contour map of water saturation at depth 6000 ft for base case @ day 900	86
Figure A- 30: Contour map of water saturation of water dump flood at depth 6000 ft for edge well injector @ day 900	87
Figure A- 31: Contour map of water saturation of water dump flood at depth 6000 ft for center well injector @ day 900	87
Figure A- 32: Contour map of water saturation at depth 8000 ft for base case @ day 900	88
Figure A- 33: Contour map of water saturation of water dump flood at depth 8000 ft for edge well injector @ day 900	88
Figure A- 34: Contour map of water saturation of water dump flood at depth 8000 ft for center well injector @ day 900	89
Figure A- 35: Contour map of underlying aquifer for base case @ day 900	89
Figure A- 36: Contour map of water saturation of underlying aquifer dump flooding via an edge well injector @ day 900	90
Figure A- 37: Contour map of water saturation of underlying aquifer dump flooding through a center well injector @ day 900	90
Figure A- 38: Contour map of water saturation for dump flooding on base case for 30API gravity @ day 900	91
Figure A- 39 Contour map of water saturation for dump flooding via an edge well injector for 30API gravity @ day 900	91
Figure A- 40: Contour map of water saturation for dump flooding through a center well injector for 30API gravity @ day 900	92
Figure A- 41: Contour map of water saturation for dump flooding on base case for 35API gravity @ day 900	92
Figure A- 42 Contour map of water saturation for dump flooding via an edge well injector for 35API gravity @ day 900	93

Figure A- 43: Contour map of water saturation for dump flooding through a center well injector for 35API gravity @ day 900.....	93
Figure A- 44: Contour map of water saturation for dump flooding on base case for 40API gravity @ day 900	94
Figure A- 45 Contour map of water saturation for dump flooding via an edge well injector for 40API gravity @ day 900	94
Figure A- 46: Contour map of water saturation for dump flooding through a center well injector for 40API gravity @ day 900.....	95
Figure A- 47: Contour map of water saturation of water dump flood via an edge well injector at day 1 @ day 900.....	95
Figure A- 48: Contour map of water saturation of water dump flood via an edge well injector at day 15 @ day 900.....	96
Figure A- 49: Contour map of water saturation of water dump flood via an edge well injector at day 30 @ day 900.....	96
Figure A- 50: Contour map of water saturation of water dump flood via an edge well injector at day 60 @ day 900.....	97
Figure A- 51: Contour map of water saturation of water dump flood via an edge well injector at day 90 @ day 900.....	97
Figure A- 52: Contour map of water saturation of water dump flood via an edge well injector at day 120 @ day 900.....	98
Figure A- 53: Contour map of water saturation of water dump flood via an edge well injector at day 150 @ day 900.....	98
Figure A- 54: Contour map of water saturation of water dump flood via an edge well injector at day 240 @ day 900.....	99
Figure A- 55: Contour map of water saturation of water dump flood via an edge well injector at day 330 @ day 900.....	99
Figure A- 56: Contour map of water saturation of water dump flood via an edge well injector at day 420 @ day 900.....	100
Figure A- 57: Contour map of water saturation of water dump flood via an edge well injector at day 510 @ day 900.....	100
Figure A- 58: Contour map of water saturation of water dump flood via an edge well injector at day 600 @ day 900.....	101

Figure B- 1: Oil production rate through a center injector with decreased in aquifer sizes	102
Figure B- 2: Water production rate through a center injector with decreased in aquifer sizes	103
Figure B- 3: Average reservoir pressure through a center injector with decreased in aquifer.....	103
Figure B- 4: Recovery factor through a center injector with decreased in aquifer sizes	104
Figure B- 5: Oil production rate through a center injector with increase in aquifer sizes ...	105
Figure B- 6: Oil recovery factor through a center injector with increase in aquifer sizes ...	105

Nomenclatures

°API	degree (American Petroleum Institute)
BHP	bottom hole pressure
LGR	local grid refinement
PVT	pressure-volume-temperature
TVDSS	true vertical depth sub sea, feet
OOIP	original oil in place, STB
PI	productivity index, BBL/day-psi
II	injectivity index, BBL/day-psi
ORF	oil recovery factor, percent
OPR	oil production rate, STB/day
WPR	water production rate, STB/day
GOR	gas- oil ratio, MSCF/STB
WCT	water cut, percent
APR	average pressure reservoir, psia

CHAPTER I

INTRODUCTION

1.1 Introduction and problem statement

Dump flooding is a secondary recovery technique developed around 1924 and still in use today. Water dump flooding is a well established process which uses the water from overlaying or underlying aquifer to waterflood (i.e. pressure support and/or oil displacement) an oil reservoir by inducing cross flow of water between the aquifer and the oil reservoir (see Figure 1-1).

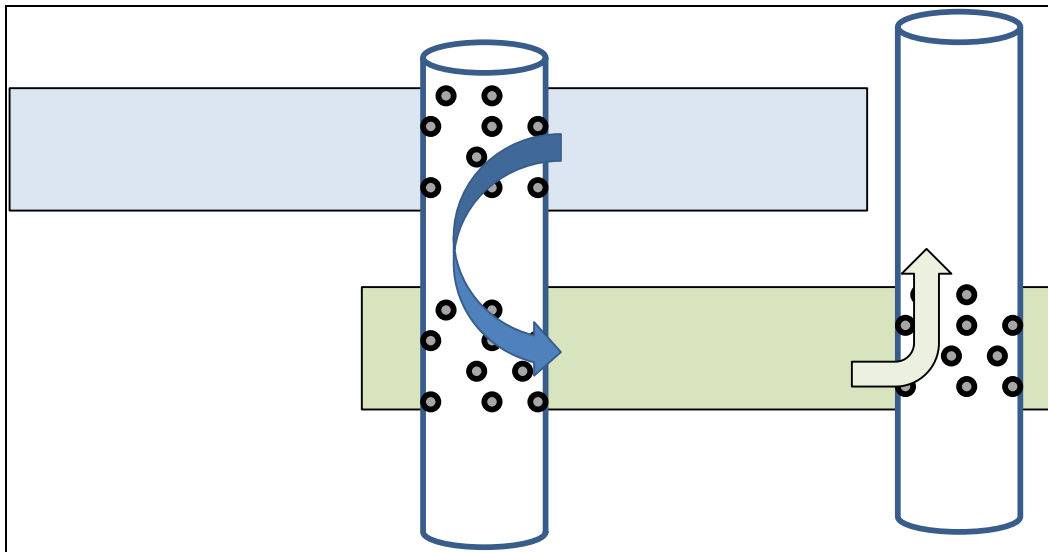


Figure 1- 1: Schematic of a dump flood using an overlaying aquifer to support production from an oil reservoir.

For a water dump flood project to succeed, it is required that the aquifer pressure is higher than the pressure in the oil reservoir and that the injectivity in the reservoir sand and productivity of the aquifer are significant enough to receive and produce enough water to support the oil production from the reservoir. Additionally, the volume of the aquifer should be large enough relative to the oil reservoir to provide support during the life of the oil production.

This thesis intends to study water dump flood in a field in Thailand. Different conditions in the reservoir have impacts on water dump flood performance. Although the same concept of water dump flood can be applied to an underlying aquifer, there are different advantages in using an overlaying or an underlying aquifer. An overlaying aquifer may have significantly higher porosity and higher deliverability (higher permeability). In addition, the reservoir temperature may be lower, thus increasing the potential to generate thermal stresses and thermal fractures (increased injectivity in the oil reservoir). On the other hand, the deeper aquifer may have higher pressures or give better wellbore accessibility and reduce well intervention work after the waterflood is finished. Other conditions such as injector position, aquifer size, well productivity index, well injectivity index, API gravity and time to begin water dump flood will be studied and simulated by reservoir simulation runs. The result from each case will be compared and discussed.

1.2 Objectives

This study aims to evaluate dump flooding in the Gulf of Thailand and identify parameters such as ratio of aquifer size to OOIP, requirements in injectivity, and productivity that yield successful projects. This technique has the potential to open many sands to secondary recovery due to constrained environment such as facility limitations and water availability.

CHAPTER II

LITERATURE REVIEW

There have been many studies on water dump flooding which reported the success of water dump flood technique.

Davies ^[1] concerned the monitoring of the dumpflood rates, a problem which has existed in the oil producing industry due to the fact that the rate may not stay constant over the life of the dumpflood project. The author presented a derivation of equations describing the fluid transfer rate, and a computer program to solve the equations has been designed to alleviate the problem of monitoring the dump flooding rates. The conclusion from investigation of dumpflooding is that the actual fluid transfer rate can be monitored, within an acceptable accuracy, for oil-field practical purposes with the condition that regular fluid level measurements and periodic rate determinations are required.

DesBrisay et al. ^[2] designed an underlying aquifer dump flooding. Unsteady-state radial flow equations were used to match the observed pressure drawdown of water zone. In addition, an aquifer analysis based upon the performance of several wells indicated that other sources would be needed. The results indicated that it was low of capable of sustained production rate. This limit due to the lower water zone was limited to area of oil reef. In order to fill the remainder of injection requirement for prolong the life of injection project, a shallower water zone was used to provide the remaining water required.

Fujita et al. ^[3] presented 5 years' operation of water dumping by shallow aquifer water into a peripheral oil zone. A reservoir simulation study was conducted to find the most economical method of maximizing the ultimate oil recovery. The injection performance of water dumping wells can be observed only at initial completion or when a work over takes place.

Yao et al. ^[4] determined the feasibility of dump-flood pilot testing. Reservoir models were built using a 3-D reservoir simulator that included the oil zone and water zone. Simulation was used to design the optimum number of injectors in these heterogeneous reservoirs. The pilot flood simulation showed that the dump flood was feasible. The modeling also showed that adding a pump accelerates the oil recovery. As the dump flood progresses, injection rates decrease as the pressures in the two zones begin to equilibrate. The water zone pressure decreases while the oil zone pressure increases. In the second step, downhole pump injection was added to maintain higher injection rates. Pump-aided reverse dump-flooding method can improve sweep efficiencies and delay breakthrough times.

Luis et al. ^[5] presented a natural water dump flooding from lower water reservoir. This natural water flooding method attempts to use water and energy from higher pressure reservoir to lower pressure reservoir. The variation of the rate due to the increasing in pressure in reservoir with time is considered. As an observation, it shows a good communication with increment of pressure after beginning of the injection. With an increment in pressure of 300 psi, the oil production rate increased from 10 to 20 BPD, and production of 230 BPD oil is obtained in the observation well.

Quttainah and Hunaif ^[6] presented a pilot project of dumpflood to prove the viability of water dump flood and quantify sweep benefits. The dumpflood proved to be an excellent way to pressure support the falling reservoir pressure, but the analysis of injectivity & water sweep still waiting on full results.

Quttainah and Maraghi ^[7] demonstrated the design to extend a production plateau of a water dump flood process. The authors considered three main development options: water injection, infill drilling and combined development options. Many simulation runs were made to evaluate the best scenario. The recommended option is combined dumpflood. Water injection and infill drilling is the optimum development option that maximizes the oil plateau extension. The dump flood operation provides pressure support and increases oil sweep, and infill producers allow the remaining swept oil to be recovered. Due to infill drilling and water dump flood, the simulation results show that the oil plateau extends to 11 years instead of 4.5 years with water dump flood under plateau extension option.

Friedel et al. ^[8] identified improved oil recovery potential for depleted reservoir using water dump flood. They investigated 2 dump flooding studies: dump flooding from a neighboring aquifer and dump flood from a deeper higher pressure aquifer. In the first case, the fluid flow between the two reservoirs is not controlled in the field (as the completions are simply commingled and water flow is entirely governed by existing pressure difference). A simulation model was used to assess the efficiency of the dump flood. When producing from the oil reservoir, the amount of dump water increases with the pressure difference. Results show that the dump flooding process is harmful to the oil recovery for some of the wells. The increase in water cut causes these wells to be shut-in earlier and lowers the predicted oil recovery. The result of this case is unfavorable. The limited initial pressure difference between the source and target reservoirs does not provide enough driving force to replace the voidage in the target reservoir and fails to keep the target reservoir pressure stable. In the second case, dump flooding from a deeper high pressure aquifer was investigated. The dump flood wellbore penetrates deeper reservoirs with significant higher pressure differential of up to 1500 psi. In order to evaluate the impact of deeper aquifer pressure, two cases were run. Bottom hole injection pressures were set to 500 psi and 1000 psi pressure differentials for two cases respectively. The result shows that the effect of the higher pressure aquifer can be noticed. With water rates more than doubled, voidage replacement ratio increases to 20%. But the resulting of water encroachment swept area is very similar to low-pressure dump flood case.

Rawding et al. ^[9] described the improved reservoir management by using intelligent completion technology and remotely controlled hydraulic Interval Control Valve in a water dumpflood well. It is a reliable and cost effective solution for a controlled dumpflood. With the ability to constantly monitor and control the flow from the aquifer to support the production reservoir, the productivity index is improved significantly from 9.8 bbl/d/psi to 30.5 bbl/d/psi.

Ming et al. ^[10] studied by using simple generic models to identify the optimal injection strategy by selecting the injector location as a function of reservoir dip, ranging from 0.5 to 3.5 degrees. The model results showed that the central injector performs better than down dip wells in a five wells line drive pattern when formation dip is less than 2.6 degree. The reason for this conclusion is not clear due to a complicated reservoir structure in this area.

Many authors have studied the practicability of water dump flood in their specific fields. However, there are no study of sensitivities to rock properties or fluid properties which can affect the production performance. The aim of this paper is to identify the factors that yield successful projects such as aquifer size, injector position, well PI, well II, aquifer location, API gravity and time to start water dump flooding. This technique has the potential to open many sands to secondary recovery due to constrained environment (i.e. facility limitations, and water availability).

CHAPTER III

THEORY AND CONCEPT

Dump flooding improves recovery mechanism by immiscible displacement with water where the rate and volume of water injected are controlled by natural interaction between the aquifer used as a water source and the reservoir with little to no control from the surface.

The performance of the waterflood will depend on the typical parameters recognized by the industry such as heterogeneity, fluid properties, wettability, rock properties, and so on. However, different from a typical waterflood where the operator has control on the injection rate and the water quality, a dump flood relies on the natural interaction of the oil reservoir and the aquifer supplying the water through the wellbore. These factors (i.e. water flow rate, level of pressure difference, and well location) have significant impacts on the recovery efficiency.

Because of the reasons previously described, dump floods could be simplified as being dominated by:

- Aquifer size and its deliverability
- Oil reservoir characteristics (rock properties)
- Injectivity, deliverability, wettability, heterogeneity, fluid properties, etc.
- Single phase flow in the tubing between aquifer and reservoir
- Compatibility of aquifer and reservoir fluids (oil & formation water)

3.1 Injectivity

When water is injected into an oil reservoir, a pressure funnel develops around the wellbore and dissipates logarithmically away from the well. This pressure profile is indicated by the dashed line in Figure 3-1.

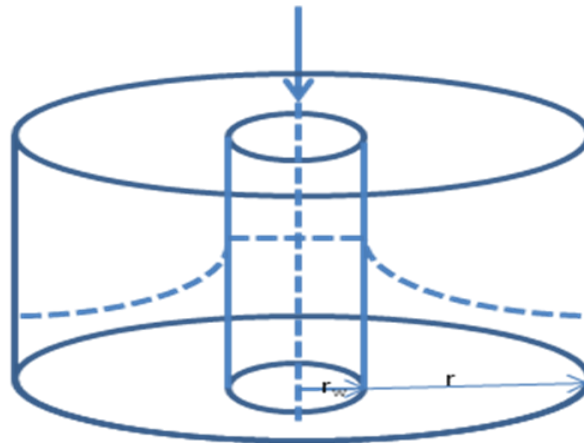


Figure 3- 1: A sketch of pressure distribution around a water injector.

The shape of this funnel (height and how it dissipates) can be described by the diffusivity equation. Physically, it represents how an excess mass placed into the reservoir can move (diffuse) away from the entry point (i.e. wellbore). For radial flow and under pseudo steady state conditions, this is described by the familiar equation:

$$q_{inj} = \frac{hk}{141.2[\ln(r_e / r_w) - \frac{3}{4} + s]} \int_{\bar{p}}^{p_{inj}} \frac{k_{rw}}{\mu_w B_w} dp \quad (3.1)$$

where

q_{inj} = injection rate, STB/day

k = permeability

k_{rw} = water relative permeability

h = reservoir thickness, ft

\bar{p} = average reservoir pressure, psi

p_{inj} = water-injection pressure, psi

r_e = well's drainage radius, ft

r_w = wellbore radius, ft

μ_w = water viscosity, cp

B_w = water formation volume factor, bbl/STB

s = skin factor

The parameters that are important here are the formation transmissibility, the injection pressure which is dependent on the aquifer pressure for water dump flood, reservoir pressure, and any potential damage or skin caused by incompatibility of waters or precipitation or scaling. Equation (3.1) indicates that a successful dump flood can be achieved when the aquifer is large enough such that the aquifer pressure stays high, and the reservoir has large permeability and or transmissibility (i.e. $k_w h$).

The water injection rate, which can vary throughout the life of the project, is influenced by many factors. The variables affecting the injection rates include the following:

- Reservoir geometry.
- Rock and fluid properties. Low injectivities are associated with tight rocks, skin, and viscous fluids.
- Mobility of fluids.

Injectivity index is an important parameter used in the evaluation of waterflood performance. It is defined as the rate of water injection over the pressure difference between water injection pressure and average reservoir pressure. It has the unit of barrels per day per pound per square inch (bbl/d/psi). Decline in water injectivity is observed during the early stages of injection into a reservoir depleted by solution gas drive. This occurs as pore spaces initially occupied by free gas are gradually filled up. Following fill-up, the injectivity of water depends upon the mobility ratio. As shown in Figure 3-2, it remains constant in the case of unit mobility ratio and increases when the mobility ratio is greater than unity (favorable for displacing oil). It is obvious from Equation (3.2) that the mobility ratio depends upon the relative permeability characteristics as well as upon the fluid viscosities. Therefore, the water injectivity index increases with greater mobility. Again, well injectivity may deteriorate noticeably during the life of a waterflood project as a consequence of formation damage around the wellbore.

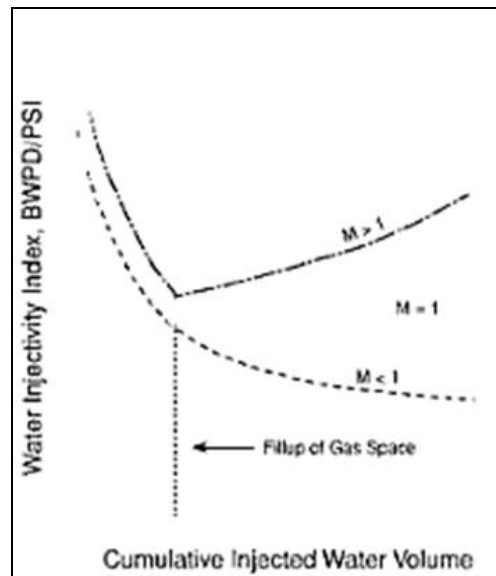


Figure 3- 2: Water injectivity variations in a radial system. [11]

The mobility ratio is defined as the mobility of the displacing phase (water) over that of displaced phase (oil). This is given as follows:

$$M = \frac{[k_{rw} / \mu_w]}{[k_{ro} / \mu_o]} \quad (3.2)$$

where

- M = water-oil mobility
- k_{rw} = water relative permeability
- k_{ro} = oil relative permeability
- μ_w = water viscosity, cp
- μ_o = oil viscosity, cp

The reference permeability is based on two different and separate regions in the reservoir during waterflood. Reference ^[1] suggested calculating the mobility ratio prior to water breakthrough, i.e., k_{rw} at the average water saturation in the swept region, and k_{ro} in the unswept zone.

Well injectivity is a function of the distance between the injector and producer, along with the pressure drop between the wells. Well injectivity is also a function of the formation thickness, oil viscosity, and effective permeability to the displaced fluid among other factors.

3.2 Productivity

The relationship between well inflow rate and pressure drawdown has often been expressed in term of a productivity index, PI . Since most of the well life is spent in a flow regime that is approximating the pseudo steady state, the productivity index is a valuable methodology for predicting the future performance of wells.

The productivity index can be numerically calculated in terms of semi steady-state flow conditions as:

$$PI = \frac{hk}{141.2[\ln(r_e / r_w) - \frac{3}{4} + s]} \left(\frac{k_{ro}}{\mu_o B_o} \right) \quad (3.3)$$

Since most of the well life is spent in a flow regime that is approximating the pseudo steady-state, the productivity index is a valuable methodology for predicting the future performance of wells. Further, by monitoring the productivity index during the life of a well, it is possible to determine if the well has become damaged due to completion, production, injection operations, or mechanical problems.

3.3 Overall recovery efficiency

The overall recovery factor (efficiency) of any secondary or tertiary oil recovery method is the product of a combination of three individual efficiency factors as given by the following generalized expression:

$$RF = E_D E_A E_V \quad (3.4)$$

where

- RF = overall recovery factor
- E_D = displacement efficiency
- E_A = areal sweep efficiency
- E_V = vertical sweep efficiency

3.3.1 Displacement efficiency

The displacement efficiency, E_D , is the fraction of movable oil that has been displaced from the swept zone at any given time or pore volume injected. Factor affecting displacement efficiencies are:

- Oil and water viscosities
- Oil formation volume factors at the start and end of flood

- Oil saturations at the start and end of flood
- Relative permeability characteristics

Displacement efficiency that is governed by rock and fluid properties is given by:

$$E_D = \frac{\frac{S_{oi} - \bar{S}_o}{B_{oi}}}{\frac{S_{oi}}{B_{oi}}} \quad (3.5)$$

where S_{oi} = initial oil saturation at start of flood
 B_{oi} = oil formation volume factor at start of flood, bbl/STB
 \bar{S}_o = average oil saturation in the flood pattern at a particular point during the flood
 B_o = oil formation volume factor at a particular point, bbl/STB

3.3.2 Sweep efficiency

Sweep efficiency is related to permeability variations, fluid properties, fluid distribution, fluid saturation and fracture systems. Adverse permeability variations result in poor sweep efficiency, rapid water breakthrough and high water production.

Volumetric sweep efficiency is a product of $E_A E_V$. It represents the overall fraction of the flood pattern that is contacted by the injected fluid.

The areal sweep efficiency, E_A , is the fractional area of the pattern that is swept by the displacing fluid. It increases steadily with injection from the start of the flood until breakthrough occurs, after which E_A continues to increase at a slower rate. The major factors determining areal sweep efficiency are:

- Fluid mobilities
- Pattern type
- Areal heterogeneity
- Total volume of fluid injected

If directional permeability trends can be identified, injection and production wells can be arranged to take advantage of the trends to enhance areal sweep efficiency. It is also possible to maximize areal sweep efficiency through a careful management of pressure distribution and proper injection–production pattern selection.

The vertical sweep efficiency, E_V , is the fraction of the vertical section of the pay zone that is contacted by injected fluids. It is a product of $E_A E_V$. The vertical sweep efficiency is primarily a function of:

- Vertical heterogeneity
- Degree of gravity segregation
- Fluid mobilities
- Total injection volume

3.4 Optimum time to waterflood

The following factors are important when determining the optimum time (or reservoir pressure) to initiate a secondary recovery project:

- Reservoir oil viscosity. Water injection should be initiated when the reservoir pressure reaches its bubble-point pressure since the oil viscosity reaches its minimum value at this pressure. The mobility of the oil will increase with decreasing oil viscosity, which in turns improves the sweeping efficiency.
- Productivity of producing wells. A high reservoir pressure is desirable to increase the productivity of producing wells, which prolongs the flowing period of the wells, decreases lifting costs, and may shorten the overall life of the project.
- A high oil relative permeability, i.e., high oil saturation, means more oil recovery with less production of the displacing fluid. On the other hand, low oil saturation means a low oil relative permeability with more production of the displacing fluid at a given time.

CHAPTER IV

RESERVOIR MODEL CONSTRUCTION

Water dump flood is a system consisting of aquifer layer and reservoir layer which are separated from one another. In order to study the behavior of water dump flood, reservoir simulator was used as a tool to predict oil production in different scenarios.

The following sections will describe the simulation models construction under the assumption on being homogeneous. Reservoir properties and fluid properties base on filed data are also presented.

4.1 Reservoir model

This study uses a finite difference, black oil, three dimensional numerical model using **Chevron's** in-house simulator called **CHEARS**. A generic model resembling the structure (i.e. the sealing bounding faults, and a small dip angle of 1 degree in the x direction and 5 degrees in the y direction) and a typical well development plan (i.e. wells along the top of the structure every 400 m and some 200 ft away from the fault) was used to create the simulation model. The grid blocks are 100ftx100ft areally and 1.5 ft thick. The grid dimensions are 39x8x22. The first layer represents the aquifer and is 60 ft thick. The oil reservoir is 300 ft below the aquifer and is represented by layers 3 to 22, and each layer is 1.5ft thick. The top of aquifer layer was located at a depth of 4,000 ft with an initial pressure of 1,650 psia and top of reservoir was located at depth of 4,360 with 1,800 psia at initial condition. A sketch of the reservoir model is shown in Figure 4-1.

Sensitivity to grid size was performed using local grid refinement (LGR) around the three wells and it was concluded that the resolution of the coarse grid was satisfactory. The LGR used a refinement of three coarse cells along well 1 to well 3. Each coarse cell was subdivided into nine cells (3x3). The coarse cells were 100ftx100ft while the LGR cells were 33ftx33ft.

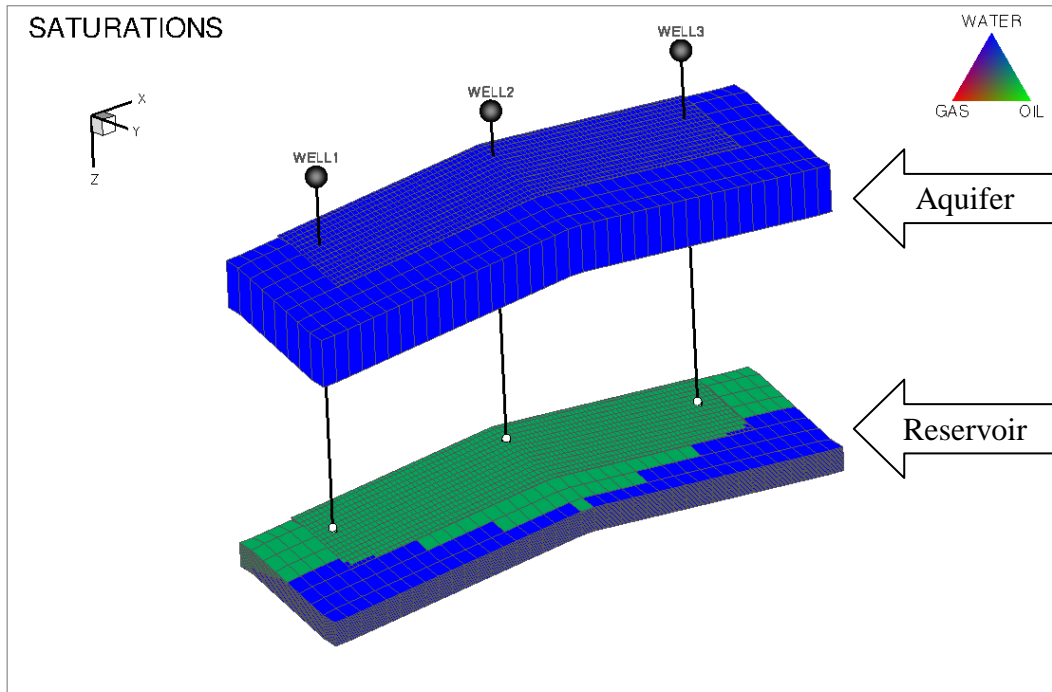


Figure 4- 1: Structural model of oil reservoir and overlaying aquifer.

A side-view of structural model is shown in Figure 4-2. Well 2 was set as center well with full to base, perforated from layer 3 to layer 22. Well 1 and well 3 were set as edge wells, being perforated from layer 3 to layer 10.

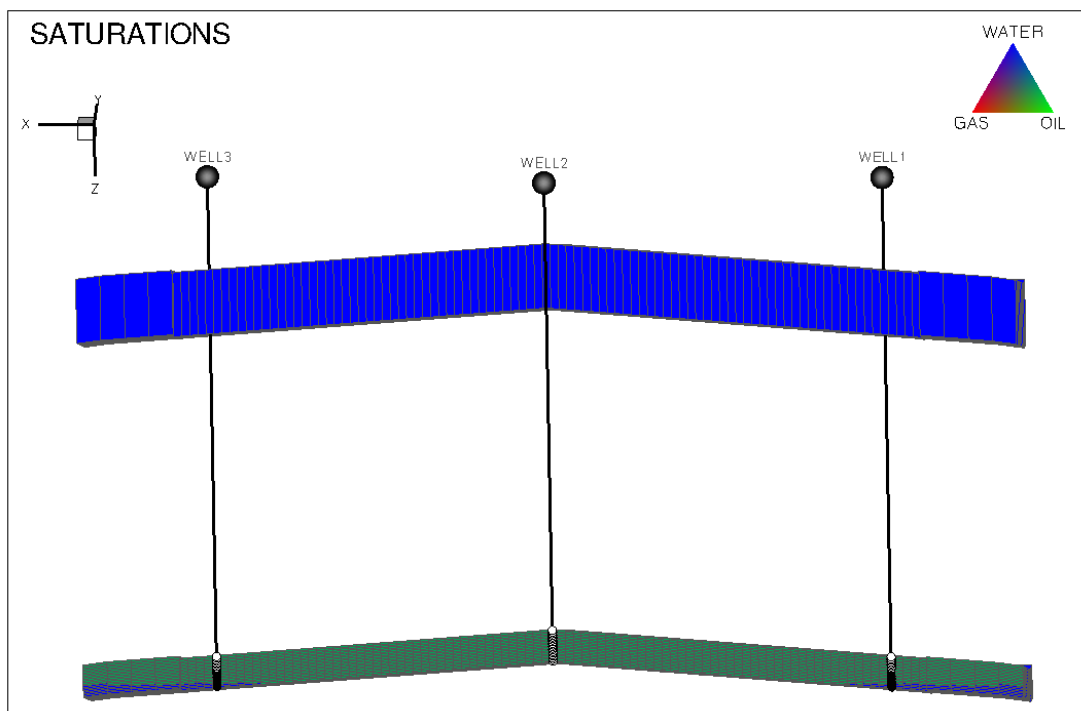


Figure 4- 2: Side view of Structural model of oil reservoir and overlaying aquifer.

4.2 Rock and fluid properties

4.2.1 Rock properties

The reservoir properties were chosen based on average trends from the basin and vary with depth (i.e. porosity, initial pressure, and temperature) and the PVT properties were chosen from a depth relationship developed from the scarce PVT analyses that exist in the oil assets. Rock properties of the oil reservoir and aquifer for the base case are shown in Table 4-1. The reservoir properties are estimated from basin trends such that porosity is about 28%, permeability is in the range of 300 to 800 mD, reservoir temperature is 200°F, and reservoir pressure is about 1800 psia.

Table 4- 1: Rock properties for base case.

Layer	Parameter	Value
1 st layer (aquifer)	Top structure (top of aquifer), ft	4000
	Thickness (1 st Layer), ft	60
	Porosity, fraction	0.3
	k_x and k_y , mD	1000
	k_z , mD	50
2 nd layer (shale)	Thickness (2 nd layer), ft	300
3 rd – 22 nd layer (oil reservoir)	Top structure (top of the reservoir), ft	4,360
	Reservoir pressure, psia	1800
	Reservoir temperature, °F	200
	Thickness (3 rd – 22 nd layer), 1.5 ft/layer	30
	Porosity, fraction	0.28
	k_x and k_y , mD	800
	k_z , mD	0.5

4.2.2 Fluid properties

Reservoir fluid properties were estimated from field data. At initial condition, the reservoir fluids consist of oil and water. The fluid properties were used to calculate water viscosity, mobility ratio, pore volume of oil and original oil in place for the base case as shown in Table 4-2. The correlations were matched with parameters by non-linear regression to make the best fit to PVT data.

Table 4- 2: Fluid properties and pore volumes for base case

Parameter	Value
Oil gravity, °API	35
Gas specific gravity	0.85 (air =1)
Water salinity, ppm	2000
CO ₂ , N ₂ , H ₂ S content	0%
P _b , R _s & B _o correlation	Glaso
Oil viscosity correlation	*Petrosky et al.
Solution gas-oil ratio @ initial condition, scf/STB	200
Bubble point pressure, psia	1017
Rock compressibility, (psi ⁻¹)	10.0E-06
Water formation volume factor @ initial condition, RB/STB	1.0412
Oil formation volume factor @ initial condition, RB/STB	1.1785
Oil viscosity, cp	1.0635
Water viscosity, cp	0.3013
Mobility ratio	1.7648
Aquifer pore volume, RBBL	9.9847E+6
Reservoir pore volume, RBBL	4.6664E+6
OOIP, STB	1.3113E+6

* Pressure-Volume-Temperature Correlations for Gulf of Mexico Crude Oils, G.E. Petrosky Jr. and F.F. Farshad.

4.3 SCAL (Special core analysis)

Fluid saturations and relative permeability curves are obtained from field data as shown in Table 4-3, Figures 4-3 and 4-4.

Table 4- 3: Parameters for relative permeability curves.

Parameter	Value
Connate water saturation, S_{wc}	0.35
Residual oil saturation to water, S_{orw}	0.35
Critical gas saturation, S_{gc}	0.05
Residual oil saturation to gas, S_{org}	0.37
Water relative permeability at S_{orw}	0.4
Oil relative permeability at S_{wc}	0.8
Water relative permeability at S_{org}	0.4
Oil relative permeability at S_{gc}	0.8
Oil Correy exponent, n_o	2.5
Water Correy exponent, n_w	2.5
Gas Correy exponent, n_g	2.5

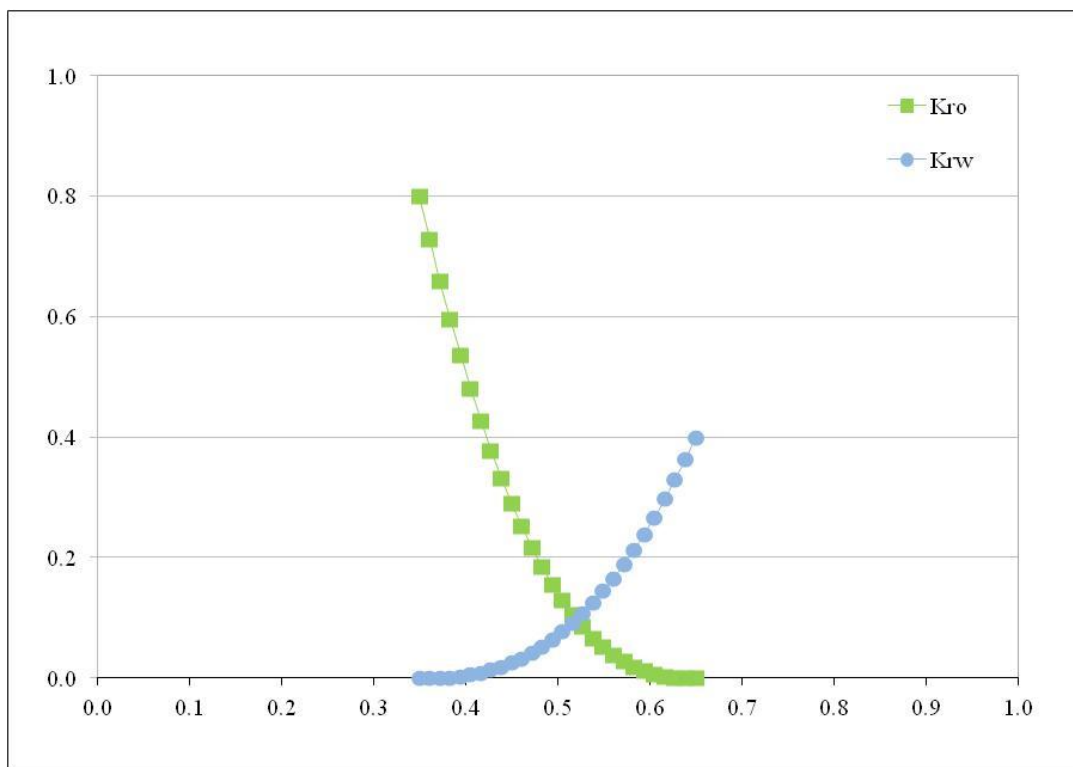


Figure 4- 3: Water/oil relative permeability curves.

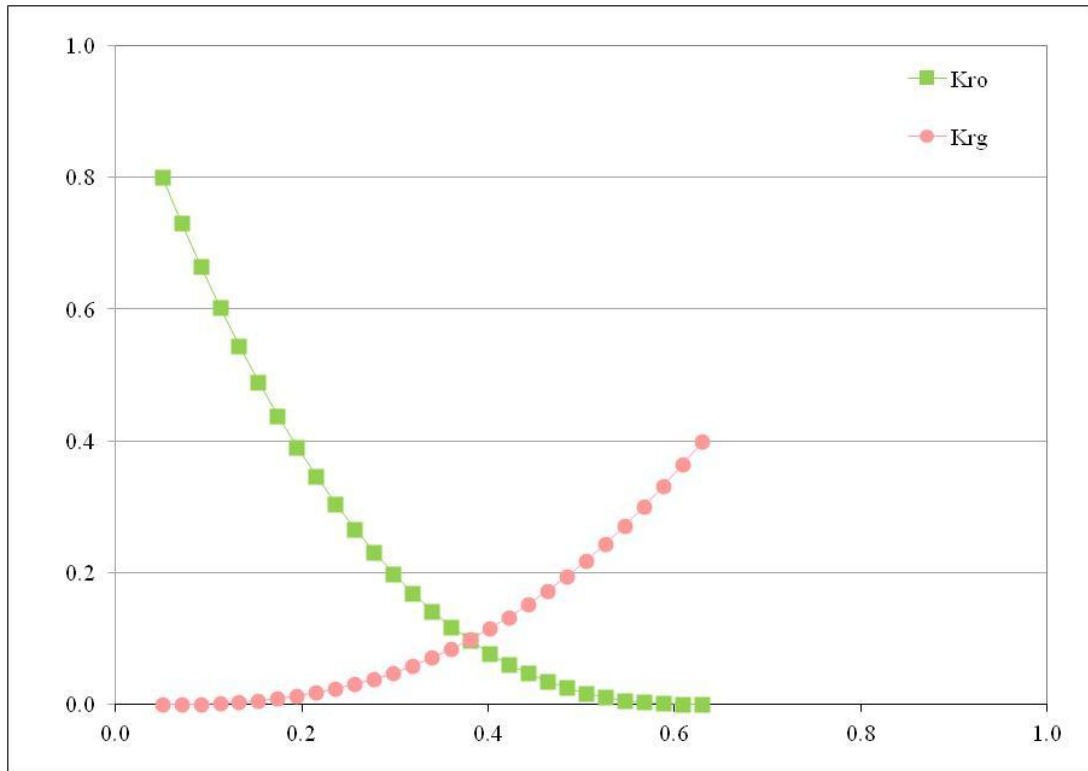


Figure 4- 4: Gas/oil relative permeability curves.

4.4 Wellbore

All wells in the model have a standard well completion design with 2-7/8 inch monobore tubing with gas lift. Gas is being injected at depth of 3,100 ft. The schematic of wellbore configuration is shown in Figure 4.5

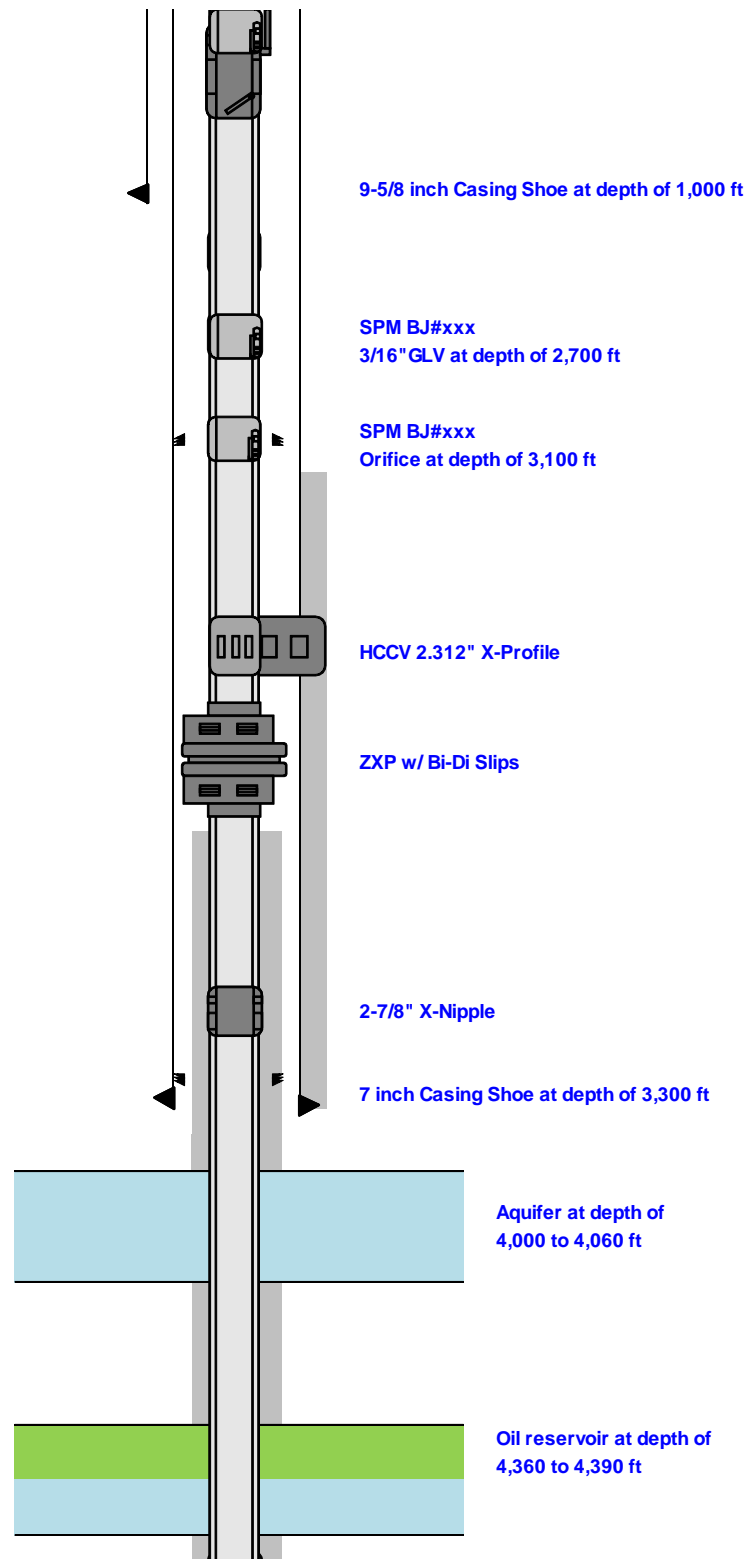


Figure 4- 5: Wellbore schematic.

4.5 Vertical flow performance

The producers were coupled to vertical lift performance tables (i.e. VLP or Flowtables) and the constraints were set to resemble those observed in the Benchamas field. The gas-lift rate for producing wells is fixed at 500 MSCF/DAY.

Production constraints and economic limit for production optimization are shown in Table 4-4. The specified wellhead pressure (minimum well head pressure) is used as a constraint for production wells. Production flow rate and wellhead pressure are related to bottom-hole pressure by using flow table. The simulator can then determine the corresponding bottom-hole pressure for any combination of phase flow rates and wellhead pressure within the range of the table. The computed bottom-hole pressure is then used in determining the limiting constraint for the well during the time step. The well will be automatically shut-in if the maximum water cut and minimum oil rate of producer exceeds the economic limit.

Table 4- 4: Production constraints and economic limit

Parameter	Value
Maximum liquid rate, STB/D	500
Minimum well head pressure, psia	114.7
Maximum water cut	0.95
Minimum oil rate, STB/D	20

4.6 Sensitivity parameters

There are many factors which can affect the production performance such as aquifer size, injector position, well PI, well II, aquifer location, API and time to start water dump flooding. In this study, the sensitivities to these factors would be performed at the shallowest depth scenario only.

CHAPTER V

WATER DUMP FLOOD RESULT

In this chapter, many scenarios were simulated to evaluate the viability of water dump flood in the Gulf of Thailand by using a generic reservoir model (previously described) with reservoir and fluid properties similar to those measured in the Gulf of Thailand. These conceptual studies are very helpful in understanding water dump flood behavior. The studies focus on understanding the impact of the following factors on oil production:

- Injector location
- Aquifer size
- Productivity/ Injectivity index
- Reservoir depth
- API gravity
- Timing of waterflood.

5.1 Impact of injector location

The objective of first set of cases is to identify the best location for the injector (between a crestal and a peripheral well along the fault). A series of simulation runs were done and compared against a base case (i.e. three wells producing under solution gas drive mechanism). Two injector locations were investigated as follows: 1) an edge well (W1), and 2) a center well (W2). The third possible location (W3) is symmetric with W1 and was therefore excluded. Dump flooding was started since day one. This numerical experiments were conducted for a reservoir depth of 4000 ft TVDSS.

Figures 5-1 and 5-2 show the comparison of oil and water performance respectively for three different cases: base case, edge well as injector, and center well as injector. Three producing wells for base case and two producing wells with one injector well for dump flood cases were conducted. The oil rate for the base case (black line) decline more rapidly than that for water dump flood cases (orange and pink lines). The water production for the dump flood cases (orange and pink lines) is higher than that for the primary case (black line). The oil production rate decreases with time until the reservoir pressure drops below the bubble point pressure (1017 psia). At this point, the oil production increases briefly due to increased GOR (lower wellbore densities and backpressure), as shown in Figure 5-3. The plot in Figure 5-4 shows that the trends of average reservoir pressure are associated with oil production rates.

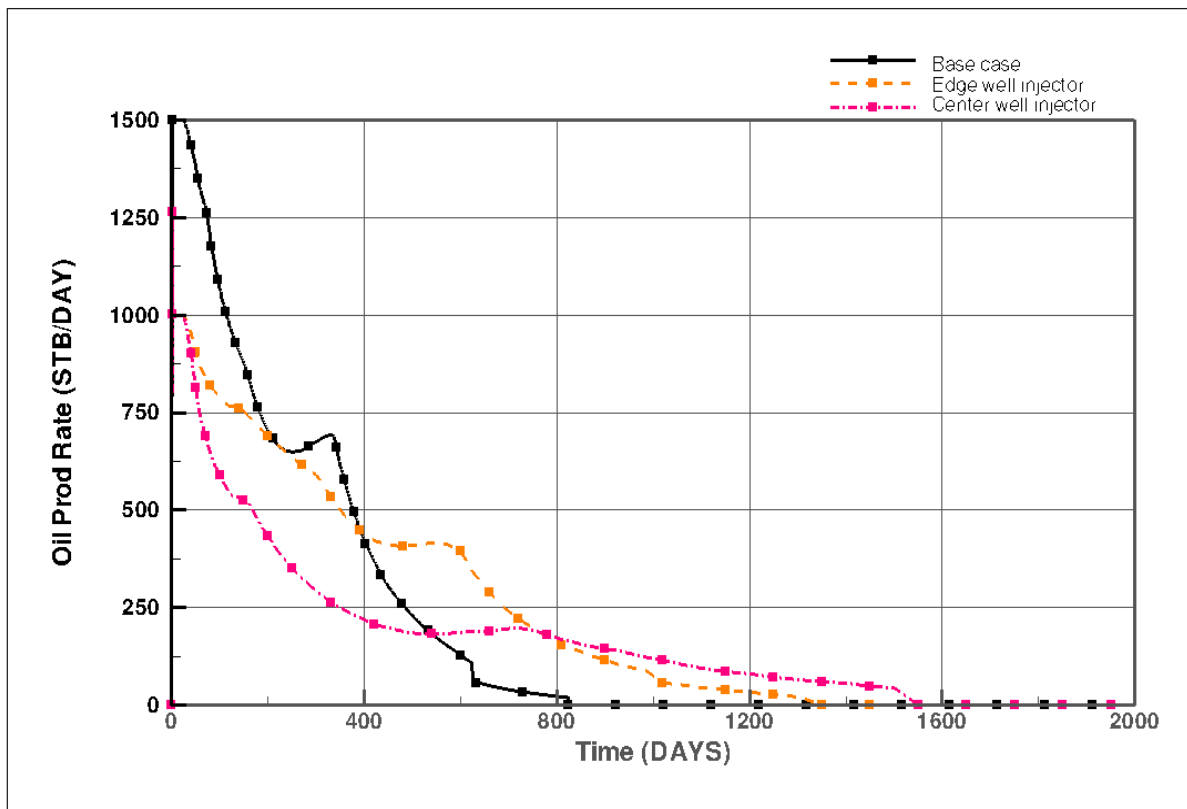


Figure 5- 1: Oil production rates for different injector locations

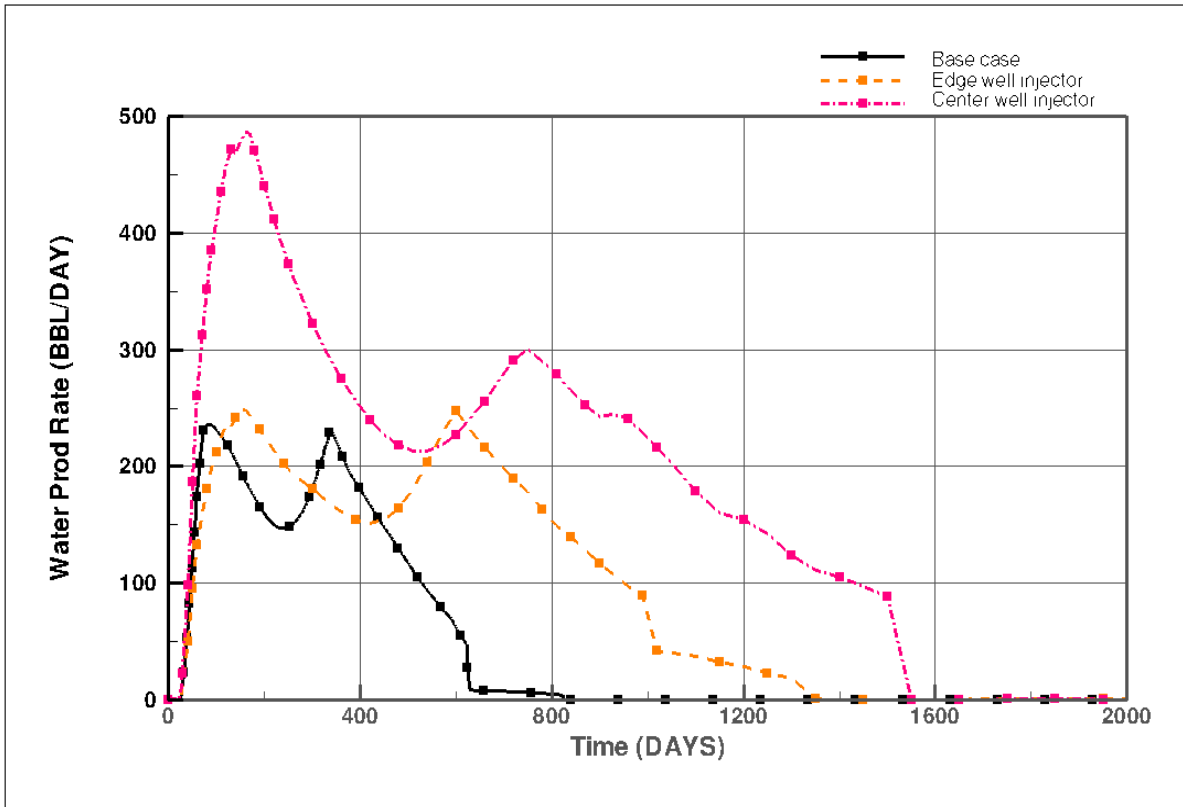


Figure 5- 2: Water production trends for different injector locations

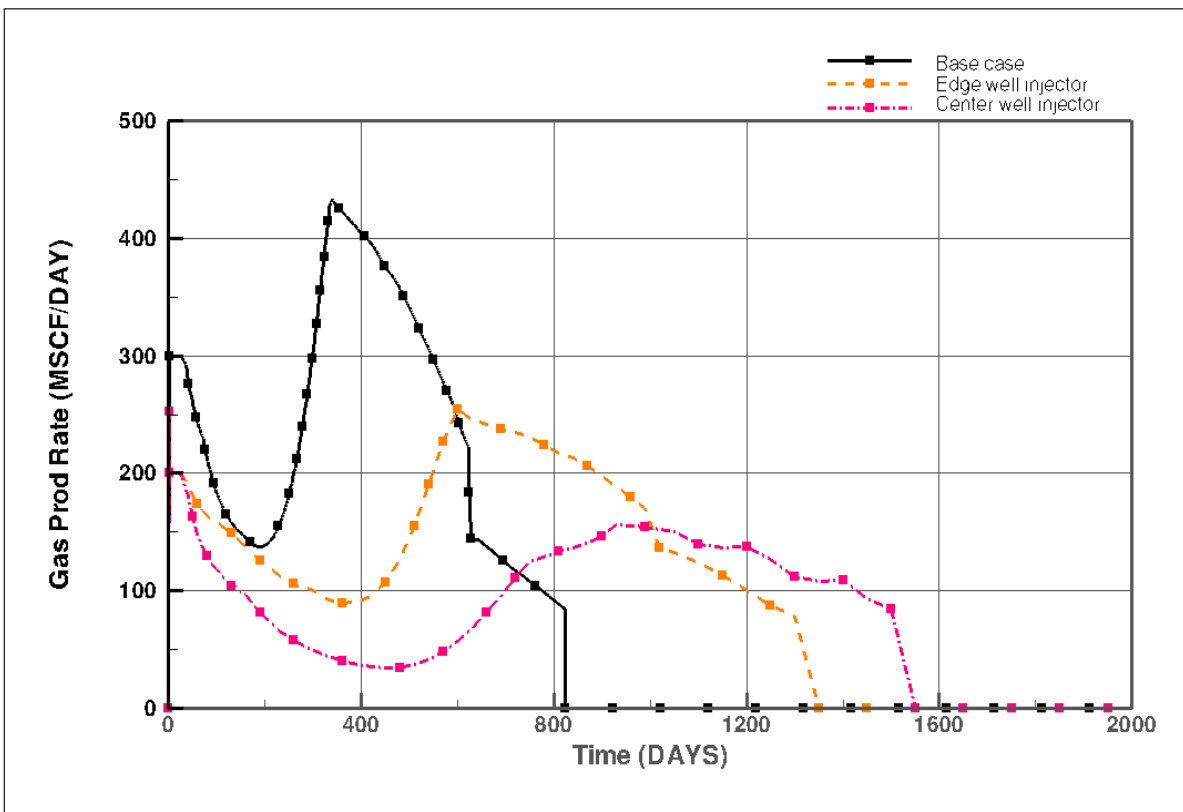


Figure 5- 3: Gas production rates for different injector locations

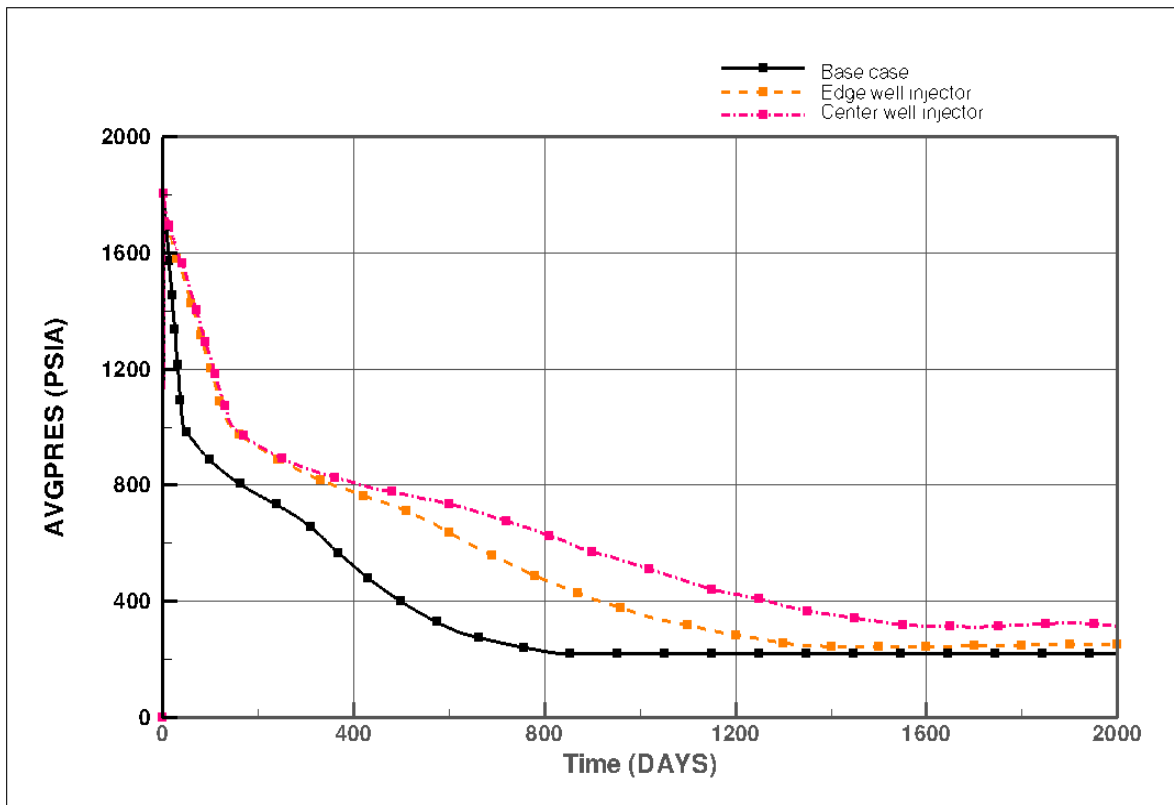


Figure 5- 4: Average reservoir pressures for different injector locations

A series of contour maps of water saturation for layers 3, 7 and 10 of the simulation model are used to show the differences in performance for the three scenarios investigated. The maps for the first scenario (base case), second scenario (edge well as injector), and third scenario (center well as injector) are shown in Figures 5-5, 5-6, and 5-7, respectively (The contour maps for all scenarios are presented in Appendix A). For the base case (Figure 5-5), water sweep only occurs as a consequence of aquifer encroachment around the edge wells due to their proximity to the oil-water contact. The areas without contour lines represent unswept zones undergoing pure primary depletion. The case of the edge injector (Figure 5-6) shows an asymmetric map with a larger area swept by the dumpflood (on the left) as compared to the aquifer encroachment swept area (on the right). The unswept areas (no contours) are much smaller in this case than those in the primary depletion case, implying larger recovery factors. The case for the center injector shows a symmetric contour map with swept areas extending from the center to the edge wells and with the effect of aquifer encroachment.

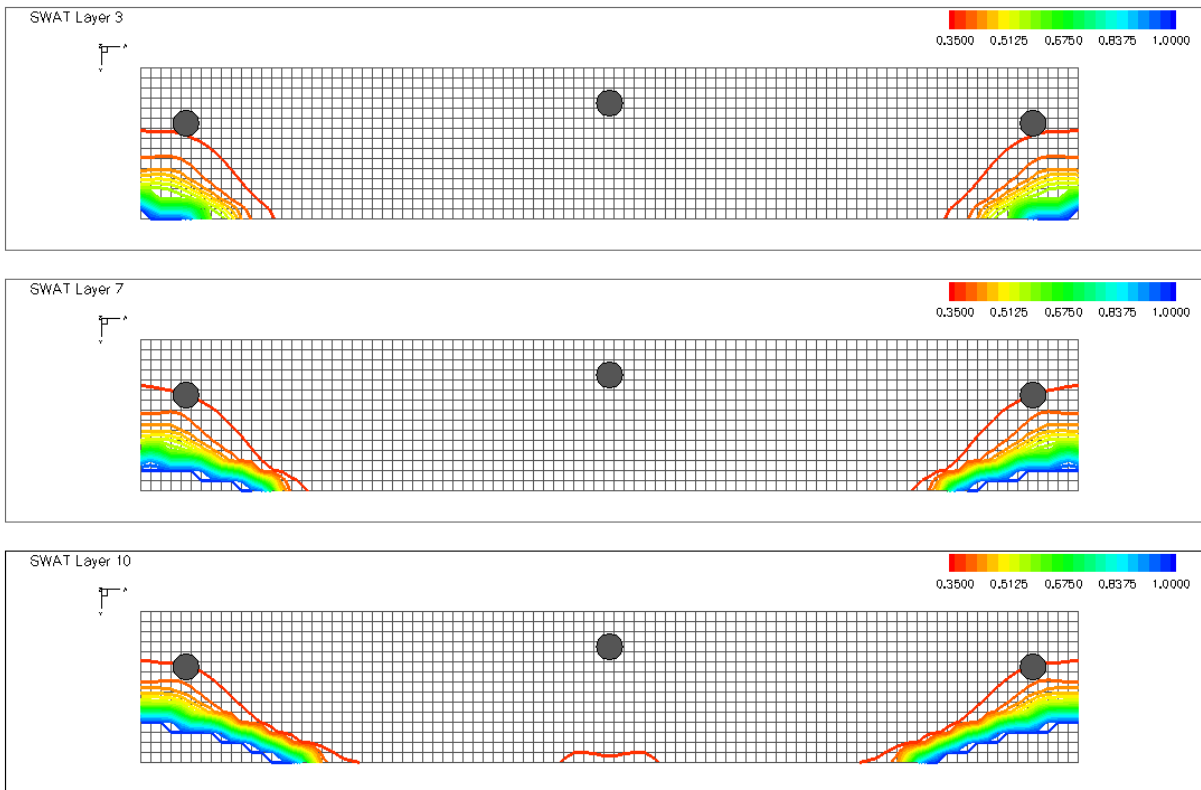


Figure 5- 5: Contour map of water saturation for base case @ day 900

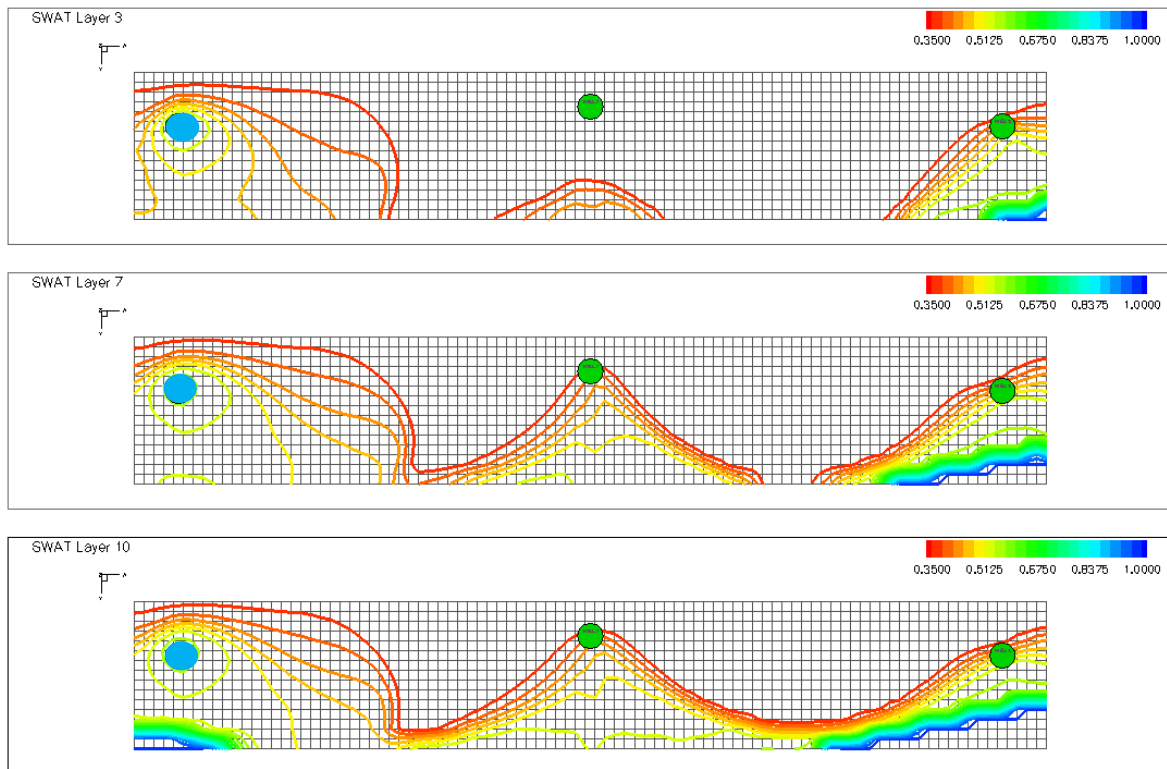


Figure 5- 6: Contour map of water saturation for dump flooding via an edge well injector @ day 900

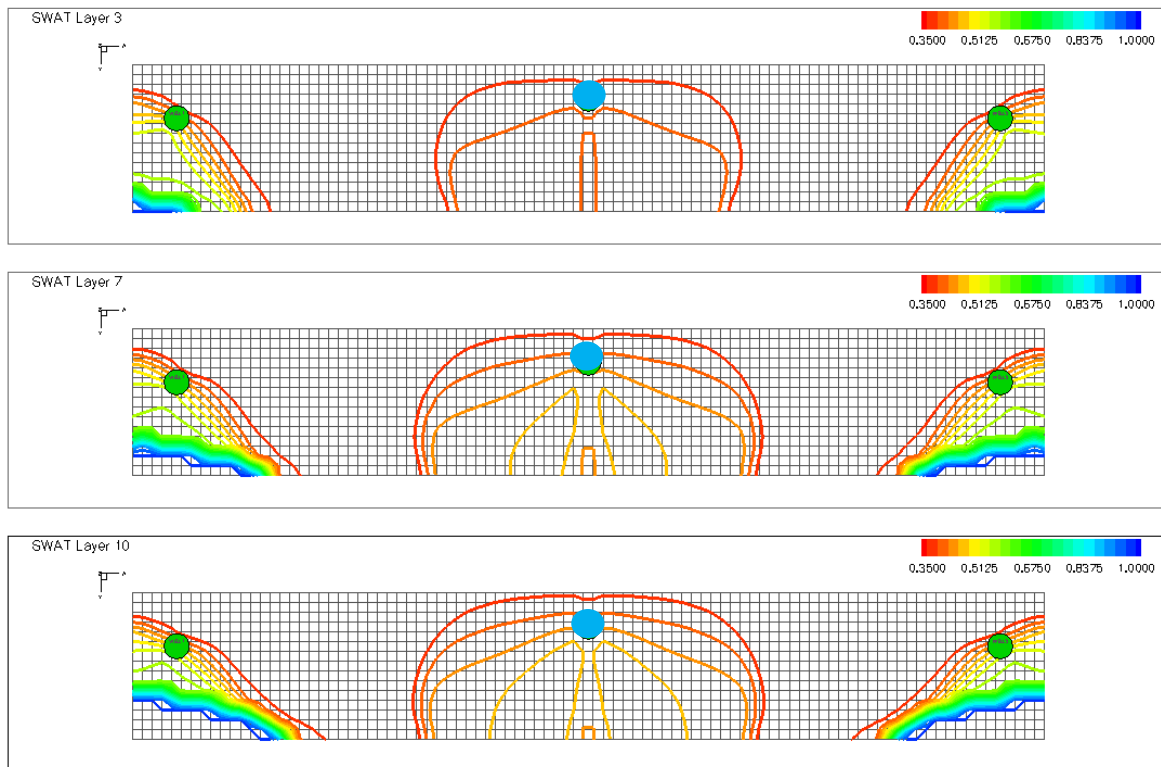


Figure 5- 7: Contour map of water saturation for dump flooding via a center well injector @ day 900

Based on all analyses, edge wells are the best choice for injection location. The results are shown numerically in Table 5-1. It is important to remember the assumption that the center well is on the crest further from the water-oil contact, a case with a flat structure along the fault was not investigated. As shown in Table 5-1, the center (i.e. crestal) well injection had a detrimental impact on recovery ($\Delta\text{RF}=-5\%$) relative to the primary depletion case, while conversion of one of the edge wells to injector increase recovery ($\Delta\text{RF}+=5\%$) relative to the primary depletion case.

Table 5- 1: Oil recovery factors for different well locations

Case	RF (%)
Base case	30.95
Edge well injector	34.05
Center well injector	25.56

5.2 Impact of aquifer volume

The impact of aquifer size on oil recovery and rate performance was investigated via pore volume multipliers that effectively increase or reduce the size of the aquifer. Enlargement of aquifer size by multipliers of 2, 3, 4, 5, 10, 20, 30, 40, 50, 100 and 150 times all showed improvements in oil recovery while reduction in the aquifer size by factors of 2, 3, 4, 5, and 10 times showed decreasing in oil recovery. The improvement in oil recovery from larger aquifers is caused by slower pressure declines in the aquifer leading to higher and more prolonged injection pressures. The following two sections describe the detailed results of the reduction on aquifer size and then the increase in aquifer size, respectively.

5.2.1 Effect of decrease in aquifer size

In this section, we studied the effect of reduction in aquifer size on oil production from water dump flood process. The aquifer size was varied by dividing the original aquifer which is 2.14 times the reservoir in terms of pore volume by a factor of 2, 3, 4, 5 and 10.

Figures 5-8 show a comparison of the dump flood cases with the original aquifer size reduction (black line) against those with reduction factors of 2,3,4,5 and 10 (color lines). The reduction in aquifer size slightly affects the production performance. The lower amount of water in the aquifer results in fairly decreased reservoir pressure, leading to little changes in oil, water and gas productions. Besides, the sweep efficiency of each case tends to be the same, as shown in Figures 5-9 and 5-10. The recovery factors of reservoirs with small overlaying aquifers are a bit smaller than those with large aquifers as summarized in Table 5-2.

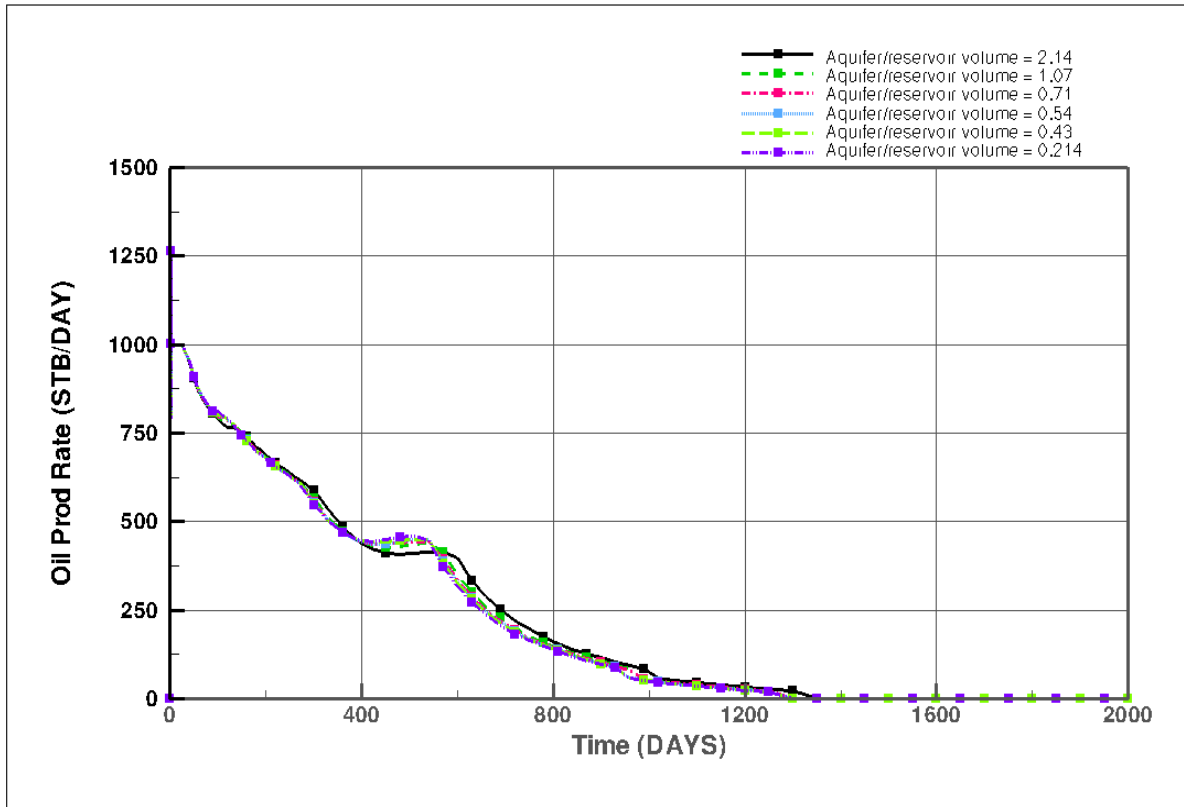


Figure 5- 8: Oil production rates for different aquifer sizes

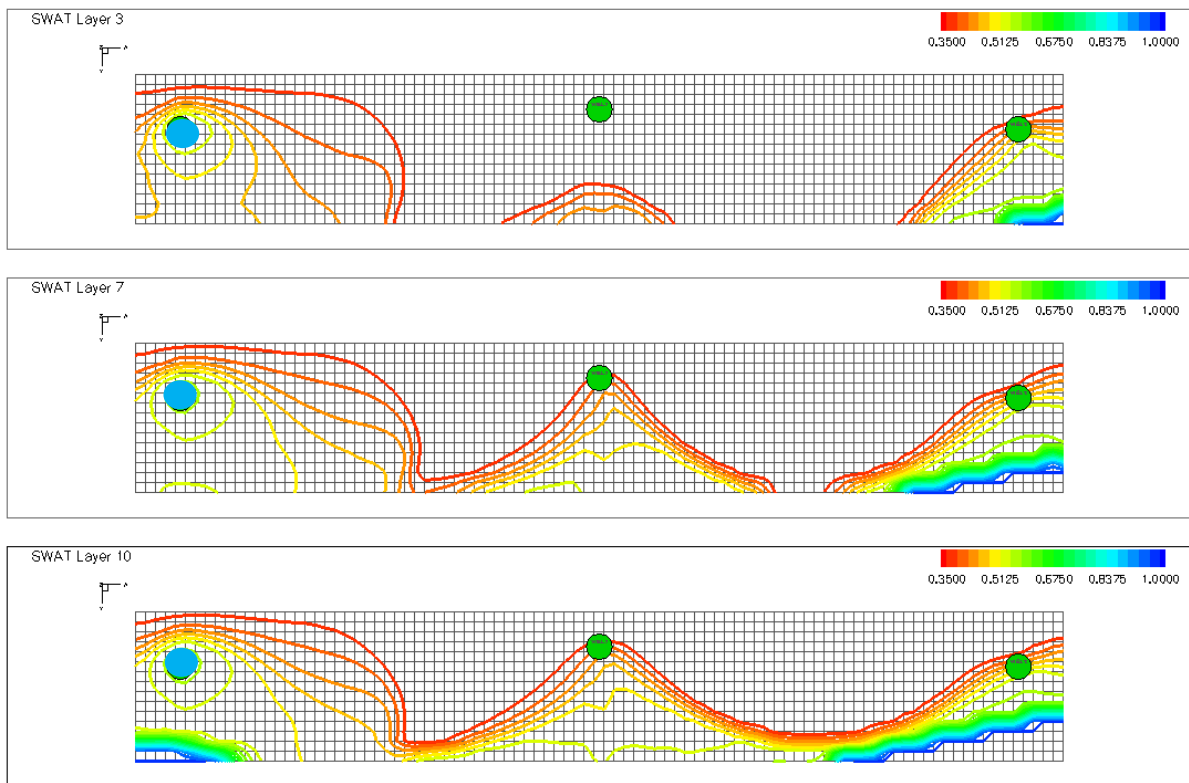


Figure 5- 9: Contour map of water saturation for dump flooding via an edge well injector with aquifer/reservoir volume of 2.14 rbl/rbl @ day 900

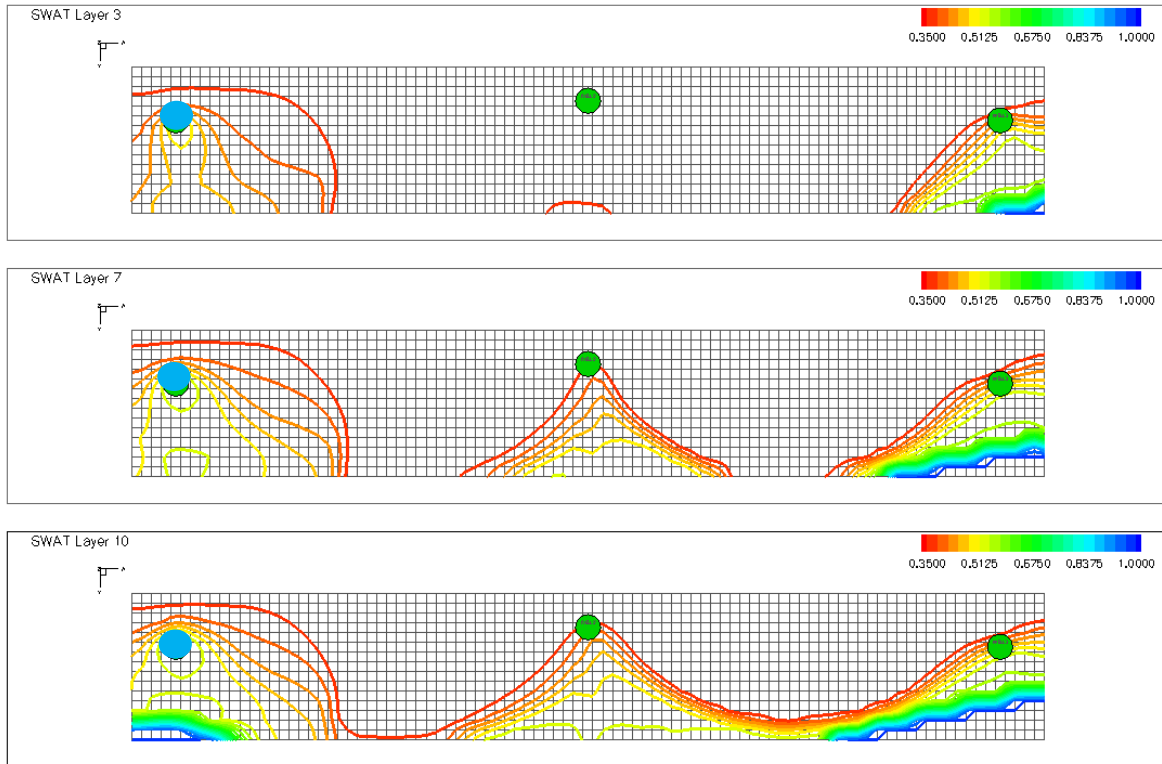


Figure 5- 10: Contour map of water saturation for dump flooding via an edge well injector with aquifer/reservoir volume of 0.214 rbl/rbl @ day 900

Table 5- 2: Oil recovery factors for different aquifer sizes

Aquifer/Reservoir ratio (RBL/RBL)	Divisor	RF (%)
2.14	1	34.05
1.07	÷ 2	33.31
0.71	÷ 3	33.09
0.54	÷ 4	32.91
0.43	÷ 5	32.81
0.214	÷ 10	32.65

5.2.2 Effect of increase in aquifer size

This section aims to study the impact of aquifer size on oil recovery and rate performance by enlargement of aquifer size by using 2, 3, 4, 5, 10, 20, 30, 40, 50, 100 and 150 multipliers.

Figures 5-11 and 5-12 show the oil and water production performance associated with aquifer size, respectively. We can see that large aquifer prolongs the production period. Figures 5-13 and 5-14 show that larger aquifer size has better sweep efficiency. However, for very large aquifer sizes (i.e. approaching infinite acting), the water continues to increase.

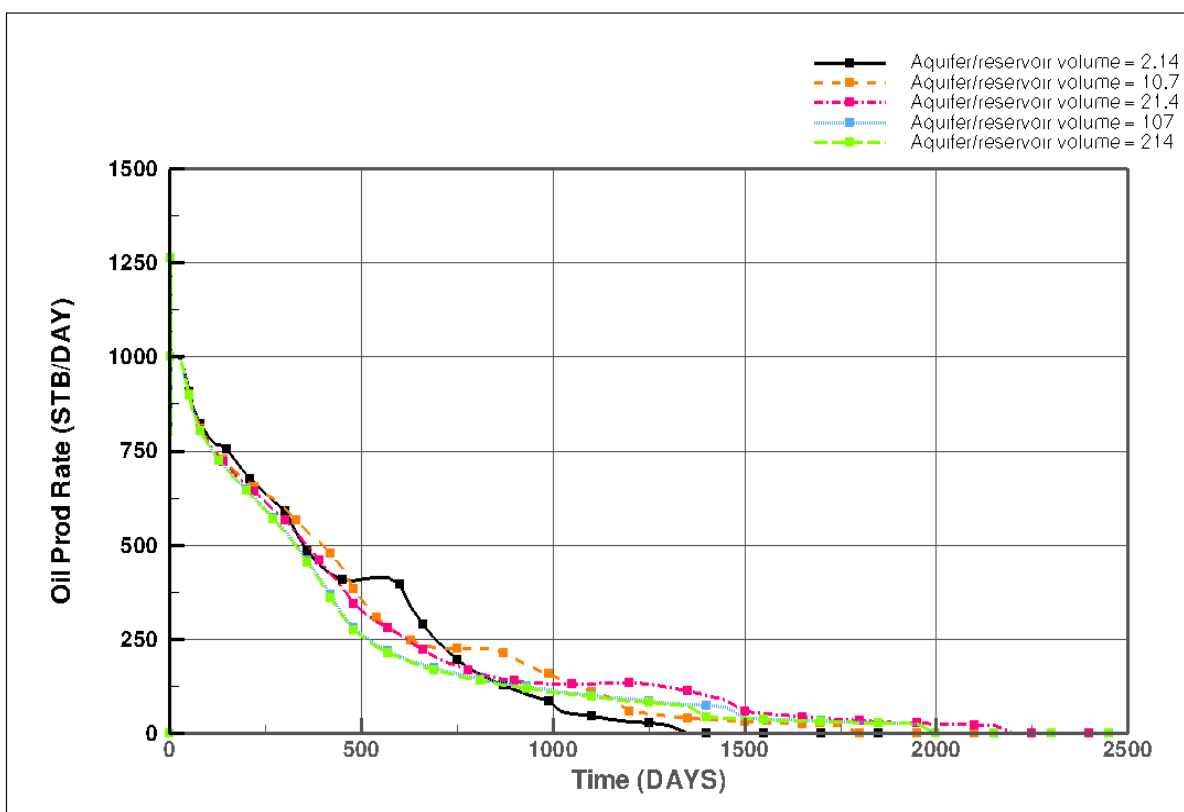


Figure 5- 11: Oil production rates for different aquifer sizes

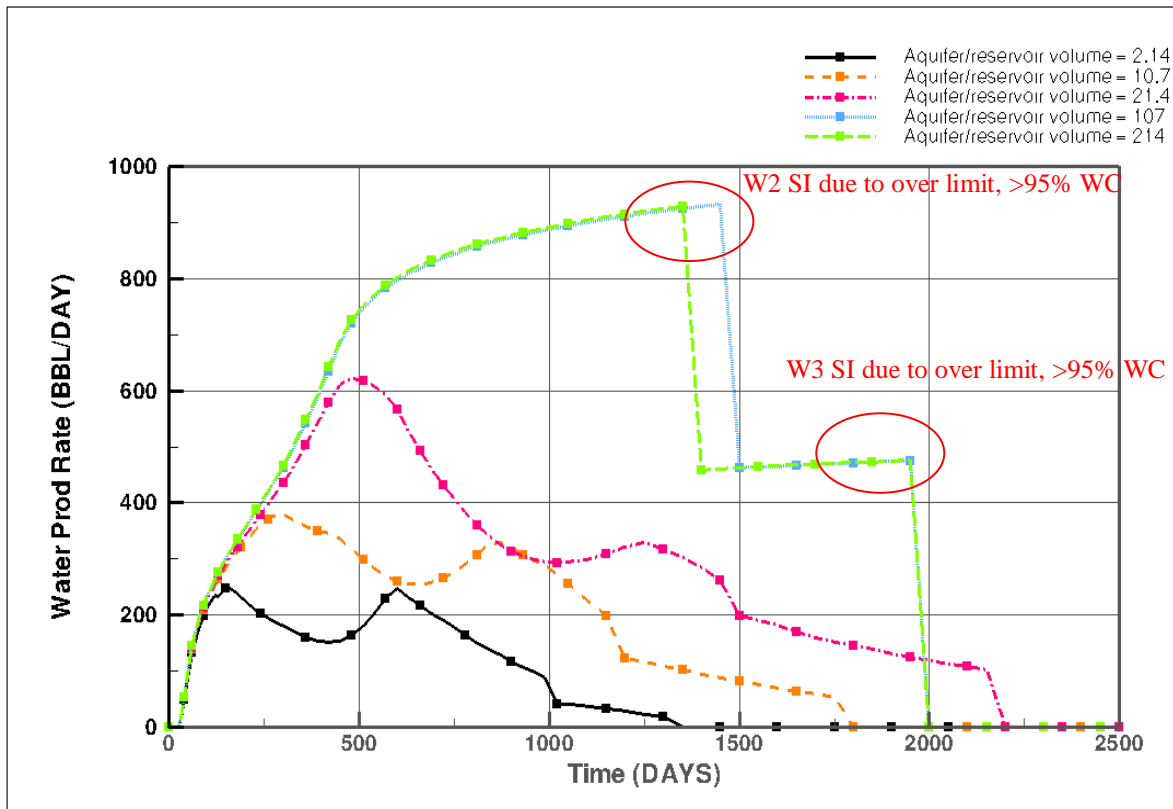


Figure 5- 12: Water production trend for different aquifer sizes

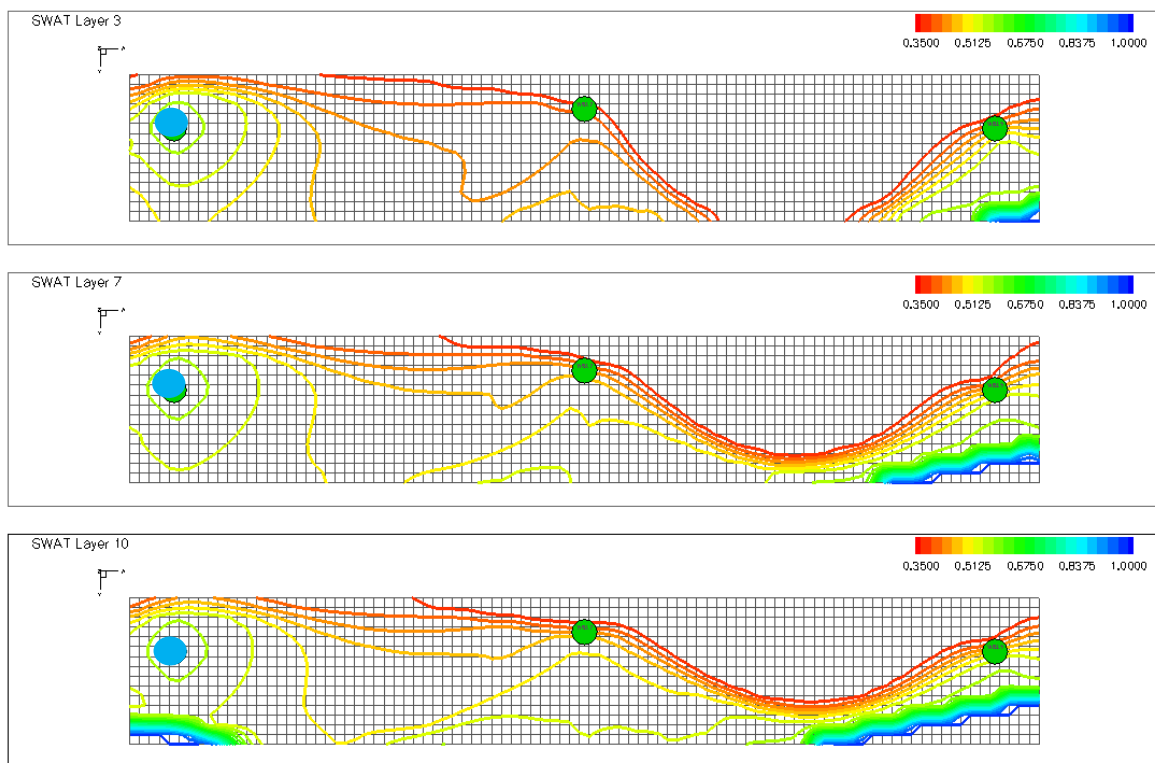


Figure 5- 13: Contour map of water saturation for dump flooding via an edge well injector with aquifer/reservoir volume of 8.56 RBL/RBL @ day 900

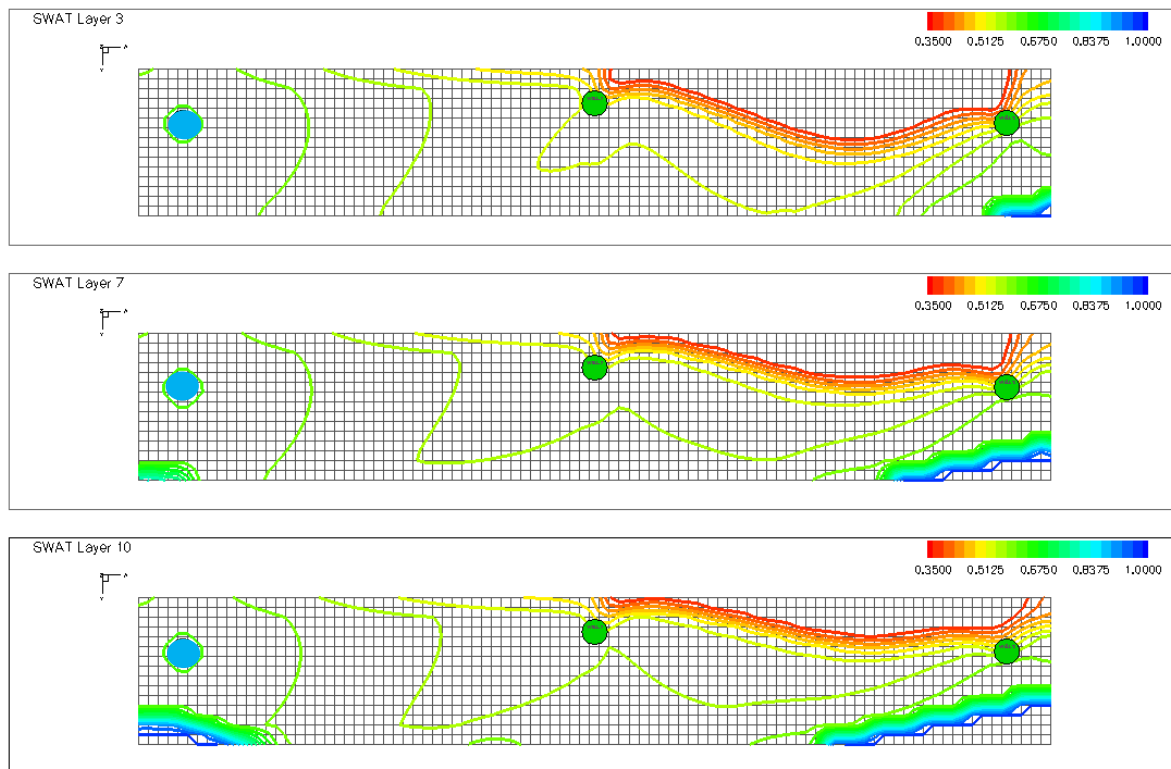


Figure 5- 14: Contour map of water saturation for dump flooding via an edge well injector with aquifer/reservoir volume of 85.6 RBL/RBL @ day 900

Table 5-3 shows that the recovery efficiency increases as aquifer volume increases. However, when the aquifer size is bigger than an aquifer-oil ratio of 42.8 RBL/RBL, the oil production becomes lower since the water production is over limit of water cut (95% WC) sooner as a result of strong water support. This is because of high viscous force due to high water flow rate. In any case, the oil recovery is still higher than that in the base case (i.e. primary production).

Table 5- 3: Oil recovery via an edge injector for increasing aquifer size

Aquifer/Reservoir ratio (RBL/RBL)	Multiplier	RF (%)
2.14	1	34.05
4.28	x 2	35.17
6.42	x 3	35.89
8.56	x 4	36.22
10.7	x 5	36.50
21.4	x 10	37.39
42.8	x 20	37.48
64.2	x 30	36.30
85.6	x 40	35.71
107	x 50	33.39
214	x 100	32.71
321	x 150	32.49

5.2.3 Effect of well location

A summary of the results evaluating the relationship between oil recovery factor and the ratio of aquifer to reservoir size for both the edge and the center well scenarios is shown in Figure 5-15. This figure shows that the maximum recovery for the center well case happens when the ratio of aquifer to reservoir is around 20RBL/RBL (The results are shown in Appendix B) while that for the edge well occurs at ratio of 20-40 RBL/RBL. That is because the aquifer size has more impact to the production well that closed to oil-water contact, as the case of center well dump flooding. For comparison purposes, the base case run has a ratio of 2.14 RBL/RBL. The oil recovery factors for the base case (no water dump flood is shown as a cubic); the oil recovery factor for case W1 (dump flood in the edge well with no aquifer multiplier) is shown as a triangle; and the oil recovery factor for case W2 (dump flood in center well with no aquifer multiplier) is shown as a circle in Figure 5-15.

For increasing in aquifer size in edge well case (pink solid line) and center well case (blue dash line), the oil recovery efficiency rapidly changes as the aquifer to reservoir size is changed from 0 to 20. When the aquifer size is greater than 20 times the reservoir size, the oil recovery begins to decline at a moderate rate as the aquifer size is increased. However, when the aquifer/reservoir size is larger than 100, there is a slightly decrease in oil recovery as the aquifer becomes larger.

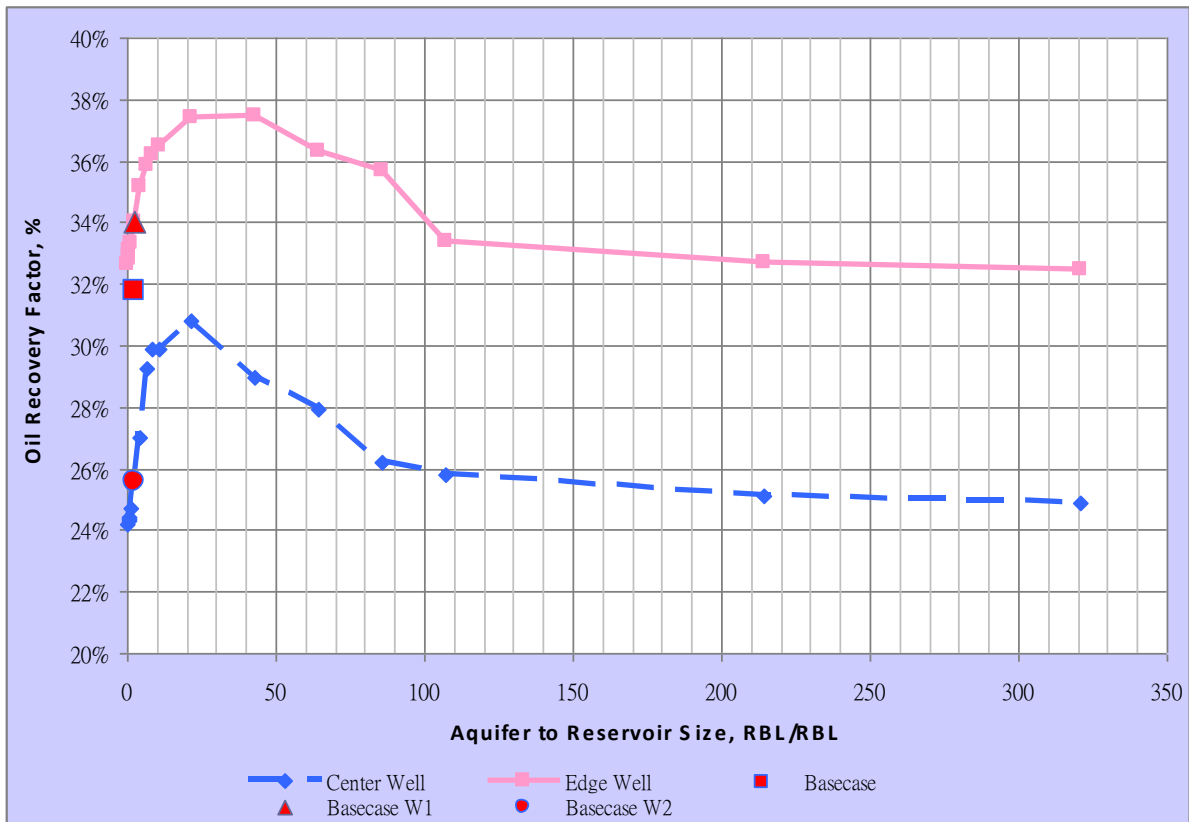


Figure 5- 15: Oil recovery factors as a function of aquifer to reservoir size and injector location

5.3 Effect of well productivity index

This section aims to evaluate the impact of well productivity index on the oil recovery for the water dump flood via an edge well. The efficiency of the well to produce is defined in terms of productivity index, PI, which is the ratio of the total liquid flow rate to the pressure drawdown:

$$PI = \frac{Q}{(p_R - p_{wf})} = \frac{Q}{\Delta p} \quad (5.1)$$

As discussed by Ahmed ^[12], the measurement of the well productivity potential is valid at pseudo steady state conditions. However, due to change in drainage area and saturation, PI varies during a water dump flood process. The results from the simulation showing the variation of PI for the three cases evaluated are shown in Figure 5-16. This figure shows the base case (where the edge well is used for dump flooding) and two other cases where the well PI is decreased by a factor of 0.5 and 0.1. At the early of production period, PI increases with time due to response to water dumpflood. Then, PI decreases with time until drawdown pressure between reservoir and wellbore are very close. Then PI becomes higher again.

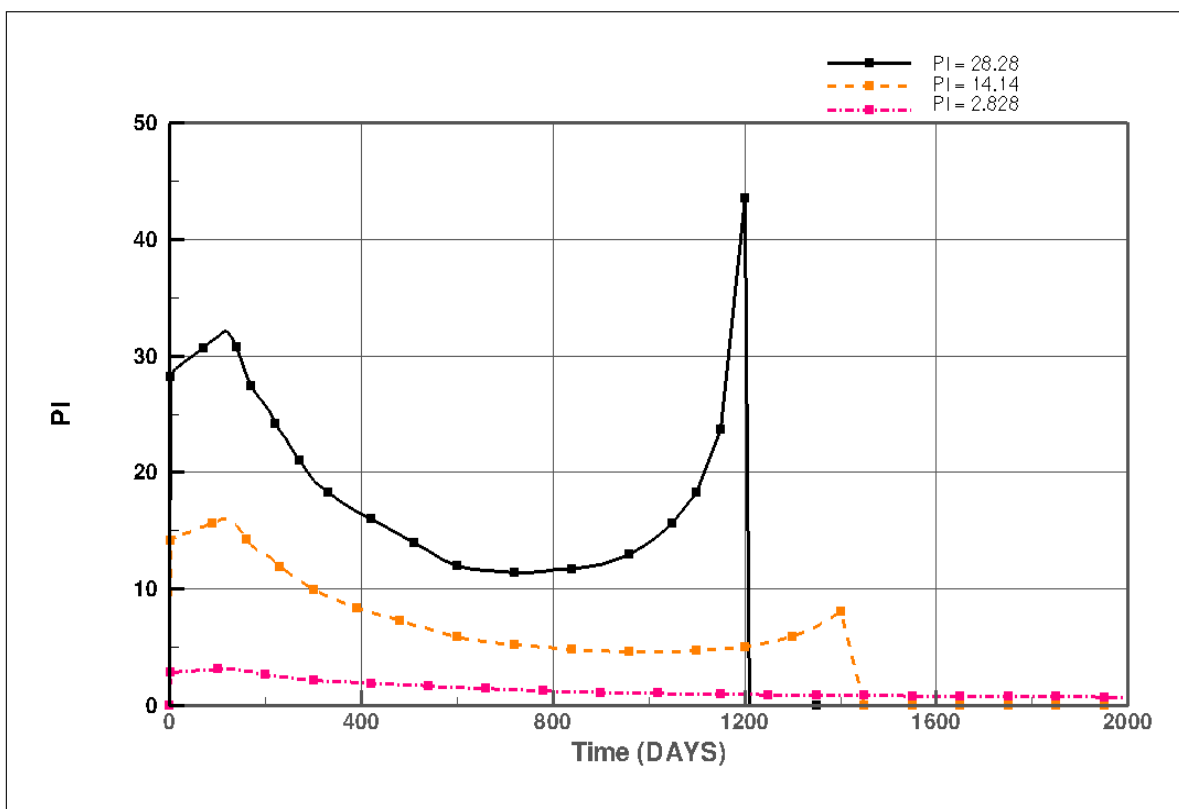


Figure 5- 16: Variation of productivity index as a function of time

Figures 5-17 and 5-18 show the oil production and water cross-flow rate, respectively. In case of decreasing PI by half (PI = 14.14), the water cross-flow rate and oil production rates are very similar compared to the base case (PI = 28.28). But for very low PI case (PI = 2.828), the water cross-flow rate and oil production rate are significantly lower. The sweep efficiency is similar for all PI cases as shown in Figures 5-19 and 5-20.

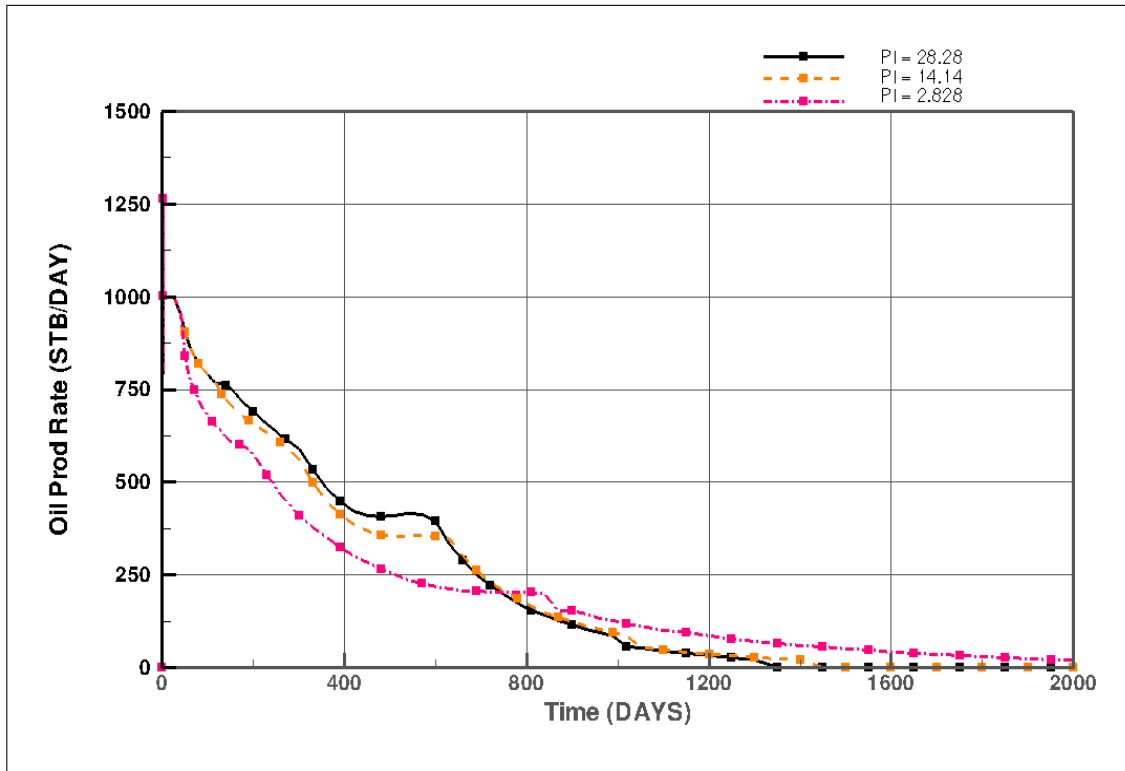


Figure 5- 17: Oil production rates for different productivity indices

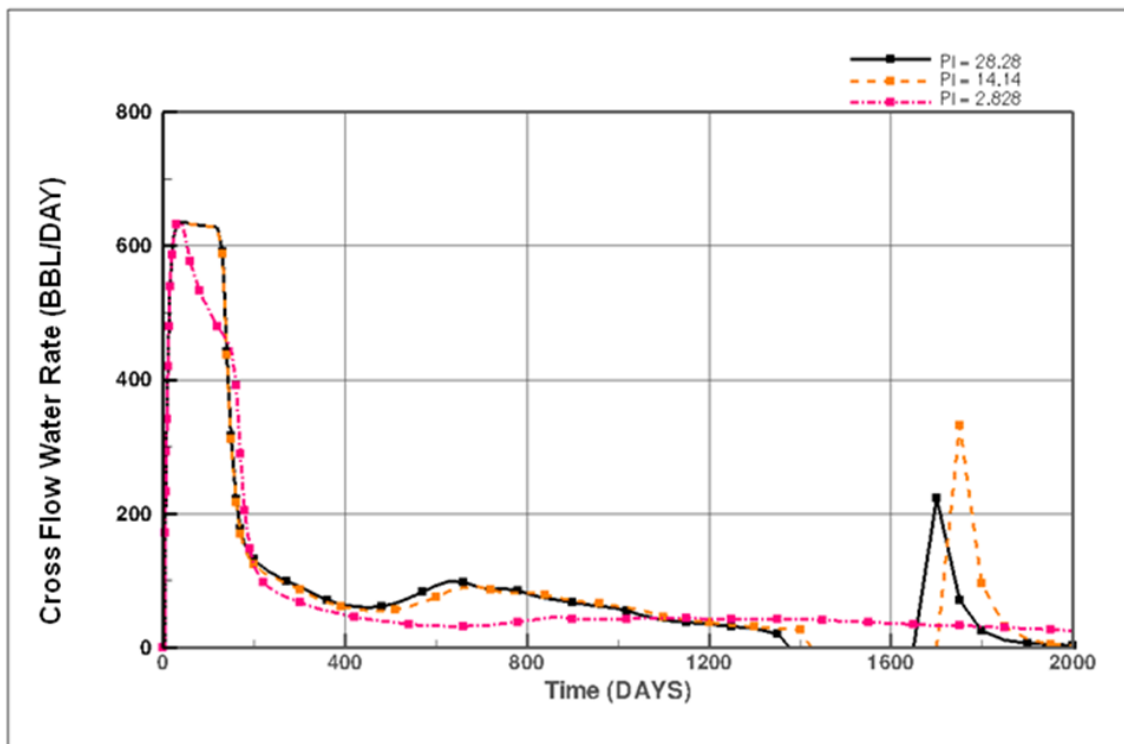


Figure 5- 18: Water cross flow rates for different productivity indices

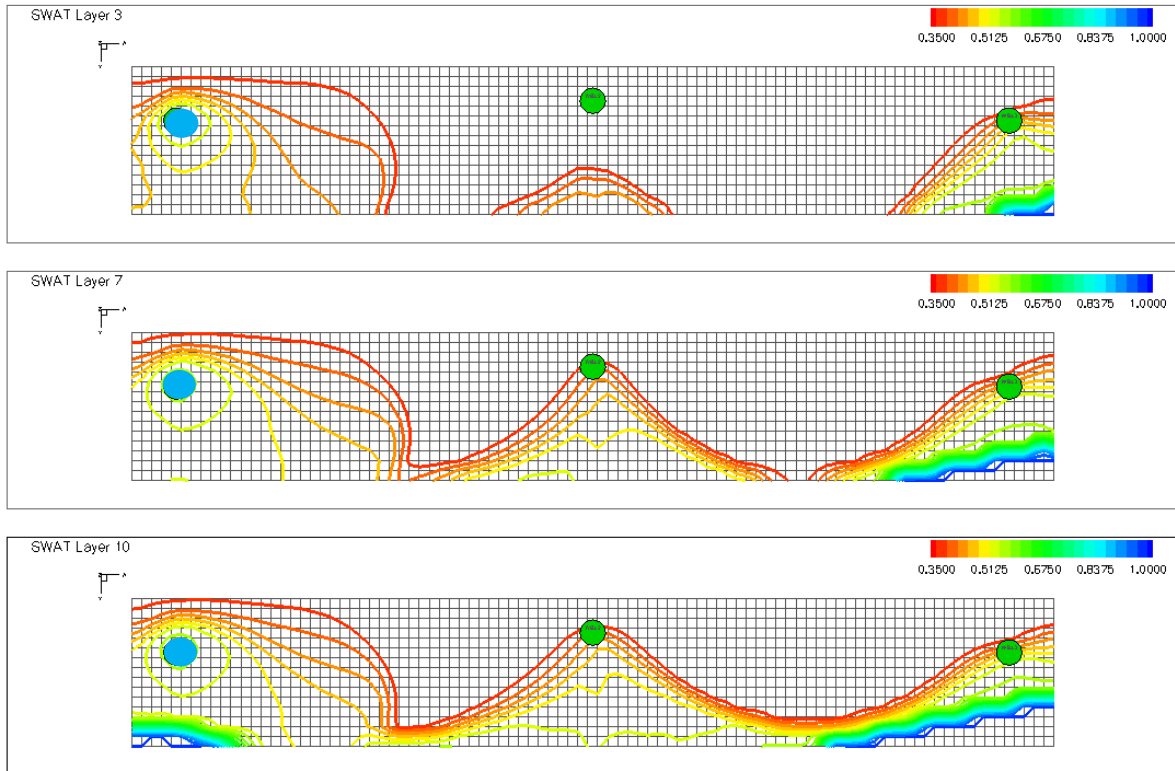


Figure 5- 19: Contour map of water saturation for dump flooding via an edge well injector for
PI of 14.14 stb/day/psi @ day 900

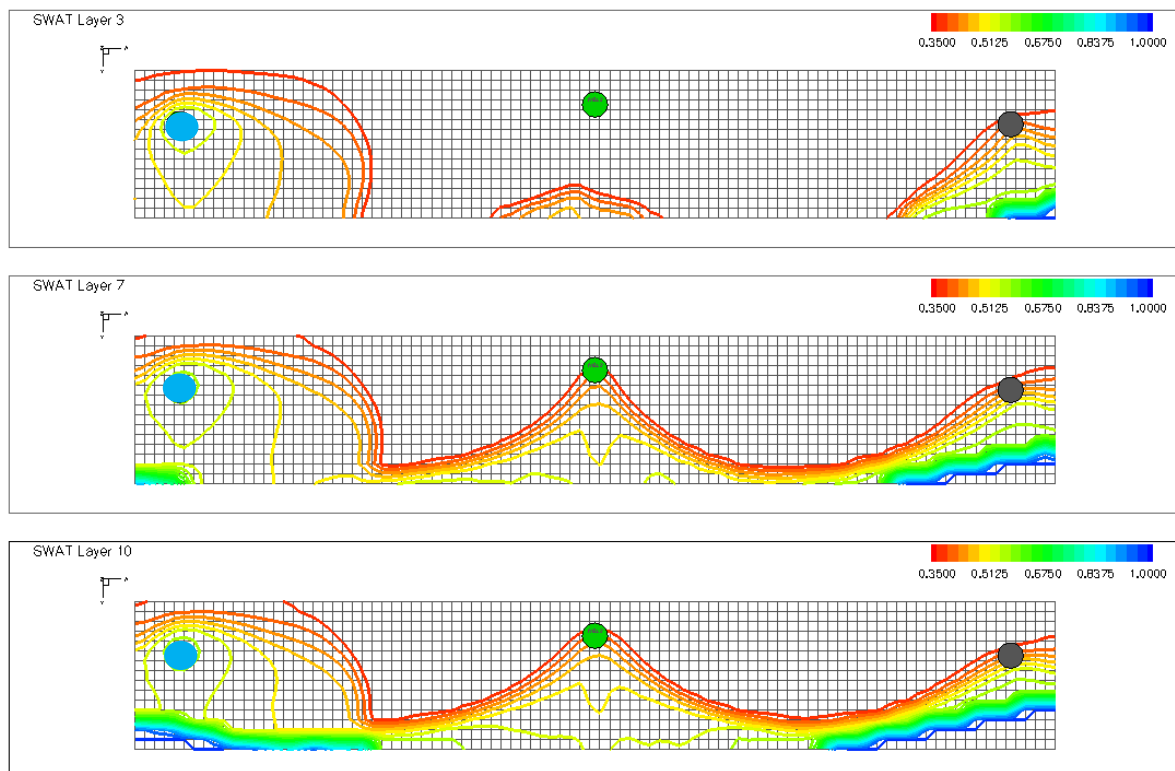


Figure 5- 20: Contour map of water saturation for dump flooding via an edge well injector for
PI of 2.828 stb/day/psi @ day 900

The summary of the recovery factors for different PI multipliers is shown in Figure 5-21 and Table 5-4. The oil recovery factor is related with PI. The higher well PI, the more oil recovery. The difference in oil recovery factor between highest and lowest case is about 2.5%. The recovery efficiency for PI of 2.828 stb/day/psi case is still higher than that for no water dump flood case.

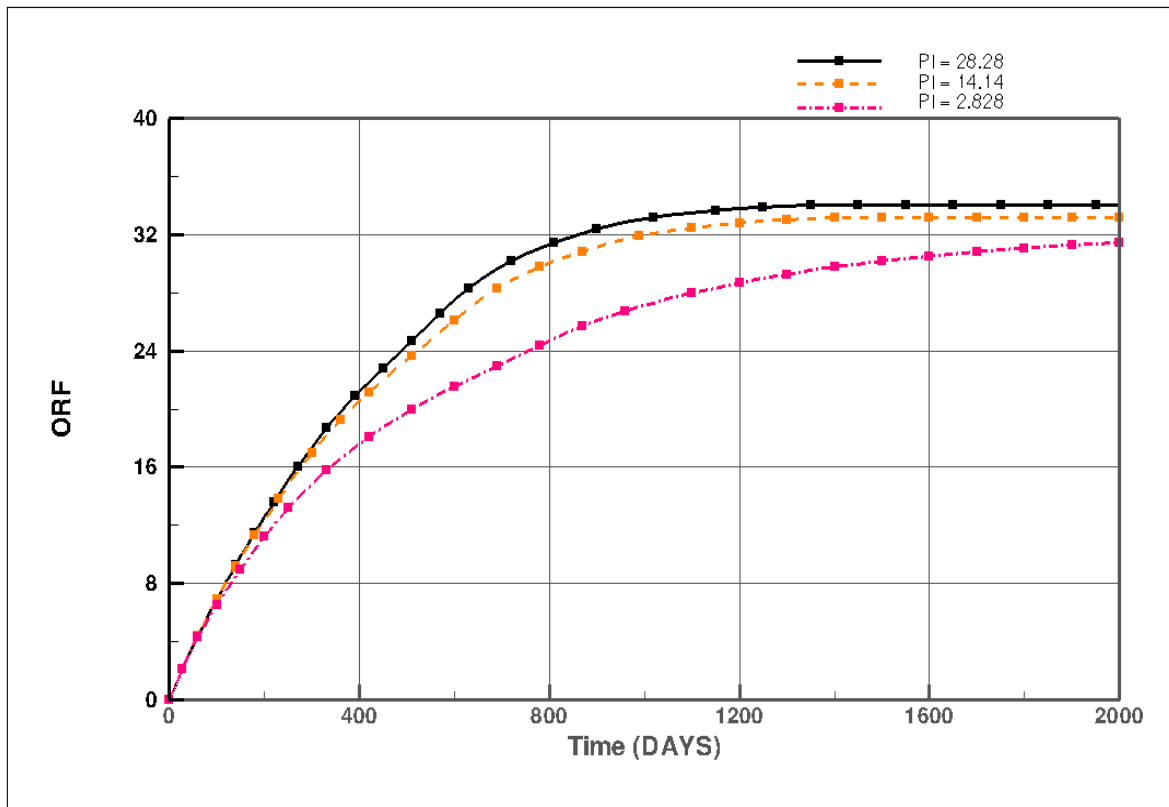


Figure 5- 21: Oil recovery factors for different productivity indices

Table 5- 4: Oil recovery factors for different productivity indices

Productivity index	PI multiplier	RF (%)
28.28	1	34.05
14.14	x 0.5	33.18
2.828	x 0.1	31.43

5.4 Effect of well injectivity index

In order to investigate the effect of injectivity index on oil recovery in water dump flood, several simulation cases were run. For injection wells, injectivity index is used in place of productivity index. Injectivity index (II) is expressed as:

$$II = \frac{Q_{inj}}{(p_{winj} - p_R)} = \frac{Q}{\Delta p} \quad (5.2)$$

The results from the simulation showing the variation of injectivity index for the five cases evaluated are shown in Figure 5-22. This figure shows the base case (where the edge well is used for dump flooding) and four other cases where the well II is decreased by a factor of 0.5, 0.1, 0.05 and 0.01. Each case has a constant II.

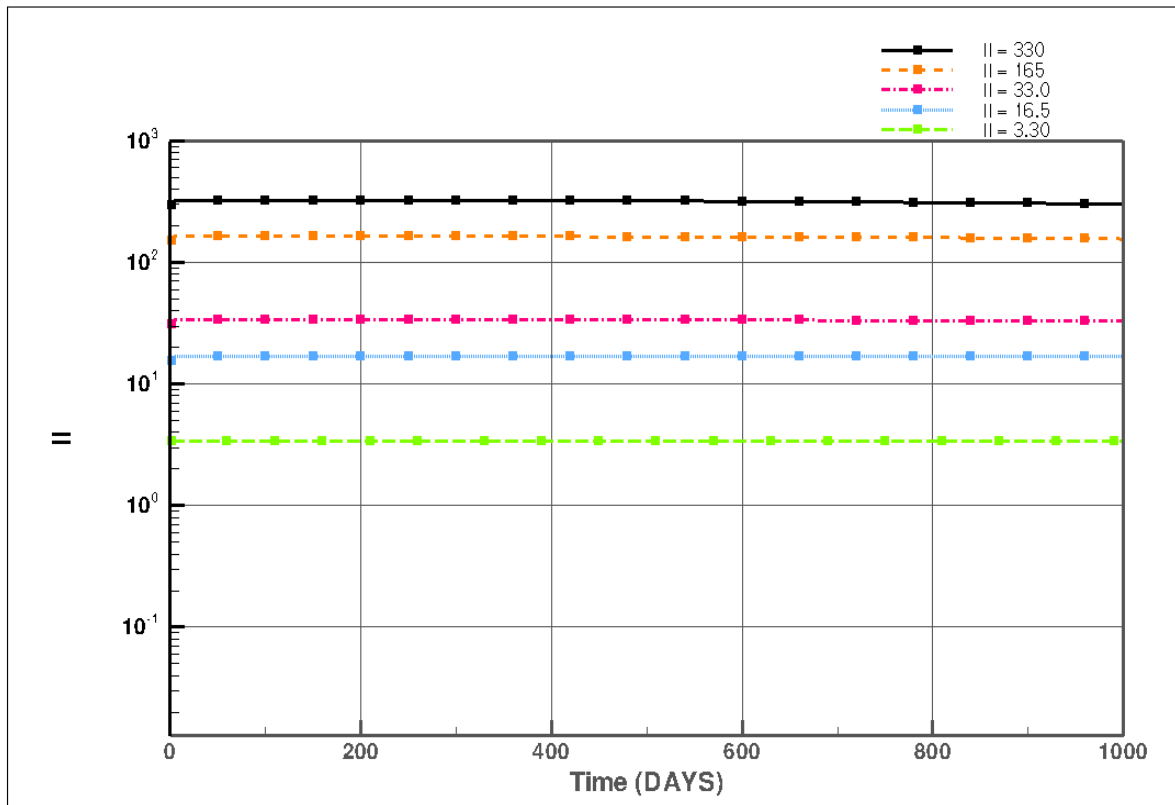


Figure 5- 22: Variation of injectivity index as a function of time

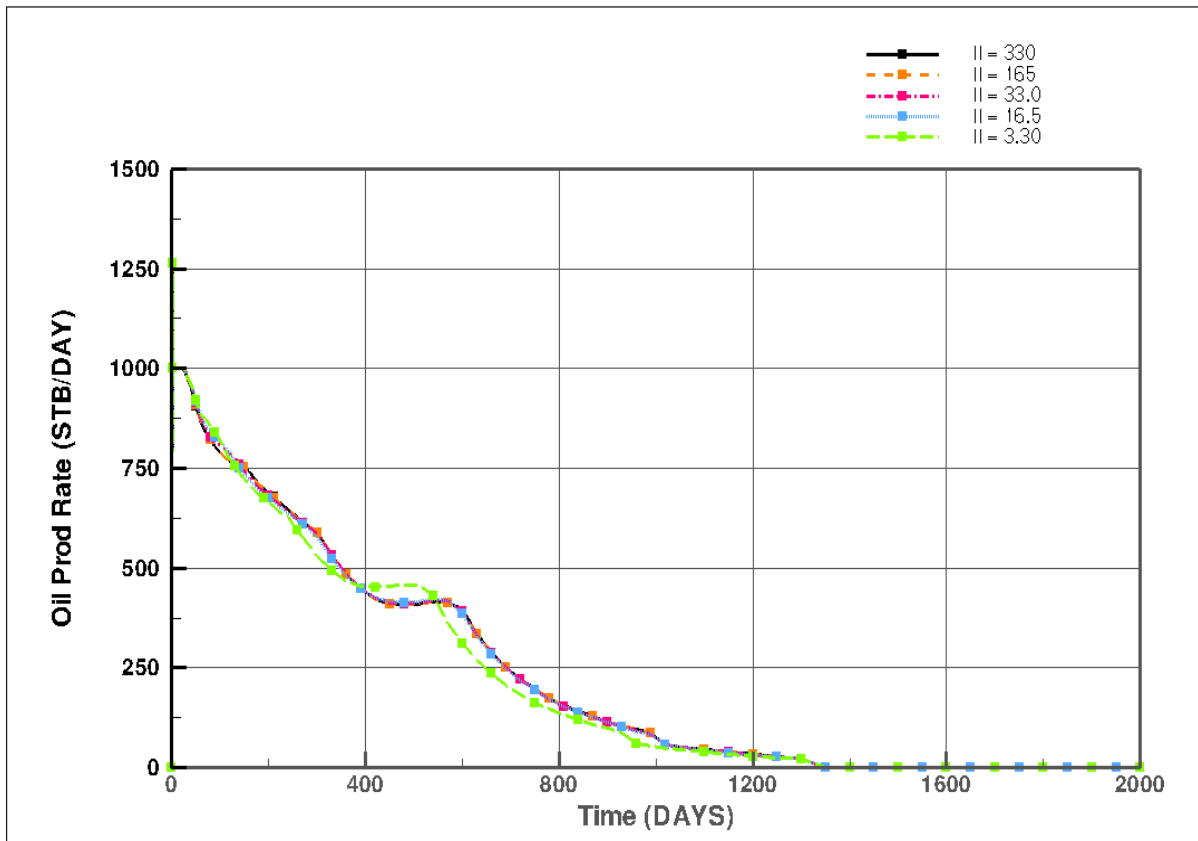


Figure 5- 23: Oil production rates for different injectivity indices

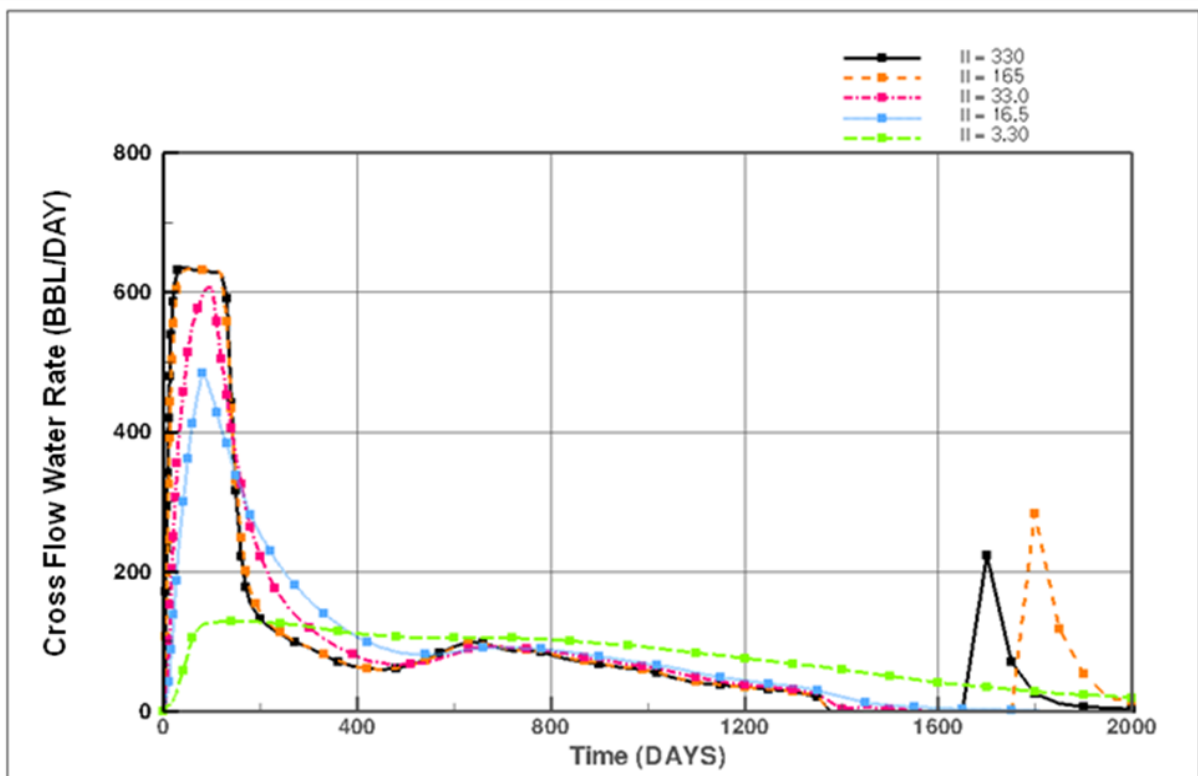


Figure 5- 24: Water cross flow rates for different injectivity indices

Figure 5-23 shows that there is about the same in oil production rate, even the water cross-flow rate is diminishing with decreasing in II as shown in Figure 5-24. But only for the case of II declined by a factor of 0.01 ($II = 3.3$), oil production performance is clearly reduced because of small water cross flow rate (about 100 bbl/day). The water saturation contour map in Figures 5-25 and 5-26 obviously illustrate the poor sweep efficiency for the case with very low II (3.3stb/day/psi). However, the simulation indicates that the water dump flood performs better than the base case in which there is no dump flood even in the case of very low II as shown Table 5-5.

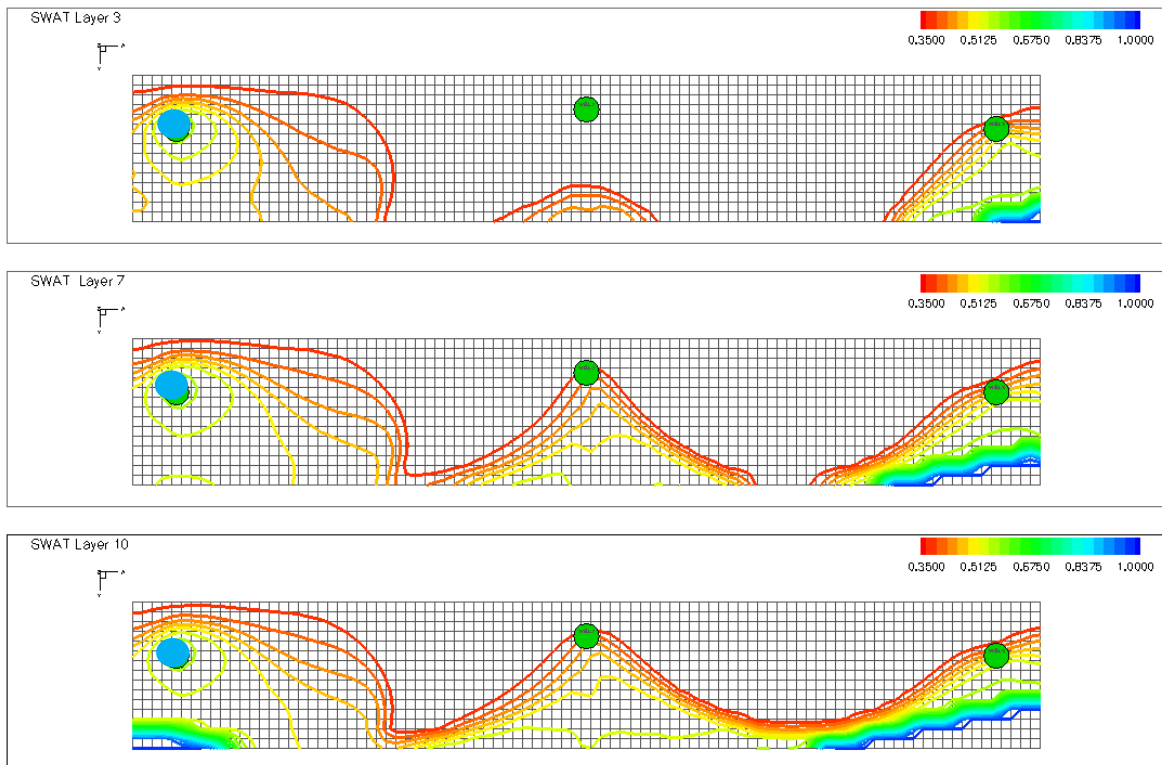


Figure 5- 25: Contour map of water saturation for dump flooding via an edge well injector for II of 33.0 stb/day/psi @ day 900

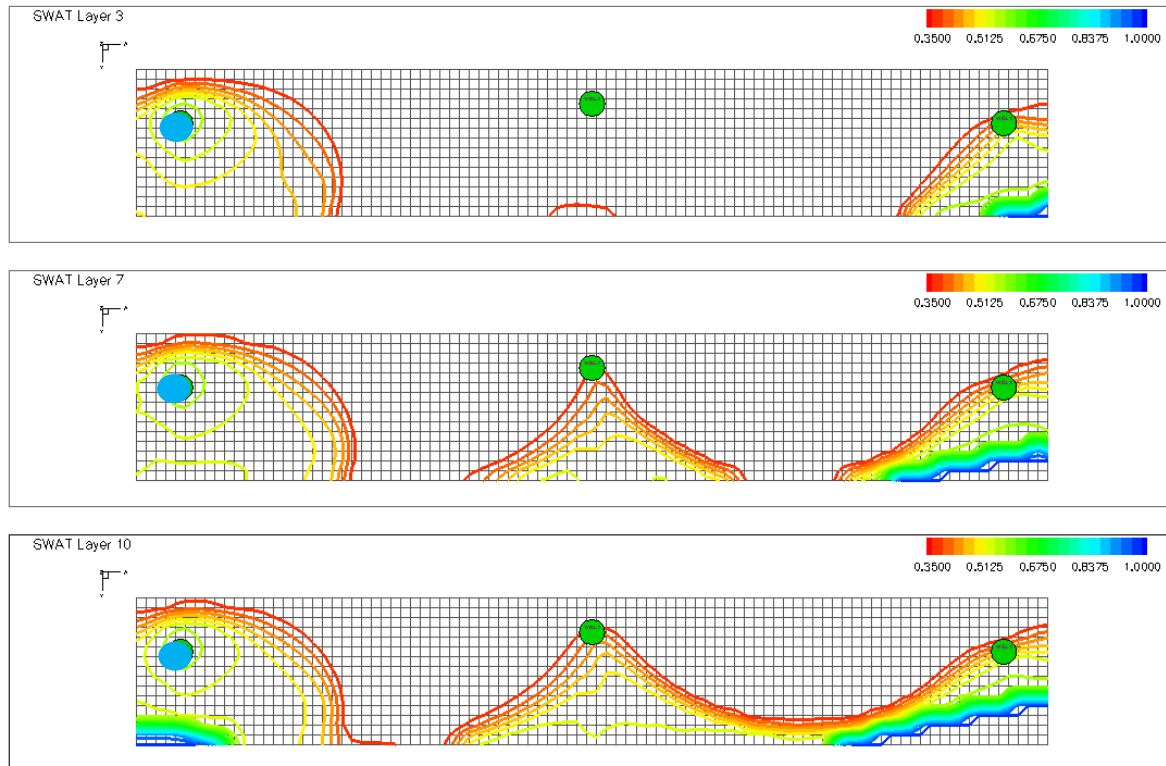


Figure 5- 26: Contour map of water saturation for dump flooding via an edge well injector for
II of 3.3 stb/day/psi @ day 900

Table 5-5 shows that the production performances for all different II cases are almost the same (about 0.1% RF). Only for the lowest II case (II = 3.3), the oil recovery factor is lower than the other cases by about 1%. For the lowest injectivity index case (II of 3.3 stb/day/psi), the oil recovery efficiency is higher than that for primary recovery.

Table 5- 5: Oil recovery factors for different injectivity indices

Injectivity index	II multiplier	RF (%)
330	1	34.05
165	x 0.5	34.04
33	x 0.1	34.04
16.5	x 0.05	33.90
3.3	x 0.01	32.58

5.5 Effect of depth-related properties

The producing interval in the field of interest typically extends from around 4000 ft TVDSS to over 9000 ft TVDSS; therefore, it is important to investigate the viability of waterflood at different depths. This study evaluated three discrete depth scenarios at 4000 (Case I), 6000 (Case II), and 8000 (Case III) ft TVDSS. The grid dimensions are the same for all depths where the first layer represents the aquifer and is 60 ft thick. The oil reservoir is 300 ft below the aquifer and is represented by layers 3 to 22, and each layer is 1.5ft thick.

Because porosity and formation volume factors are change with depth, the OOIP and WIIP also change with depth. The parameters, fluid properties and pore volumes for various depth scenarios are shown in Tables 5-6 and 5-7.

Table 5- 6: Parameters for various depth scenarios.

Layer	Parameter	Case I	Case II	Case III
1 st layer (aquifer)	Top structure (top of aquifer), ft	4000	6000	8000
	Thickness (1 st Layer), ft	60	60	60
	Porosity, fraction	0.3	0.25	0.2
	k_x and k_y , mD	1000	581	62
	k_z , mD	50	124	22
2 nd layer (shale)	Thickness (2 nd layer), ft	300	300	300
3 rd – 22 nd layer (oil reservoir)	Top structure (top of the reservoir), ft	4,360	6,360	8,360
	Reservoir pressure, psia	1800	2600	3500
	Reservoir temperature, °F	200	250	300
	Thickness (3 rd – 22 nd layer), 1.5 ft/layer	30	30	30
	Porosity, fraction	0.28	0.23	0.18
	k_x and k_y , mD	800	252	21
	k_z , mD	0.5	66	10

Table 5- 7: Fluid properties and pore volumes for various scenarios

Parameter	Case I	Case II	Case III
Gas specific gravity	0.85 (air =1)		
Water salinity, ppm	2000		
CO ₂ , N ₂ , H ₂ S content	0%		
P _b , R _s & B _o correlation	Glaso		
Oil viscosity correlation	Petrosky et al.		
Oil gravity, °API	35	40	45
Solution gas-oil ratio, scf/STB	200	400	600
Bubble pressure, psia	1017	1340	1780
Rock compressibility, (psi ⁻¹)	10.0E-06	6.0E-06	3.0E-06
Water formation volume factor, RB/STB	1.0412	1.0608	1.0808
Oil formation volume factor, RB/STB	1.1785	1.3295	1.5481
Oil viscosity, cp	1.0635	0.6279	0.4361
Water viscosity, cp	0.3013	0.23	0.1857
Mobility ratio	1.7673	1.365	1.1741
Aquifer pore volume, RBBL	9.9848E+6	8.3258E+6	6.6668E+6
Reservoir pore volume, RBBL	4.6664E+6	3.8335E+6	3.0005E+6
OOIP, STB	1.3113E+6	1.0226E+6	0.74349E+6

5.5.1 Reservoir depth of 6000 ft TVDSS (Case II)

The viability of water dump flood was evaluated at a depth of 6000 ft by identifying the best location for an injector. A series of simulation runs were done and compared against the base case (three wells producing under solution gas drive mechanism). Two injector locations were investigated as follows: 1) an edge well (case W1), and 2) a center well (case W2). The third possible location (case W3) is symmetric with case W1 and was therefore excluded.

Figure 5-27 shows that the oil production rate for the base case (black line) declined rapidly compared to the water dump flood cases (orange and pink lines) since water drive mechanism of water dump flood cases is stronger than solution gas drive mechanism. Similar results are observed in the case of 4,000 ft.

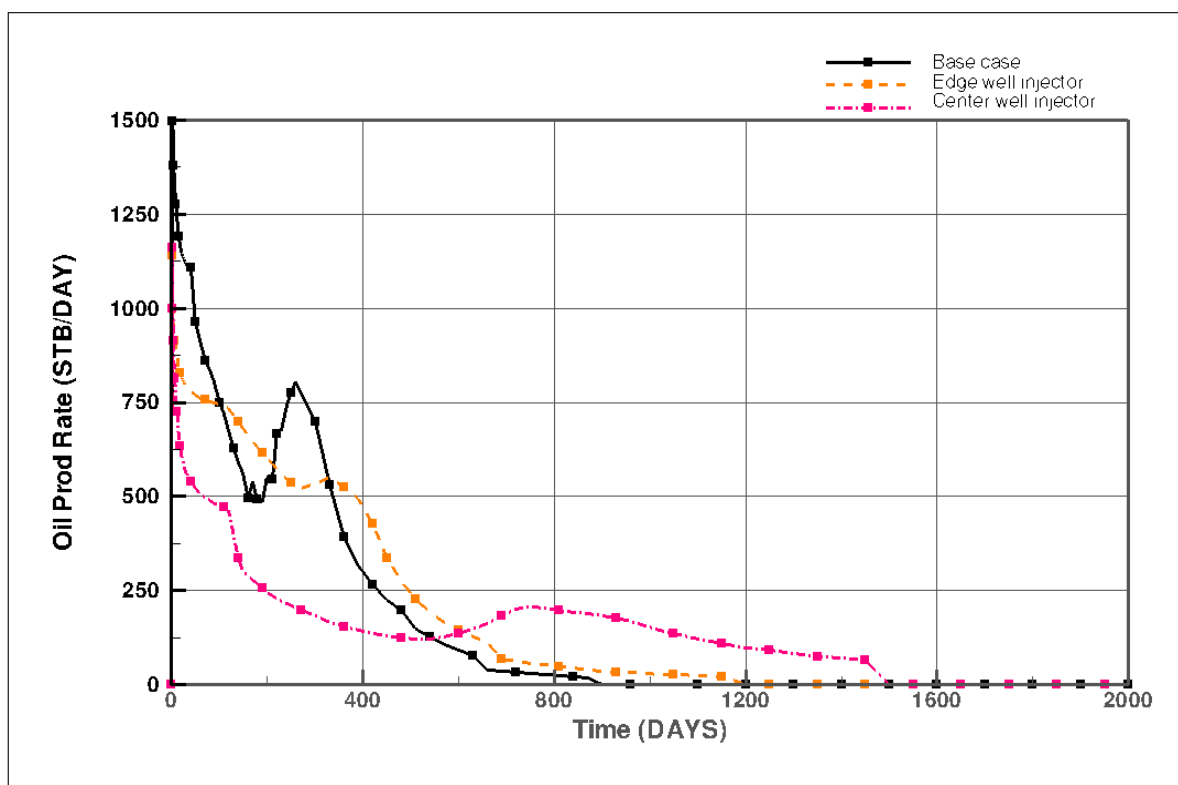


Figure 5- 27: Oil production rates of water dump flood at depth of 6000 ft for different injector locations

In Figures 5-28 to 5-30, the water saturation contour maps show water saturation at day 900 for different injector locations. The edge well injector case shows the highest sweep efficiency. The summary of oil recover efficiency is shown in Table 5-8.

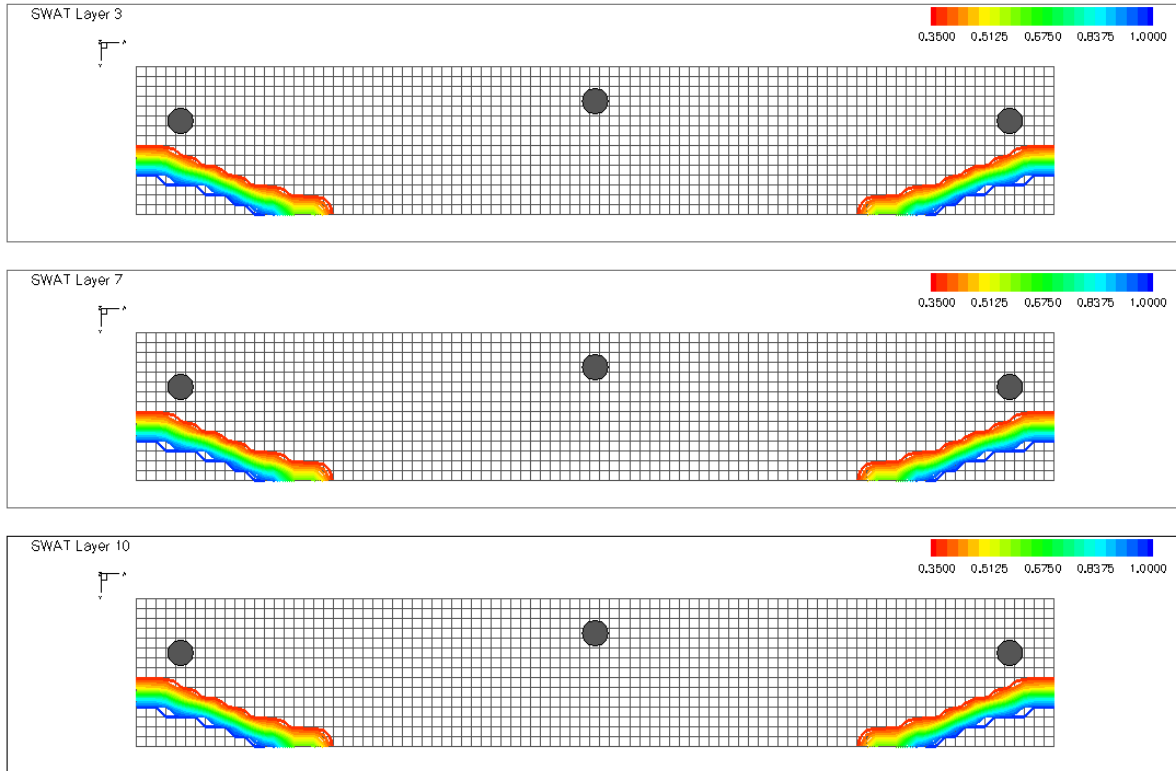


Figure 5- 28: Contour map of water saturation at depth of 6000 ft for base case @ day 900

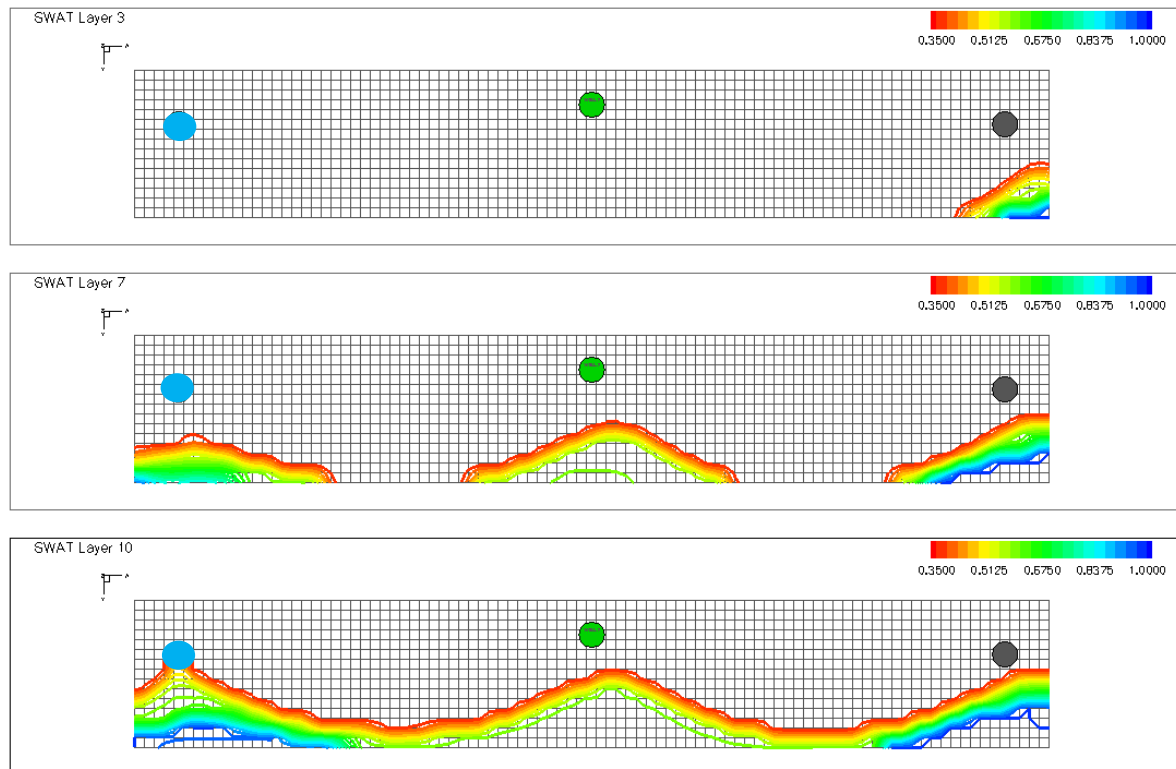


Figure 5- 29: Contour map of water saturation of water dump flood at depth of 6000 ft for edge well injector @ day 900

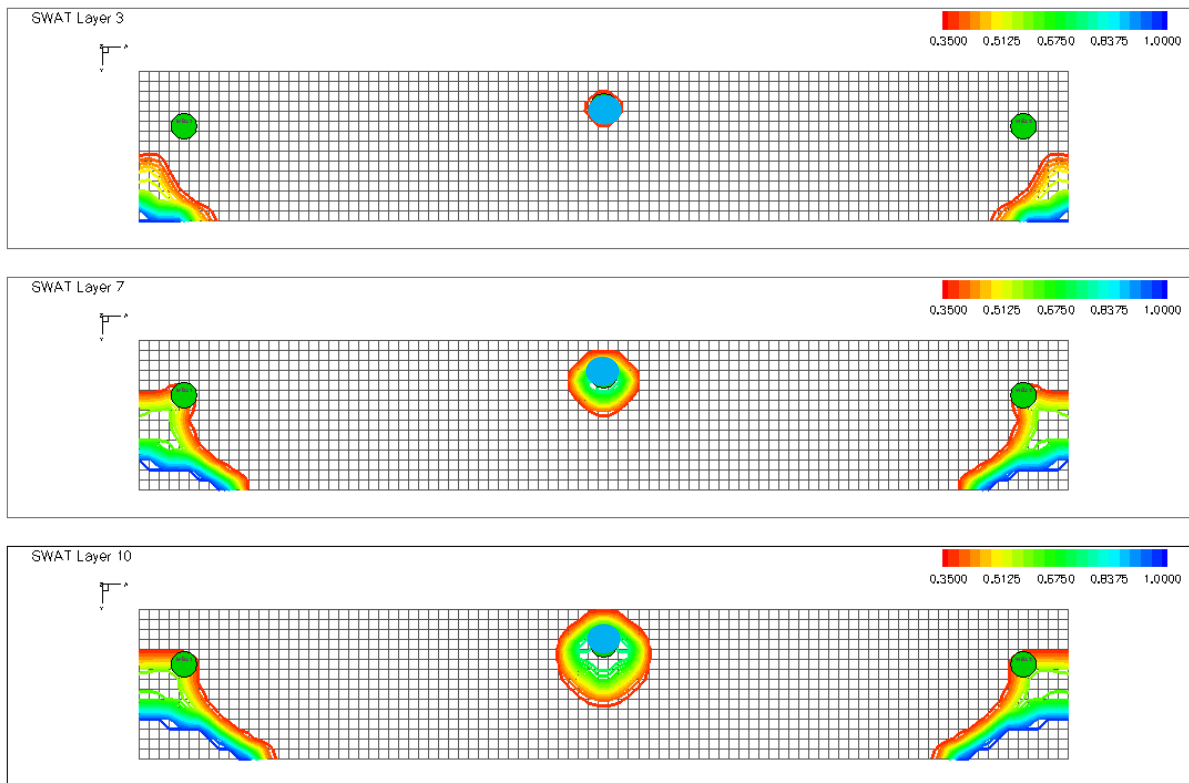


Figure 5- 30: Contour map of water saturation of water dump flood at depth of 6000 ft for center well injector @ day 900

Based on the summary of oil recovery efficiency as shown in Table 5-8, edge well is the best location of dump flood at depth of 6000 ft. While edge well as an injector increases recovery ($\Delta RF = +2\%$) relative to the primary depletion case, the center well injector decreases recovery ($\Delta RF = -4\%$) relative to the primary depletion case.

Table 5- 8: Oil Recovery factors of water dump flood at depth of 6000 ft for different injector locations

Case	RF (%)
Base case	30.64
Edge well injector	32.73
Center well injector	26.43

5.5.2 Reservoir depth of 8000 ft TVDSS (Case III)

The deepest case of water dump flood is at a depth of 8000 ft. The simulations were run to evaluate the viability of water dump flood by identifying the best location for an injector. A series of simulation runs were done and compared against the base case (three wells producing under solution gas drive mechanism). Two injector locations were investigated as follows: 1) an edge well (case W1), and 2) a center well (case W2). The third possible location (case W3) is symmetric with case W1 and was therefore excluded.

Figure 5-31 shows that the oil production rate for all cases has a very steep slope due to the low permeability at this depth. Dump flood at this depth and this low permeability is detrimental because losing one producer cannot be compensated by the swept areas in a reservoir with such low permeability.

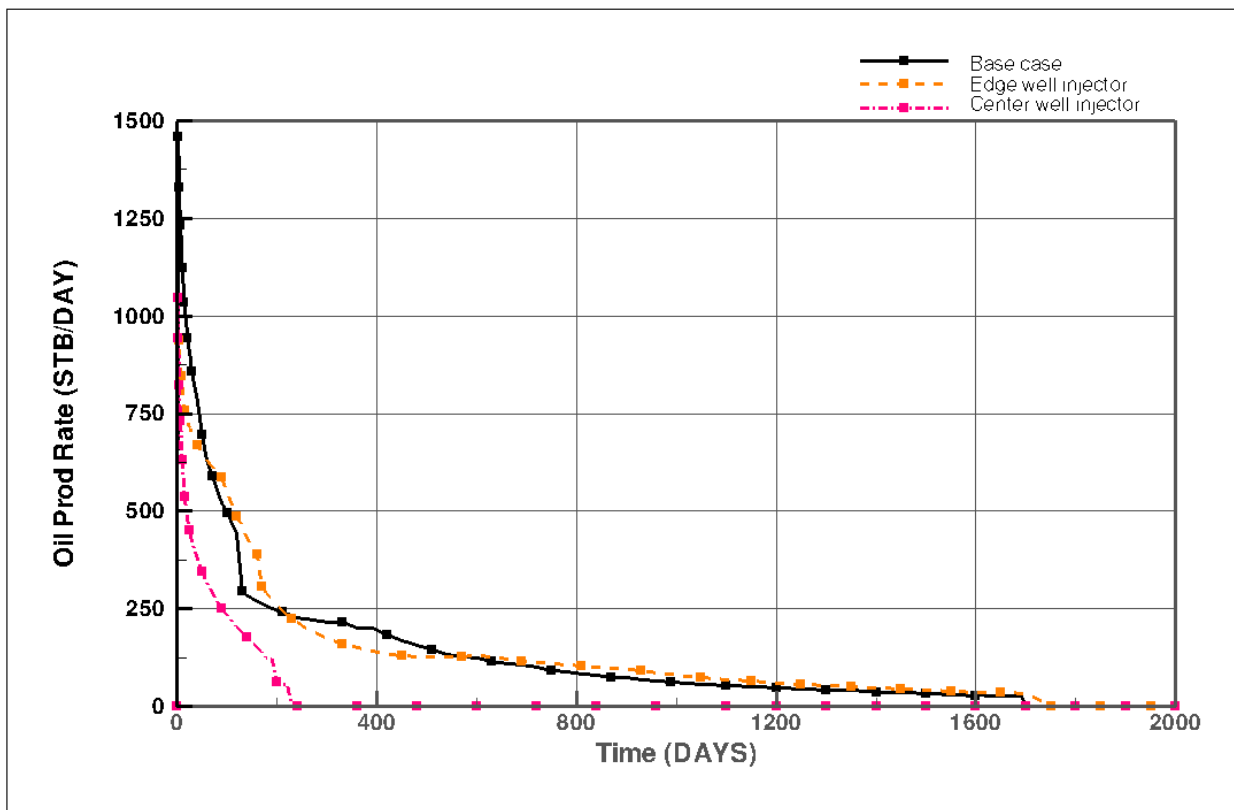


Figure 5- 31: Oil production rates of water dump flood at depth of 8000 ft for different injector locations

As depicted in contour map of water saturation in Figure 5-32 to 5-34, the water saturation shows that the water sweep in edge well injector case gives the highest sweep efficiency and the best performance from an oil recovery perspective. The results are shown in Table 5-9.

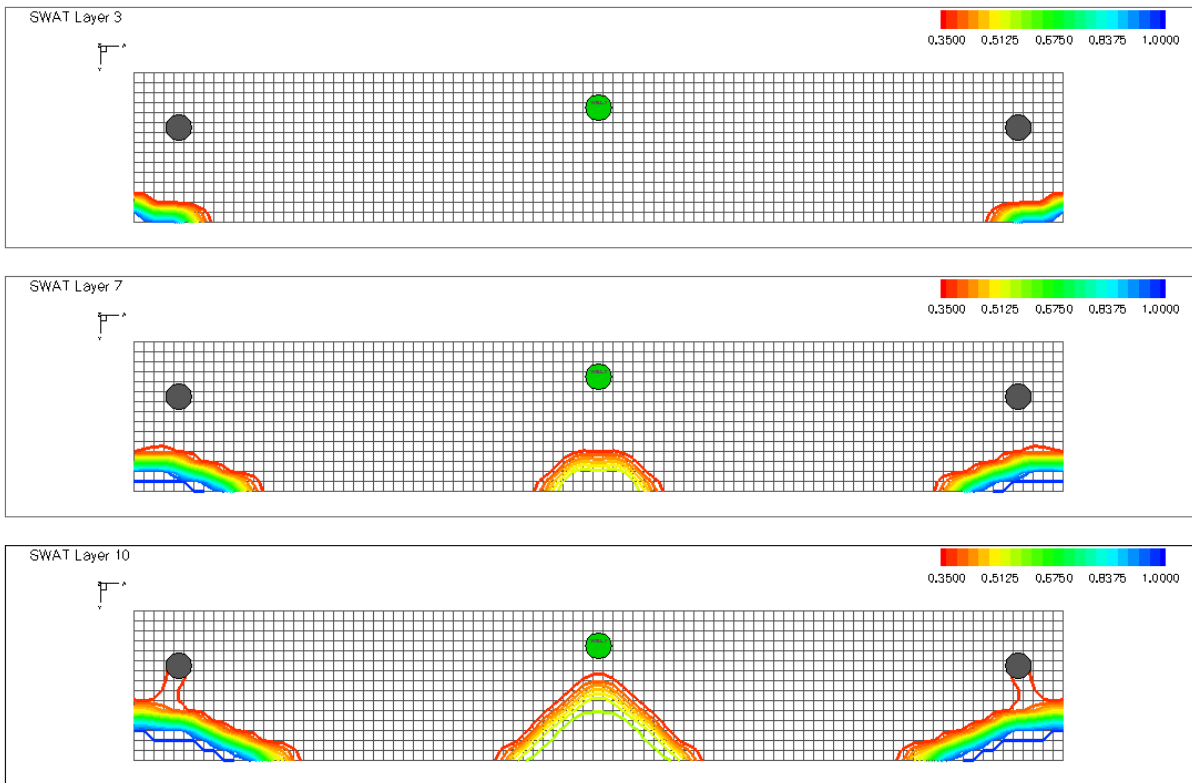


Figure 5- 32: Contour map of water saturation at depth of 8000 ft for base case @ day 900

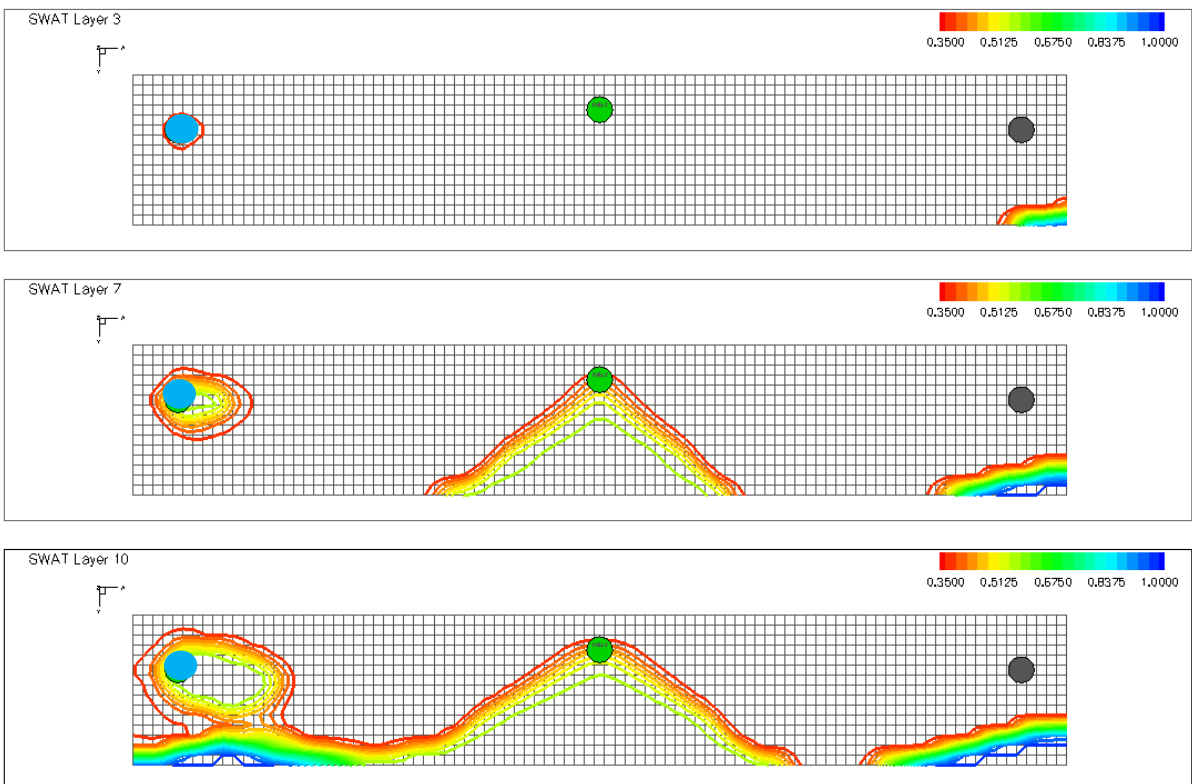


Figure 5- 33: Contour map of water saturation of water dump flood at depth of 8000 ft for edge well injector @ day 900

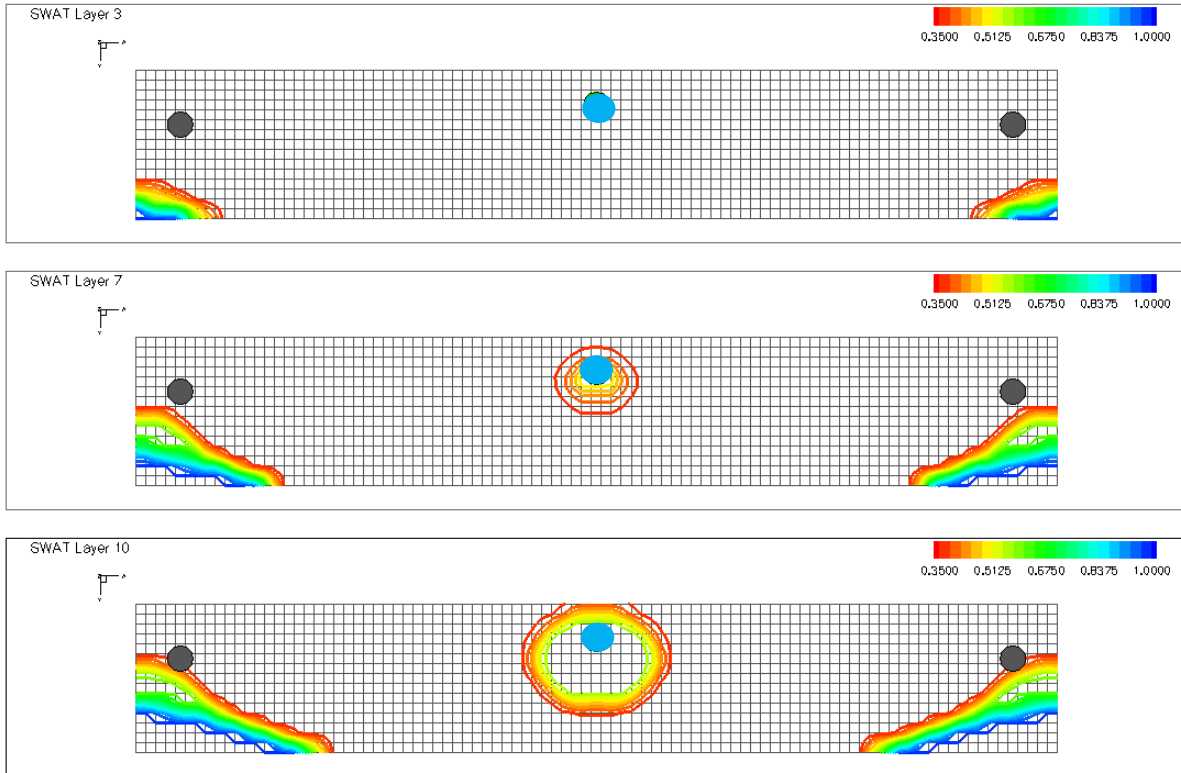


Figure 5- 34: Contour map of water saturation of water dump flood at depth of 8000 ft for center well injector @ day 900

The summary of oil recovery efficiency as shown in Table 5-9 shows that edge well is the best location of dump flood at depth of 8000 ft. The edge well as an injector increases recovery ($\Delta\text{RF}=+1\%$) relative to the primary depletion case while the center well injector decreases recovery ($\Delta\text{RF}=-25\%$) relative to the primary depletion case.

Table 5- 9: Oil recovery factors of water dump flood at depth of 8000 ft for different injector locations

Case	RF (%)
Base case	32.13
Edge well injector	33.02
Center well injector	7.55

5.5.3 Comparison of water dump flood performance at different reservoir depths

In order to determine the impact of water dump flood at different depths (4000 ft, 6000 ft, and 8000 ft TVDSS), the results of all depth scenarios (base case, edge well injector and center well injector) and comparative plot of oil recovery factor are presented in Table 5-10 and Figure 5-35, respectively.

All depth scenarios have the same trend that the highest oil recovery occurs in the center well injector case, and the lowest oil recovery occurs in the center well injector case.

However, the recovery efficiency of water dump flood in the base case, edge well injector case, and center well injector case does not decrease with depths due to the fact that there are more than one factors varied at greater depths, which caused the different trends with depth for different situations.

Table 5- 10: Oil recovery factors of water dump flood at different depths

Depth	RF (%)		
	Base case	Edge well injector	Center well injector
4000	30.95	34.05	25.57
6000	30.02	33.15	26.73
8000	33.62	35.32	13.08

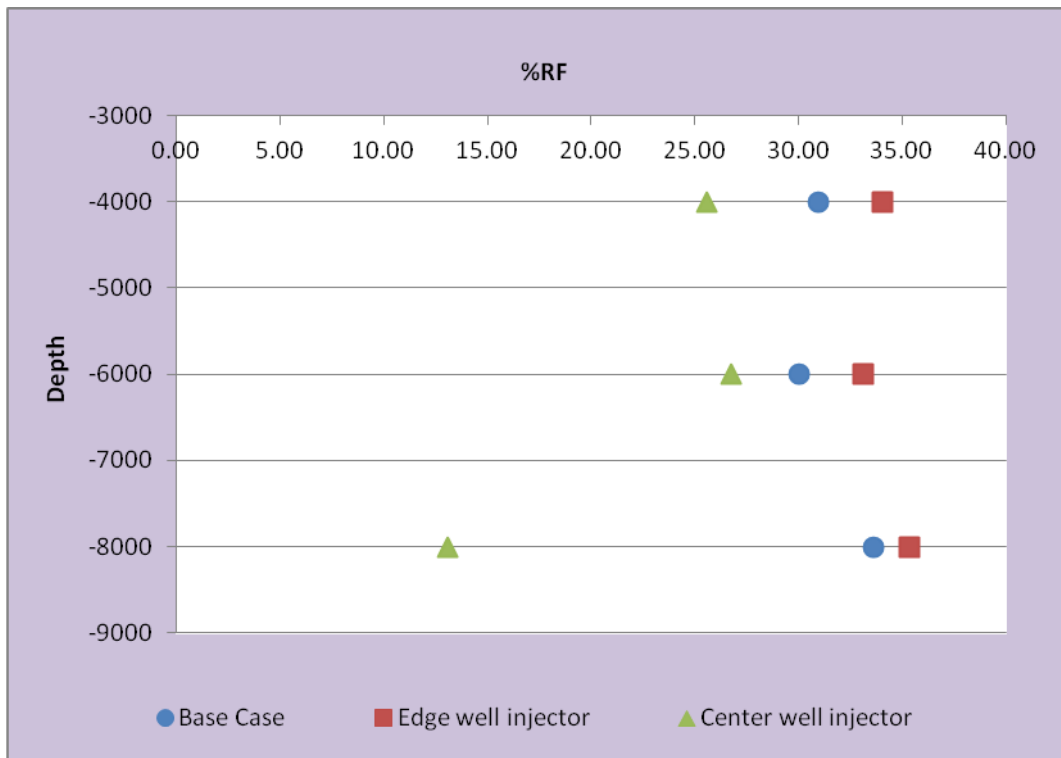


Figure 5- 35: Oil recovery factors for reservoir at depth of 4000, 6000 and 8000 ft

5.6 Viability of water dump flood of underlying aquifer

Water source for water dump flood can be obtained from either overlaying or underlying aquifer as long as the pressure of the aquifer is higher than the reservoir pressure. This section of the study evaluates the viability of using an underlying aquifer as the source of water for the dump flood. A series of simulation runs were done and compared against the base case (three wells producing under solution gas drive mechanism). Two injector locations were investigated as follows: 1) an edge well (case W1), and 2) a center well (case W2). The third possible location (case W3) is symmetric with case W1 and was therefore excluded. This numerical experiments were conducted at a reservoir depth of 4000 ft TVDSS. The top of oil reservoir layer is located at a depth of 4,000 ft with an initial pressure of 1,650 psia and top of aquifer layer is located at depth of 4,330 with 1,800 psia at initial condition. The structural model and reservoir properties are shown in Figure 5-36.

The LGR uses a refinement of three coarse cells along well 1 to well 3. Each coarse cell is subdivided into nine cells (3x3). The coarse cells are 100ftx100ft while the LGR cells are 33ftx33ft.

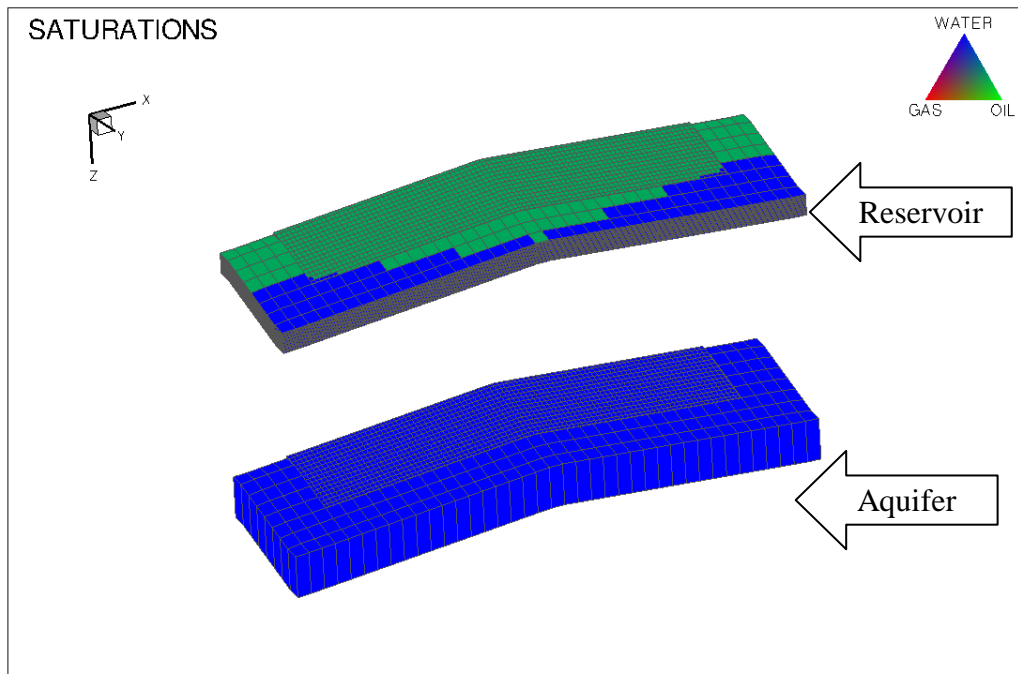


Figure 5- 36: Structural model of underlying aquifer

Rock properties of the oil reservoir and aquifer for the base case are shown in Table 5-11. The reservoir property of oil reservoir is 30%, reservoir temperature is 200°F, and reservoir pressure is about 1650 psia.

Table 5- 11: Variable parameter values for underlying aquifer model

Layer	Parameter	Value
1 st – 20 th layer (oil reservoir)	Top structure (top of the reservoir), ft	4,360
	Reservoir pressure, psia	1800
	Reservoir temperature, °F	200
	Thickness (1 st – 20 th layer), 1.5 ft/layer	30
	Porosity, fraction	0.28
	k_x and k_y , mD	800
	k_z , mD	0.05
21 st layer (shale)	Thickness (21 st layer), ft	300
22 nd layer (aquifer)	Top structure (top of aquifer), ft	4,690
	Thickness (22 nd Layer), ft	60
	Porosity, fraction	0.26
	k_x and k_y , mD	600
	k_z , mD	0.03

Reservoir fluid properties are shown in Table 5-12. The solution gas-oil ratio, water formation volume factor and oil formation volume factor are the properties that perform under initial reservoir pressure condition.

Table 5- 12: Fluid properties and pore volumes for various scenarios

Parameter	Value
Oil gravity, °API	35
Gas specific gravity	0.85 (air =1)
Water salinity, ppm	2000
CO ₂ , N ₂ , H ₂ S content	0%
P _b , R _s & B _o correlation	Glaso
Oil viscosity correlation	Petrosky et al.
Solution gas-oil ratio, scf/STB	200
Bubble pressure, psia	1017
Rock compressibility, (psi ⁻¹)	10.0E-06
Water formation volume factor, RB/STB	1.3503
Oil formation volume factor, RB/STB	1.0773
Oil viscosity, cp	1.0638
Water viscosity, cp	0.3013
Mobility ratio	1.7654
Aquifer pore volume, RBBL	8.6786E+6
Reservoir pore volume, RBBL	4.6664E+6
OOIP, STB	1.3182E+6

5.6.1 Performance of water dump flood from underlying aquifer

This part demonstrates impact of location of the aquifer for water dump flood. Figure 5-37 shows that the production periods of water dump flood cases (orange and pink lines) are longer than that for the base case (black line). Moreover, the center well injector shows the longest production period. The result of water displacement at day 900 is shown in Figure 5-38 to Figure 5-40. The swept areas of the edge well injector case are larger than those for the center injector case. Therefore, the center injector case needed more time to displace the unswept zone. Even, the recovery factor is lowest for center well injector case as shown in Table 5-13.

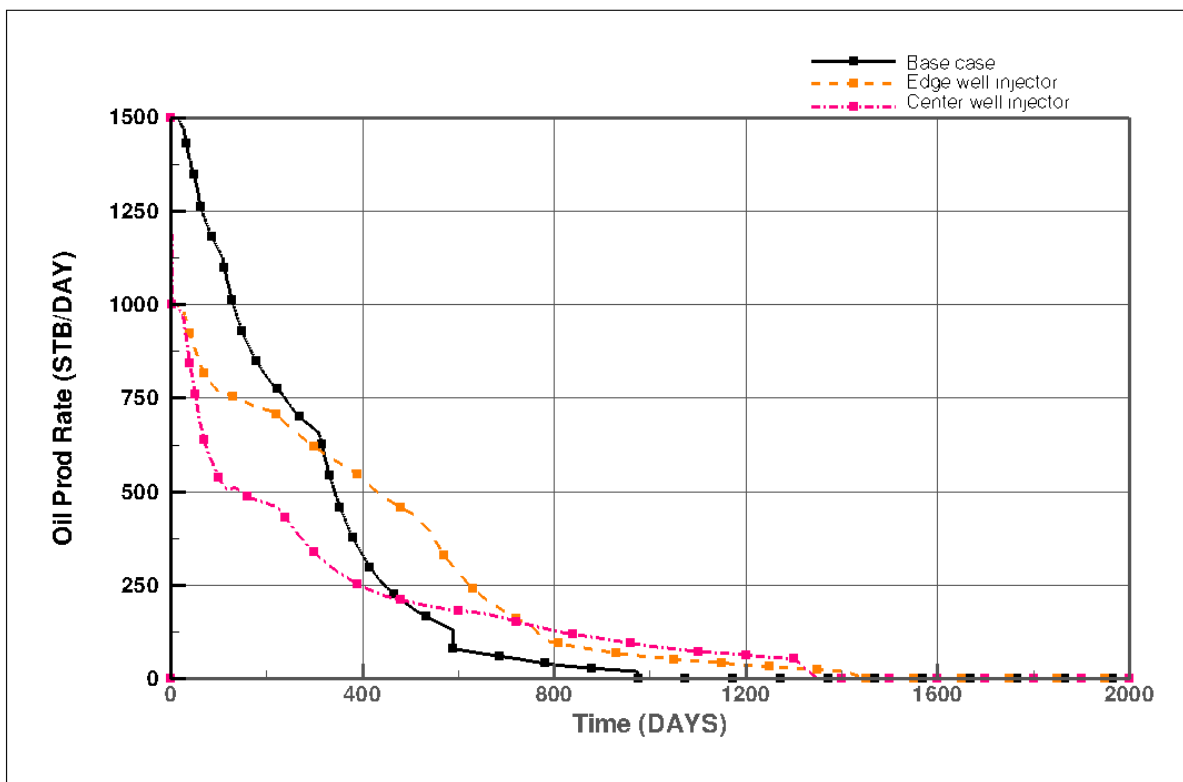


Figure 5- 37: Oil production rates of an underlying aquifer for different injector locations

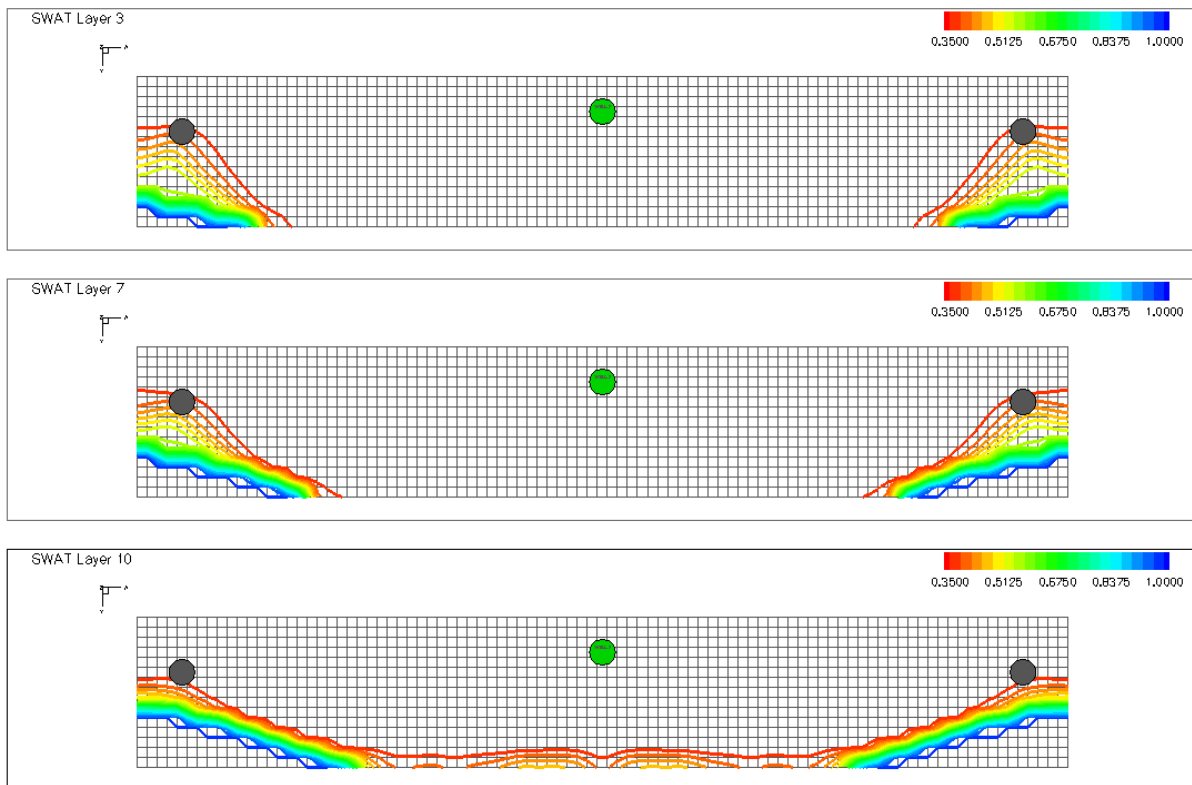


Figure 5- 38: Contour map of underlying aquifer for base case @ day 900

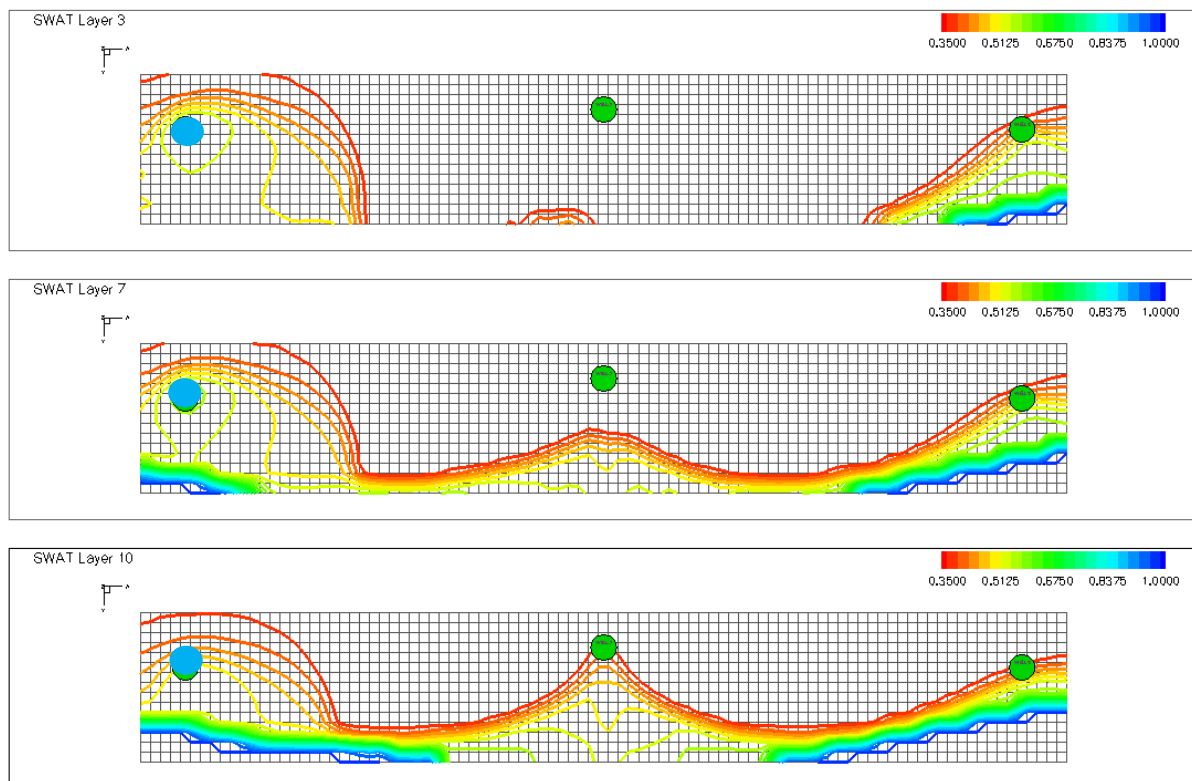


Figure 5- 39: Contour map of water saturation of underlying aquifer dump flooding via an edge well injector @ day 900

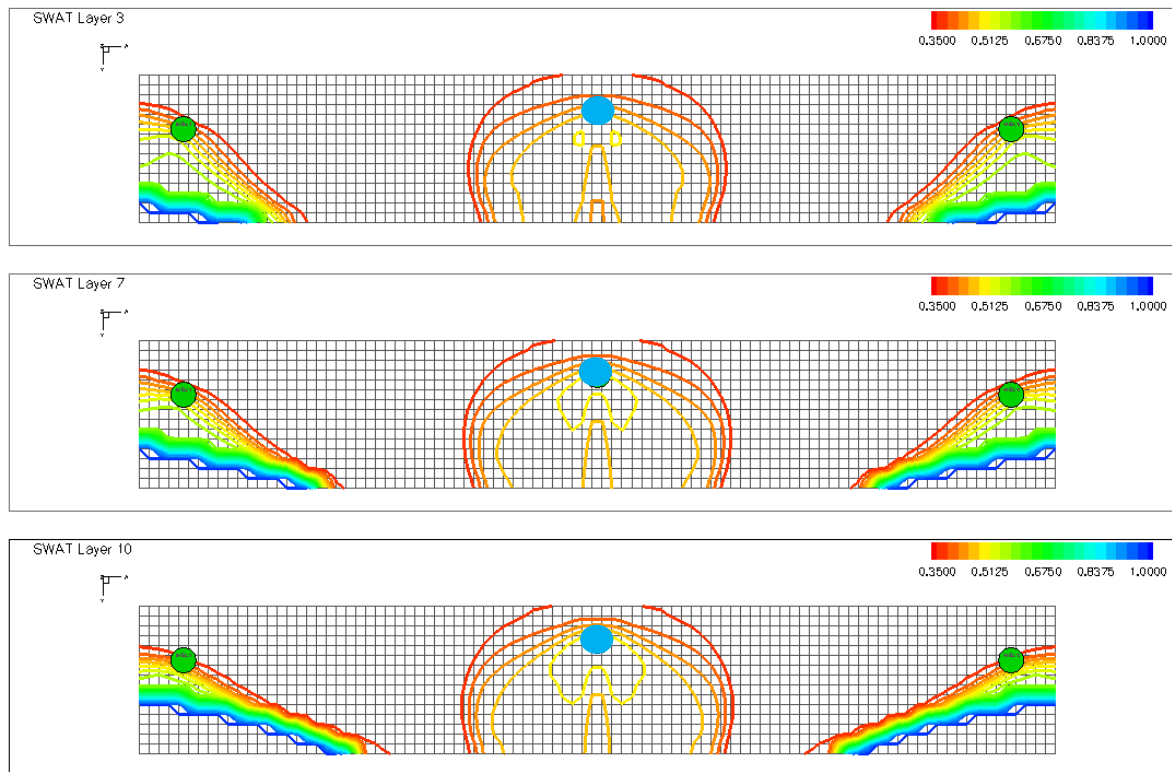


Figure 5- 40: Contour map of water saturation of underlying aquifer dump flooding via a center well injector @ day 900

The summary of oil recovery efficiency in Table 5-13 shows that impact of injector location of underlying aquifer dump flood cases is the same as in previous studies, i.e., edge well injector is the best location for water dump flooding. The edge well as an injector increases recovery ($\Delta\text{RF}=+1\%$) relative to the primary depletion case while the center well injector decreases recovery ($\Delta\text{RF}=-12\%$) relative to the primary depletion case.

Table 5- 13: Oil recovery factors of an underlying aquifer for different injector locations

Case	RF (%)
Base case	30.79
Edge well injector	33.25
Center well injector	23.73

5.6.2 Performance comparison of water dump flood from an overlaying and underlying aquifers via an edge well injector

This section compares the performance of overlaying and underlying aquifer dump flooding through edge well injector. As shown in Figure 5-41 and Figure 5-42, the oil production performances for the two cases are slightly different because the overlaying aquifer provides somewhat similar water cross flow rates compared to the underlying aquifer. The recovery factor of two cases is 2% different. However, the overlaying aquifer still yields higher recovery factor. This is due to the reason that the hydrostatic force of overlaying aquifer causes the water cross-flow rates to be higher compared to the cross-flow rates from underlying aquifer.

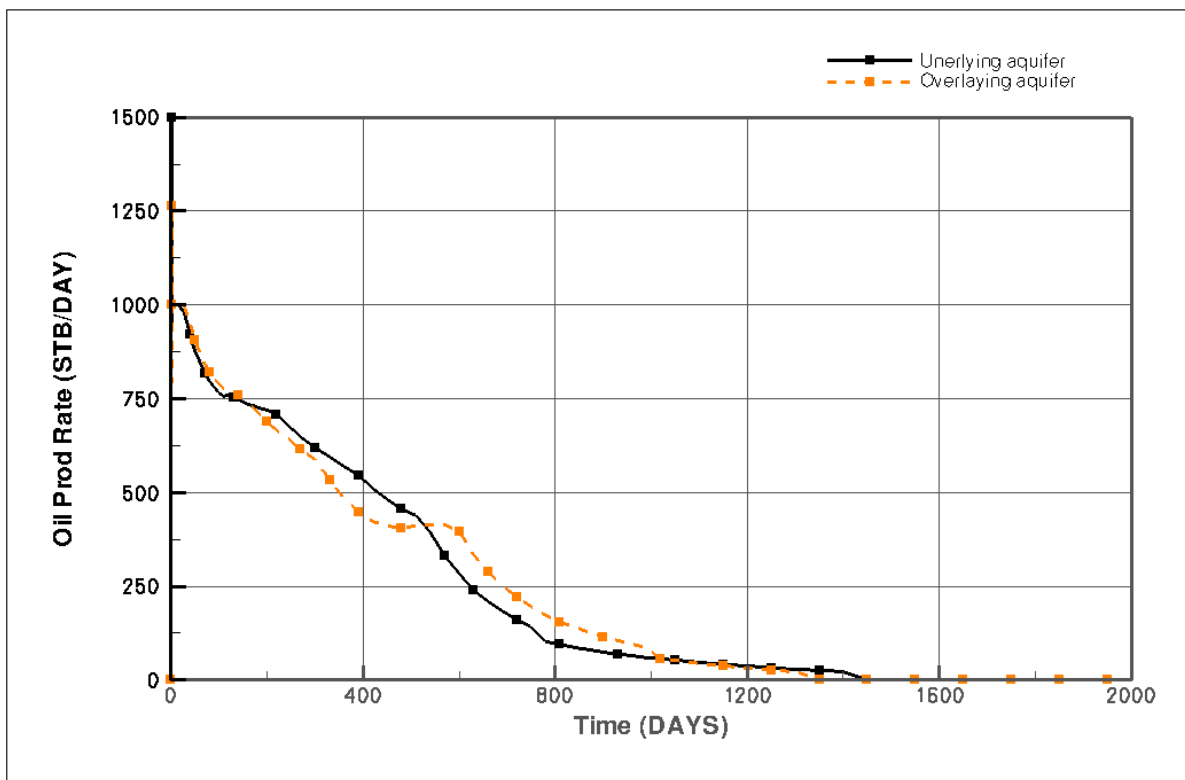


Figure 5- 41: Oil production rates for an overlaying and underlying aquifer dump flooding via an edge well injector

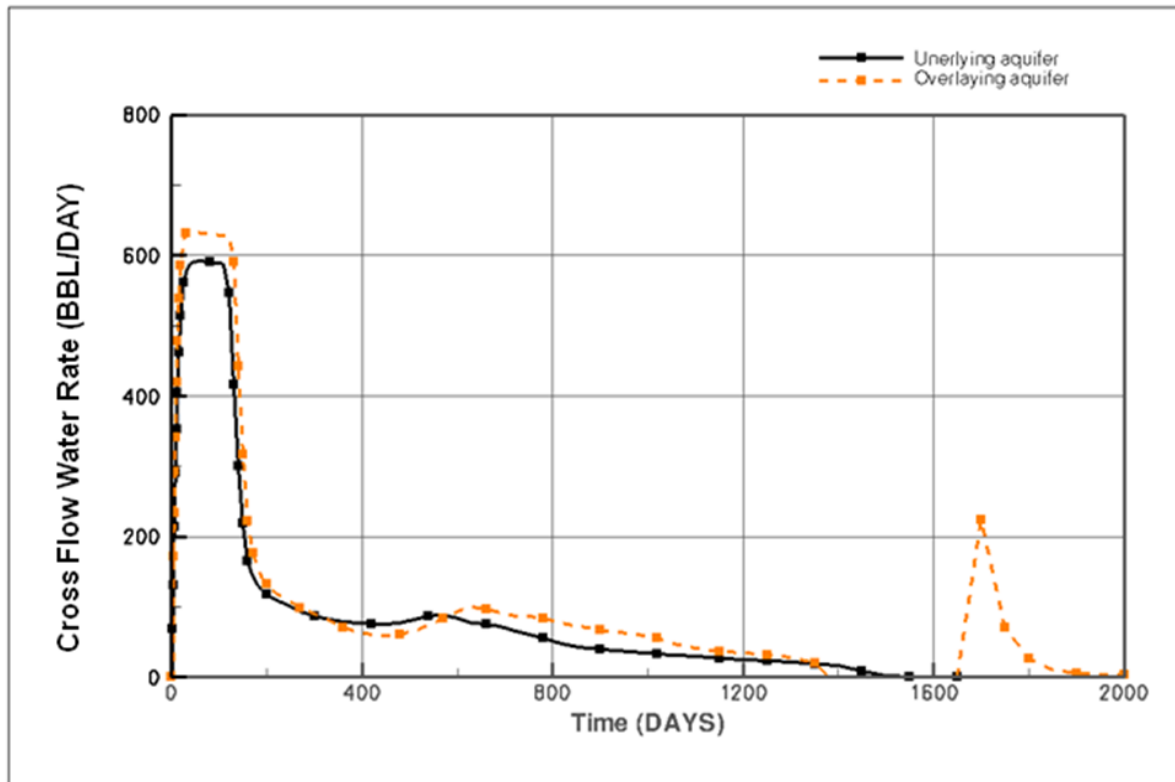


Figure 5- 42: Water production rates for an overlaying and underlying aquifer dump flooding via an edge well injector (water cross flow into reservoir)

Table 5- 14: Oil recovery factors for an overlaying and underlying aquifer dump flooding via an edge well injector

Aquifer position	RF (%)
Underlying aquifer	33.25
Overlaying aquifer	34.05

5.7 Impact of API gravity

This section compares water dump flood performance when the oil API gravity varies. A series of simulation runs were done and compared against the base case (three wells producing under solution gas drive mechanism). Two injector locations were investigated as follows: 1) an edge well (case W1), and 2) a center well (case W2). The third possible location (case W3) is symmetric with case W1 and was therefore excluded. This numerical experiments were conducted at a reservoir depth of 4000 ft TVDSS with 30, 35 and 40 °API gravity. The properties of various °API cases are shown in Table 5-15.

Table 5- 15: Fluid properties and pore volumes for various °API scenarios @ 4000 ft

Parameter	°API		
	30	35	40
Water viscosity, cp	0.3013	0.3013	0.3013
Oil viscosity, cp	1.3864	1.0635	0.8298
Mobility ratio	2.3007	1.7648	1.3770
Aquifer pore volume, RBBL	9.9847E+6	9.9847E+6	9.9847E+6
Reservoir pore volume, RBBL	4.6663E+6	4.6663E+6	4.6663E+6
OOIP, STB	1.3242E+6	1.3113E+6	1.3111E+6

As shown in Figure 5-43, the oil production performance of all °API gravity decreases with time until the pressure drops below the bubble point pressure. At this point, the oil production increases briefly due to increased GOR. The swept areas for various °API scenarios are all the same as shown in Figure 5-44.

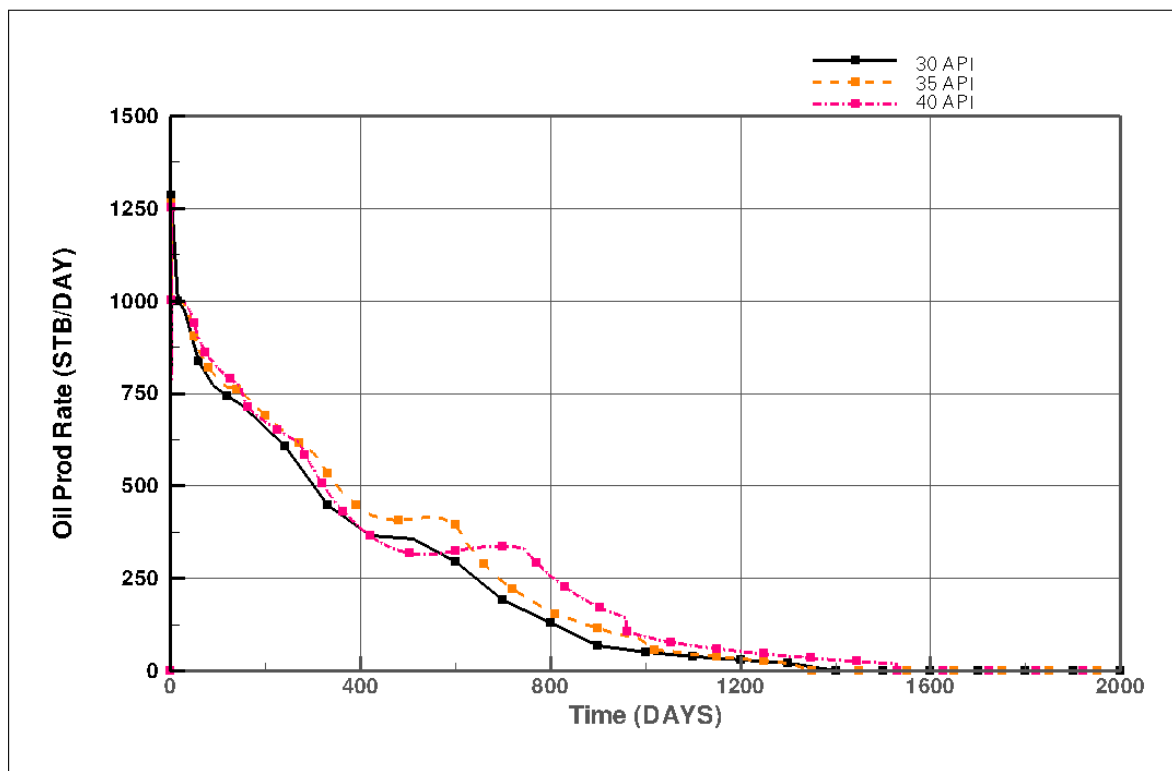


Figure 5- 43: Oil production rates of water dump flood via an edge well injector for oil with different API gravities

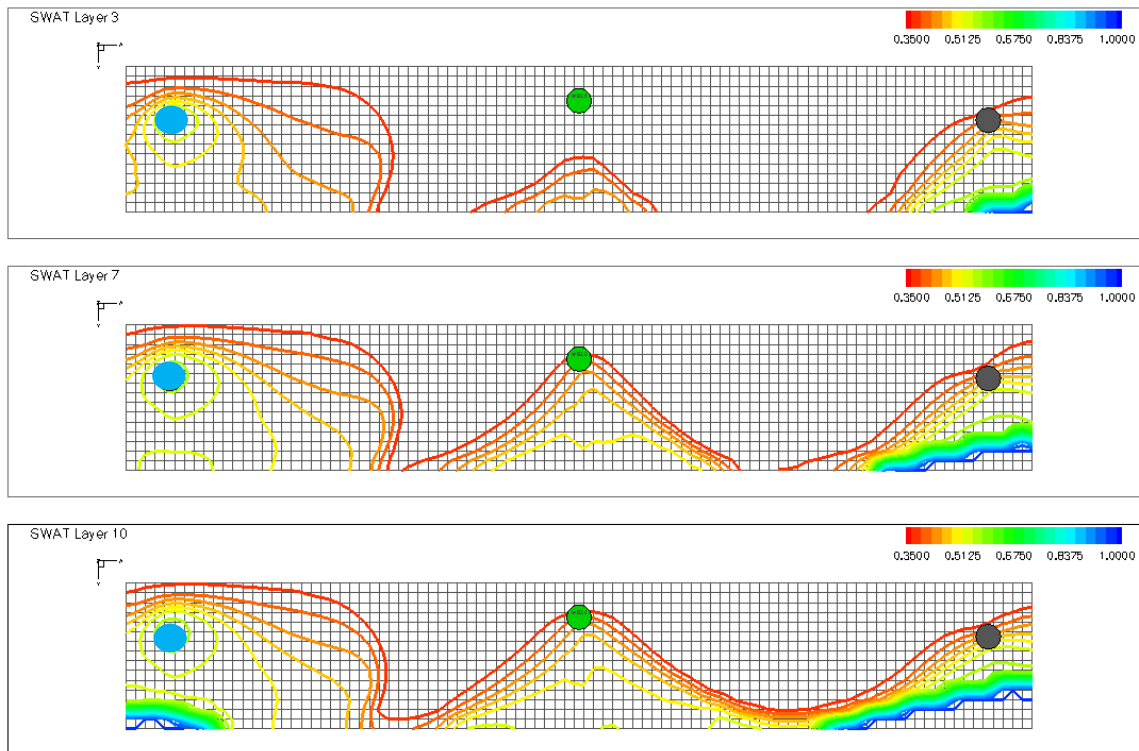


Figure 5- 44: Contour map of water saturation for water dump flood via an edge well injector for 30 °API oil

For various °API scenarios at depth of 4000 ft, the results of all °API gravity scenarios (base case, edge well injector and center well injector) and comparative plot of oil recovery factor are presented in Table 5-16 and Figure 5-45., respectively.

All °API scenarios have the same trend that the highest oil recovery occurs in the center well injector case, and the lowest oil recovery occurs in the center well injector case. the recovery efficiency of water dump flood in the base case, edge well injector case, and center well injector case increases with higher °API gravity.

Table 5- 16: Oil recovery factors of water dump flood with different API gravities

Specific gravity (°API)	RF (%)		
	Base Case	Edge well injector	Center well injector
30	25.80	29.94	21.36
35	30.95	34.05	25.57
40	33.54	35.52	28.62

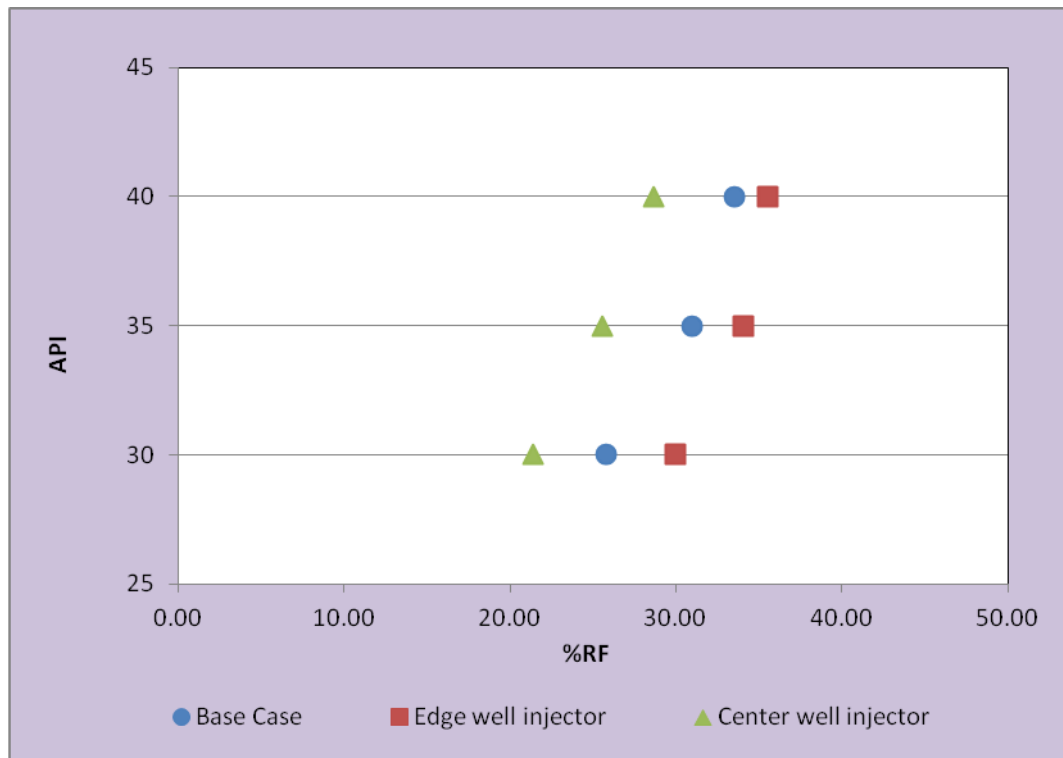


Figure 5- 45: Oil recovery factors of water dump flood with different API gravities

5.8 Effect of time to start water dump flood

A series of simulation runs were done to simulate the optimal time to initiate water dump flood via an edge well injector. Day 1, 15, 30, 60, 90, 120, 150, 240, 330, 420, 510 and 600 were chosen for the study. This numerical experiments were conducted at a reservoir depth of 4000 ft TVDSS.

The contour maps of water saturation in Figures 5-45 and 5-46 show that the water sweeping trend when water dump flood is started at day 15 and 240 are about the same as depicted by a large area swept by water dump flood (on the left) and a smaller area swept by aquifer encroachment (on the right). But the water sweeping trend of the case when water dump flood is started at day 600 is obviously different as shown in Figure 5-47. The reason of water sweeping trend when water dump flood is started at day 600 differ from others is that the reservoir pressure is down below bubble point pressure. At this point, the secondary gas cap is presented in the reservoir.

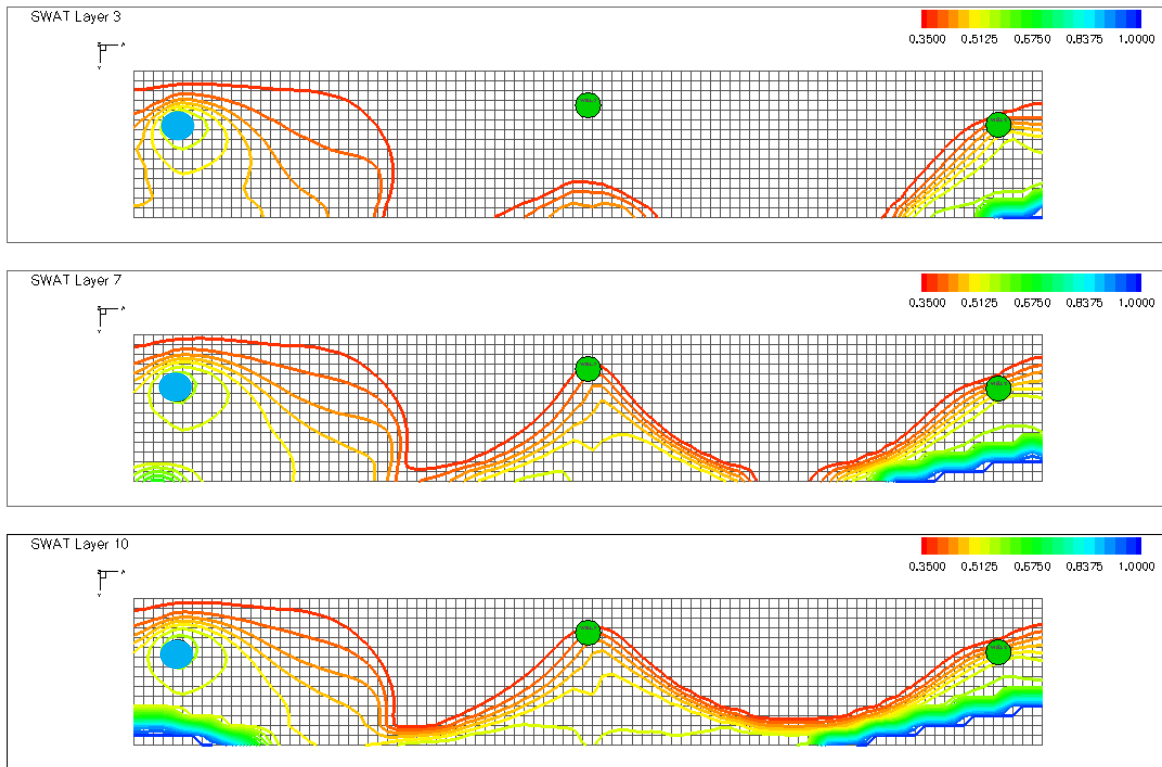


Figure 5- 46: Contour map of water saturation for water dump flood via an edge well injector at day 15 @ day 900

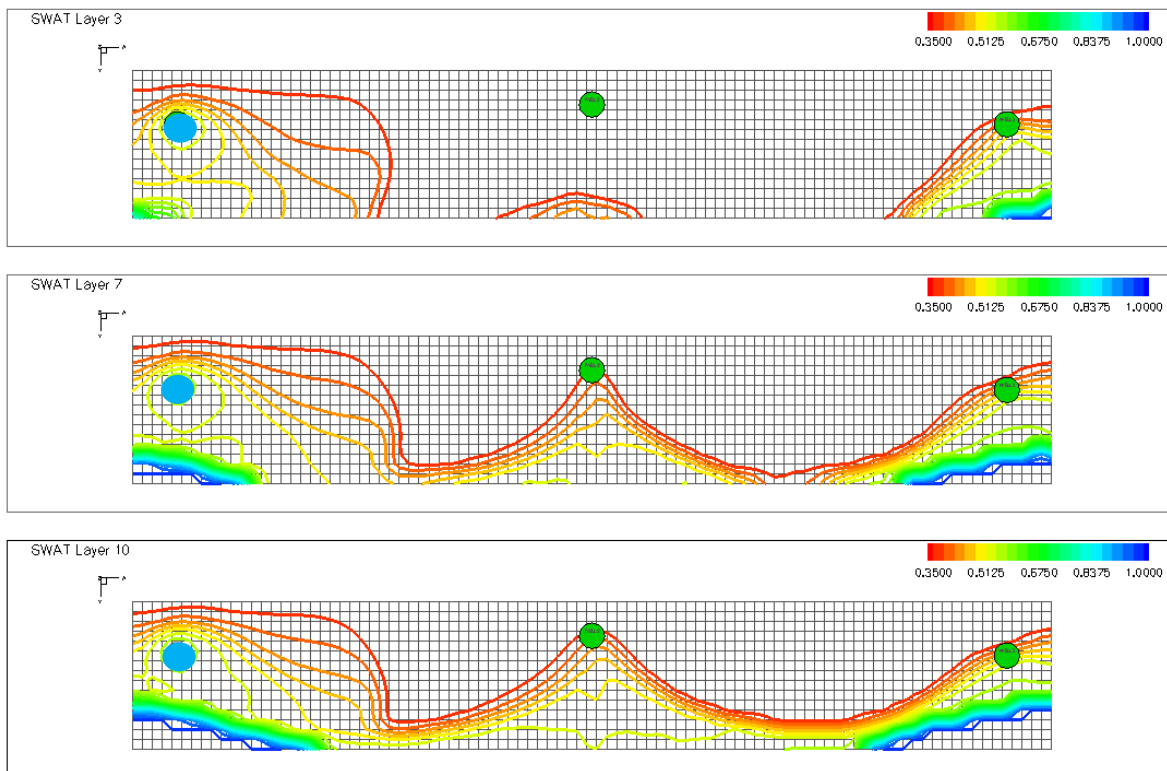


Figure 5- 47: Contour map of water saturation for water dump flood via an edge well injector at day 240 @ day 900

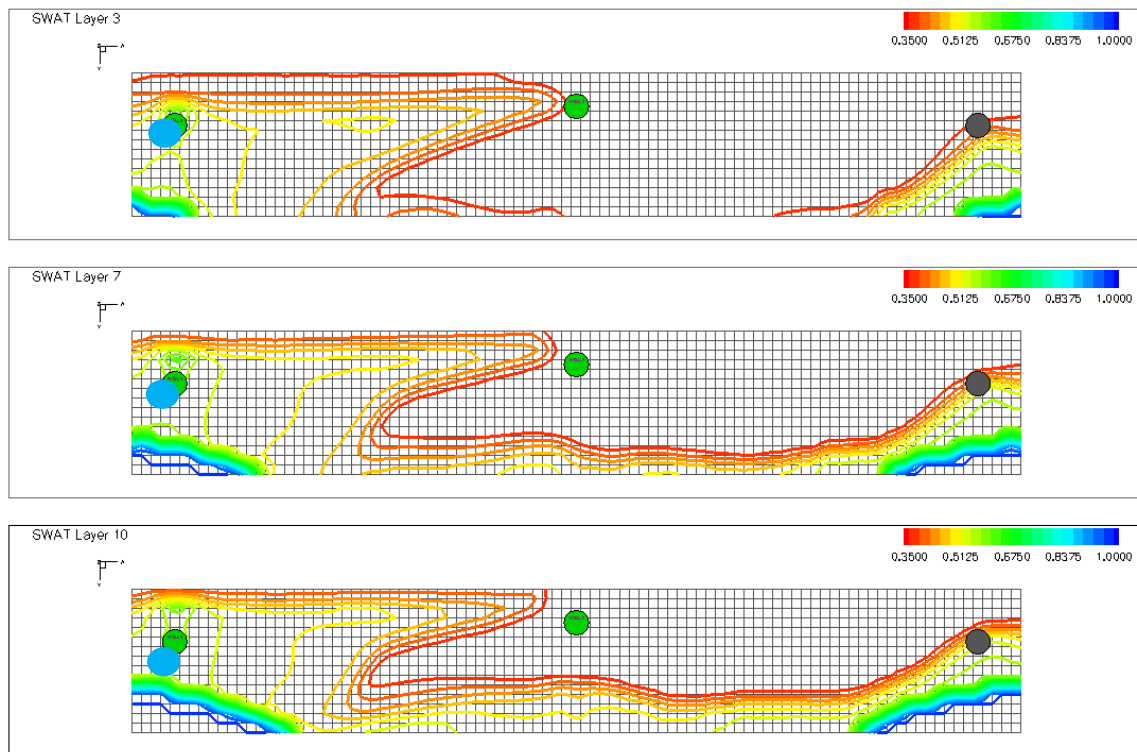


Figure 5- 48: Contour map of water saturation for water dump flood via an edge well injector at day 600 @ day 900

Table 5-17 and Figure 5-48 show that the highest recovery efficiency case when water dump flood at day 240 for the reason that at point 1, free gas begins to flow, causing the smallest mobility. Thereafter, a significant reduction in oil recovery efficiency is seen due to the declining reservoir pressure with increasing in gas oil ratio until point 2. In any case, the oil recovery efficiency is still higher than that in the base case (i.e. primary production).

Table 5- 17: Oil recovery factors for different times to start water dump flood via an edge well injector

Time to start water dump flood (day)	RF (%)
1	34.05
15	34.33
30	34.61
60	35.12
90	35.32
150	35.82
240	36.66
330	35.65
420	34.47
510	33.90
600	33.25

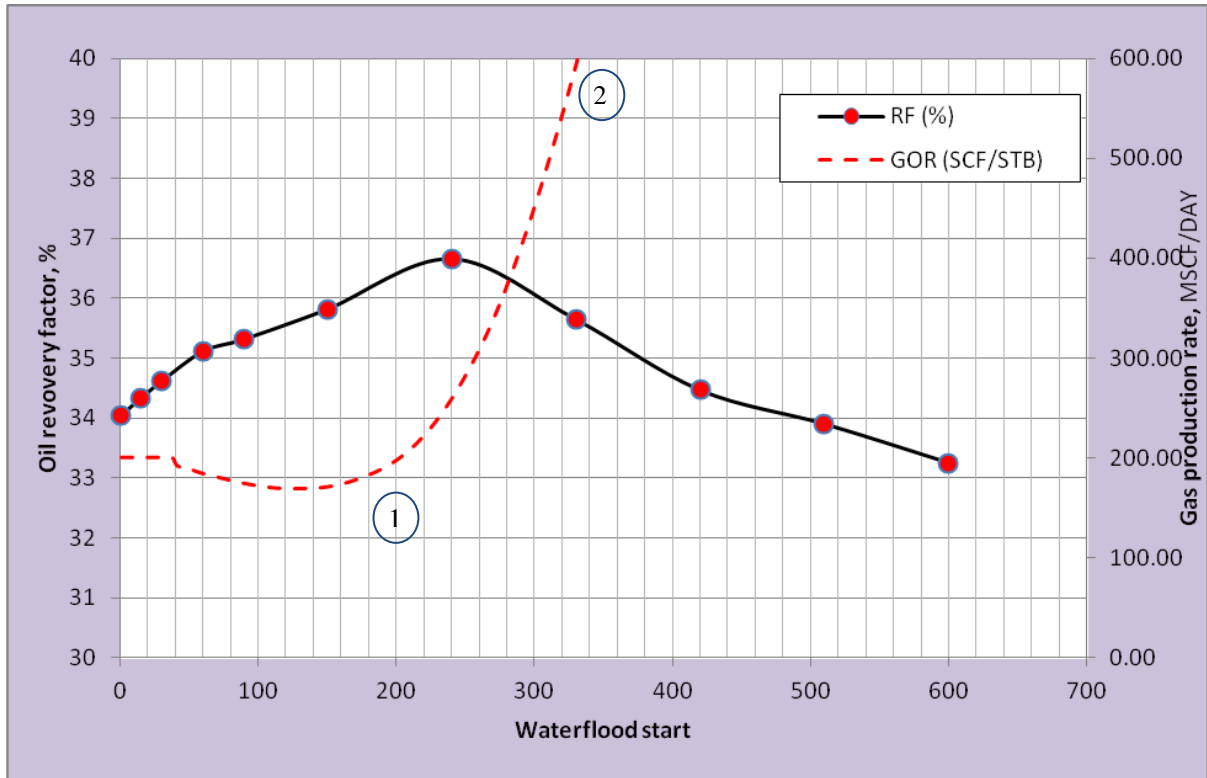


Figure 5- 49: Oil recovery factors for different times to start water dump flood via an edge well injector

CHAPTER VI

CONCLUSIONS AND RECOMMENDATIONS

This water dump flooding study provides information that will help to improve understanding of dump flooding behavior. The study was conducted by varying several parameter, which include reservoir rock or fluid properties.

6.1 Conclusions

The simulation study was conducted by using a 3D, finite difference, black oil reservoir simulation model. The simulation results describe the impact of different parameters investigated. The details of conclusions are as follows:

1. From simulation study, it has been shown that water dump flood can improve recovery efficiency because water from the aquifer can provide a significant source of energy (as compared pure solution gas drive).
2. The injector location has a strong impact on oil production performance. Based on assumption that the center well is on the crest further away from the water-oil contact, the edge well injector is the best choice to improve estimate ultimate recovery factor. If the center well is used to connect between the aquifer and the oil reservoir, the oil recovery is actually lower than that with primary recovery.
3. The oil production performance correlates to the average reservoir pressure performance. A small aquifer size leads to lower reservoir pressure and this leads to lower oil and water rates.
4. The ratio of aquifer to reservoir volume has a moderate impact on recovery. The incremental recovery factor can be up to 3.5% (i.e. from 34% to 37.5%) when the ratio of aquifer to reservoir ratio is 43 RBL/RBL. However, for very large aquifer sizes (i.e. approaching infinite acting), the water production continues to increase, the oil performance drops due to high water cut.
5. Higher well productivity index will yield higher producing rate for a given drawdown. So, early production will be benefited by higher productivity index. However, average reservoir pressure decreases related to high GOR. Thus the production rate drops more rapidly.

6. Decreasing in well injectivity index, oil production performances are obviously reduced. However, the simulation indicates that the water dump flood still performed than primary production even when the injectivity index is low.
7. The result shows that the recovery efficiencies do not follow the same trend for different depths due to the fact that there are more than one factors changed at deeper depths.
8. The study shows that water dump flood is viable at any depth within the producing interval evaluated (i.e. from 4000 to 8000 ft TVDSS).
9. The overlaying aquifer provides higher cross flow rates compared to the underlying aquifer dump flood case. Thus, the performances of overlaying aquifer are better compared to the underlying aquifer case.
10. Water dump flood is still a better choice than primary recovery when API gravity was varied between 30 to 40 °API provided that the well that connects the aquifer with the reservoir is the edge well.
11. The oil recovery for different times to start water dump flood varies between 33% and 37%. In all cases, the cumulative oil production is higher than the base case (no water dump flood).

6.2 Recommendations

1. For more accuracy, the sensitivity to temperature differences between (overlaying or underlying) aquifer and oil reservoir and tendencies to thermally fracture should be investigated.
2. This study is based on the assumption that the center well is on the crest further away from the water-oil contact. A case with a flat structure along the fault was not investigated. Therefore, other reservoir model construction should be investigated.
3. In this study, the gas-lift rates were fixed. To minimize lift gas usage in attaining the maximum production rate, gas-lift rate optimization should be used to seek an optimum lift-gas rate.

REFERENCES

- [1] Davies, C.A. The theory and practice of monitoring and controlling dump floods. paper SPE 3733 presented at European Spring Meeting. 1972.

- [2] DesBrisay, C.L., and Daniel, E.L. Supplemental Recovery Development of The Intisar “A” and “D” Reef Fields, Libyan Arab Republic. paper SPE 3438. 1972.

- [3] Fujita K. Pressure Maintenance by Formation Water Dumping for the Ratawi Limestone Oil Reservoir, Offshore Khafji. paper SPE 9584 presented at Middle East Oil Technical Conference and Exhibition held in Bahrain. 9-12 March 1982

- [4] Yao, C.Y., Hill, N.C., and McVay, D.A. Economic Pilot-Floods of Carbonate Reservoirs Using a Pump-Aided Reverse Dump-Flood Technique. paper SPE 52179 presented at Mid-Continent Operations Symposium held in Oklahoma City, Oklahoma. 28-31 March 1999.

- [5] Luis, R.J., and Navia, W. Natural Waterflooding, Campo La Peña. paper SPE 69633 presented at Latin American and Caribbean Petroleum Engineering Conference held in Buenos Aires, Argentina. 25-25 March, 2001.

- [6] Quttainah, R., and Al-Hunaif, J. Umm Gudair Dumpflood Pilot Project, The Applicability of Dumpflood to Enhance Sweep & Maintain Reservoir Pressure. paper SPE 68721 presented at Asia Pacific Oil and Gas Conference and Exhibition held in Jakarta, Indonesia. 17-19 April, 2001.

- [7] Quttainah, R., and Al-Maraghi, E. Umm Gudair Production Plateau Extension. The Applicability of FullField Dumpflood Injection to Maintain Reservoir Pressure and Extend Production Plateau. paper SPE 97624 presented at International Improved Oil Recovery Conference in Asia Pacific held in Kuala Lumpur, Malaysia. 5-6 December, 2005.
- [8] Friedel, T. et al. Identifying the Improved Oil Recovery Potential for a Depleted Reservoir in the Betty Field, Offshore Malaysia. paper SPE 100984 presented at Asia Pacific Oil & Gas Conference and Exhibition held in Adelaide, Australia. 11-13 September, 2006.
- [9] Rawding, J., Al Matar, B.S., and Konopczynski, M.R. Application of Intelligent Well Completion for Controlled Dumpflood in West Kuwait. paper SPE 112243 presented at Intelligent Energy Conference and Exhibition held in Amsterdam, The Netherlands. 25-27 Febuary, 2008.
- [10] Chang, M.M., Cullen, R., and Utomo, B. Optimizing Waterflooding Considering Dip in the Wafra Field. paper SPE 125916 presented at North Africa Technical Conference and Exhibition held in Cairo, Egypt. 14-17 Febuary, 2010.
- [11] Abdus, S., Ghulam, M., and James, L.B. Practical Enhanced Reservoir Engineering. Tulsa: Penn Well books, 2007.

APPENDICES

APPENDIX A

The Contour map of water saturation of water dump flood at day 900 for all cases

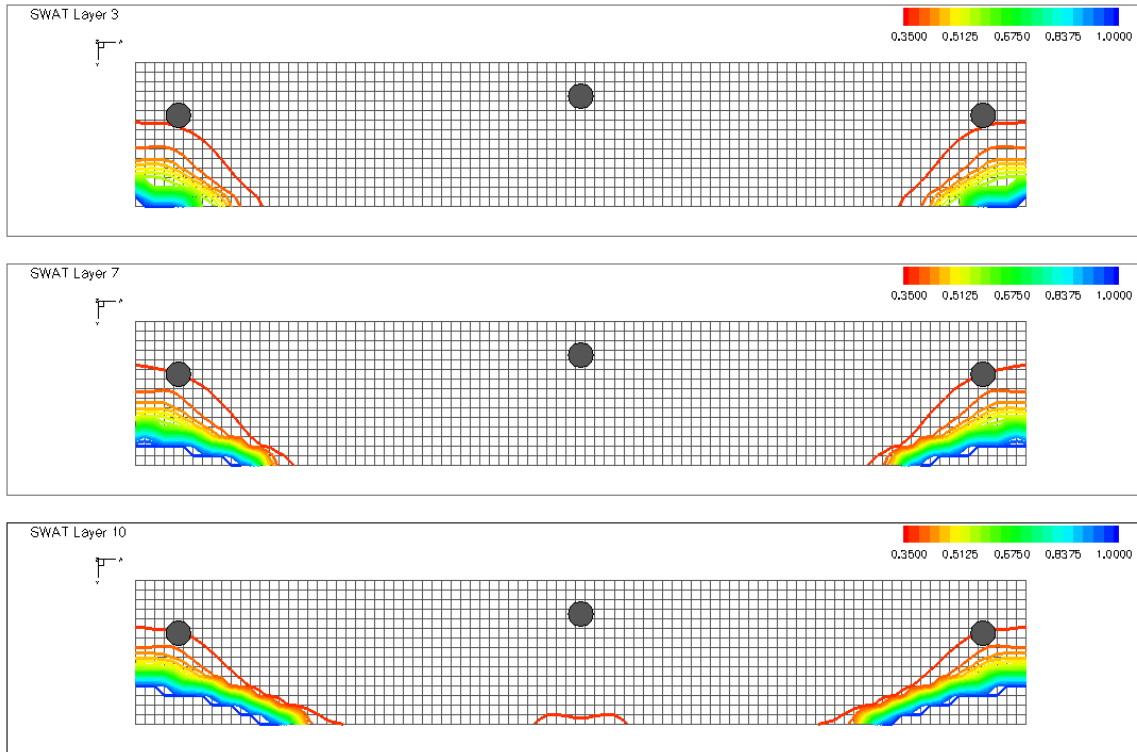


Figure A- 1: Contour map of water saturation for base case @ day 900

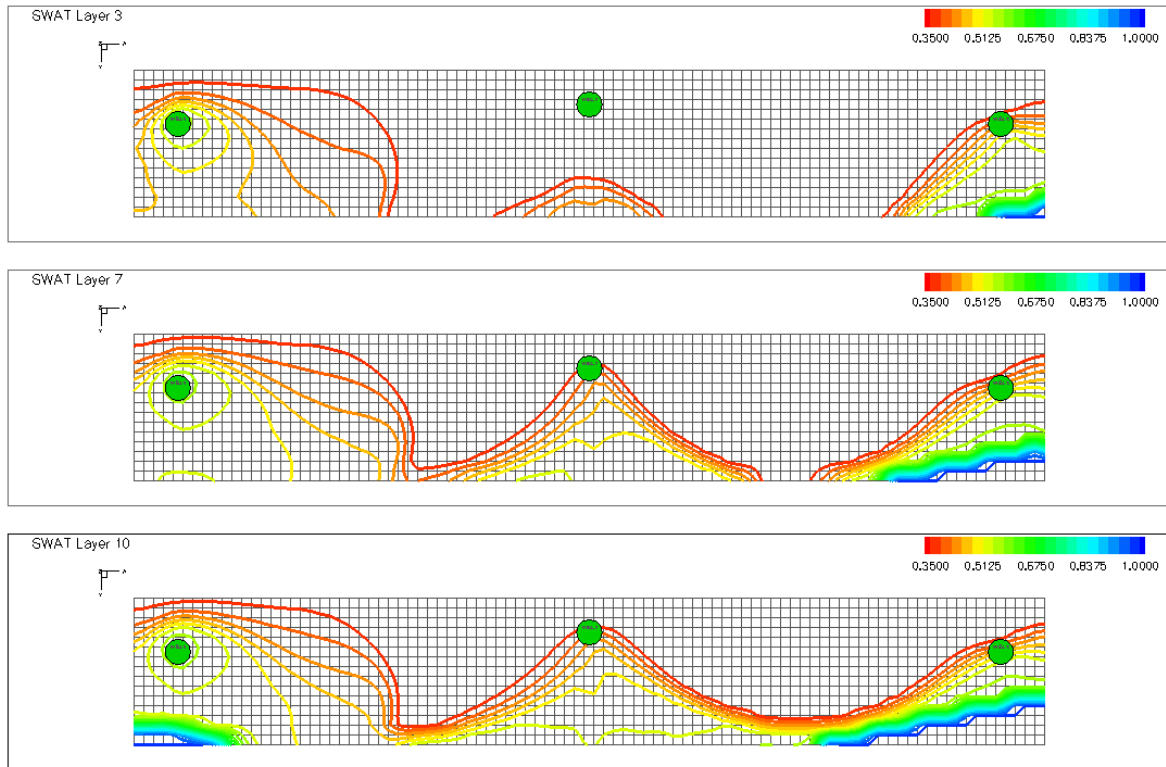


Figure A- 2: Contour map of water saturation for dump flooding via an edge well injector @ day 900

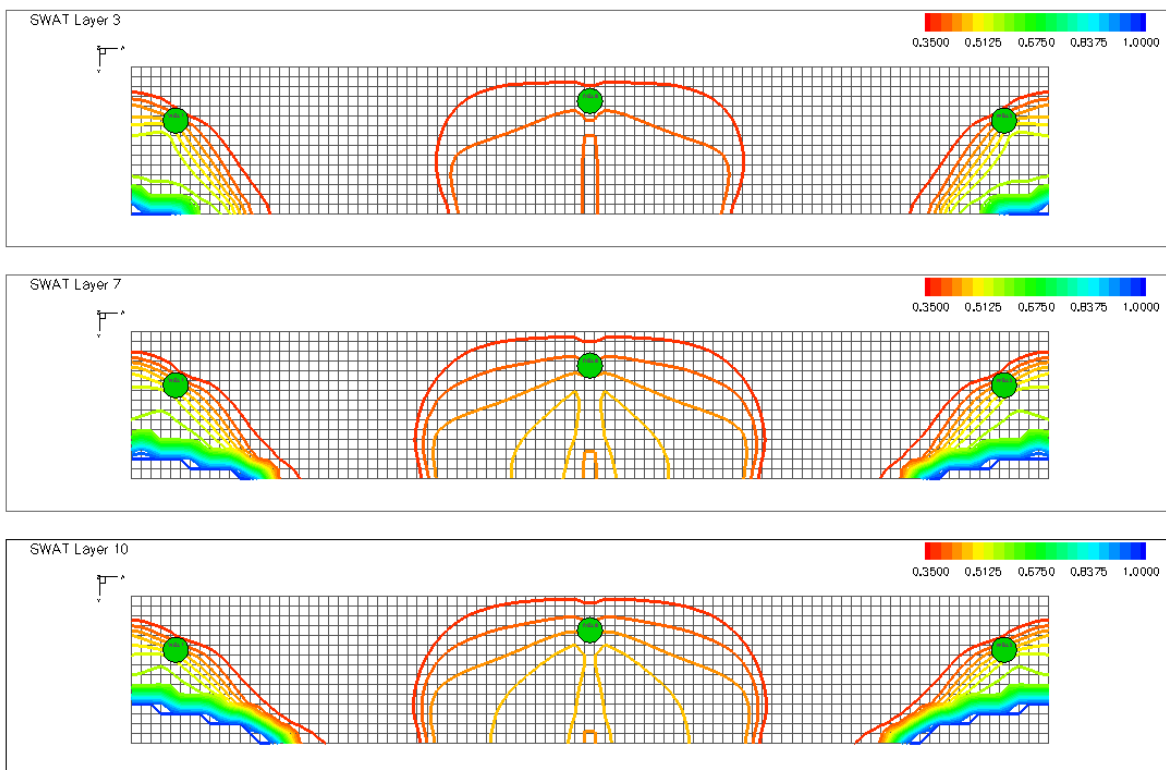


Figure A- 3: Contour map of water saturation for dump flooding via a center well injector @ day 900

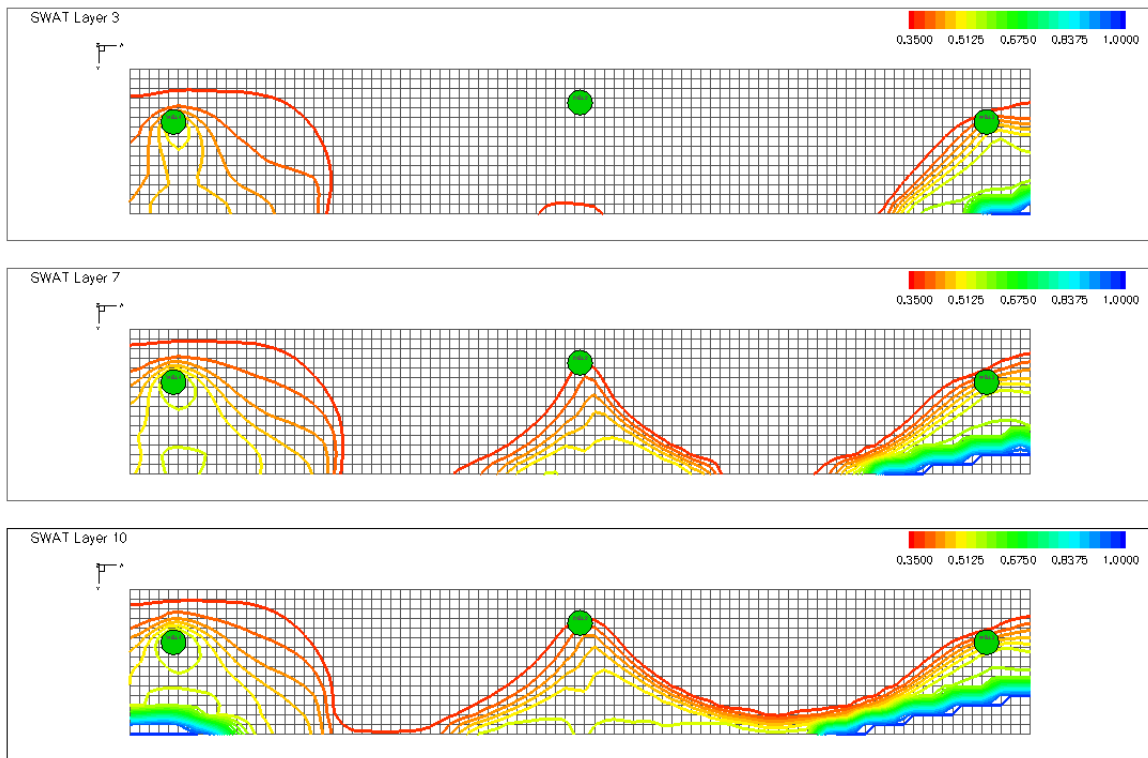


Figure A- 4: Contour map of water saturation for dump flooding via an edge well injector with aquifer/reservoir volume of 0.214rbl/rbl @ day 900

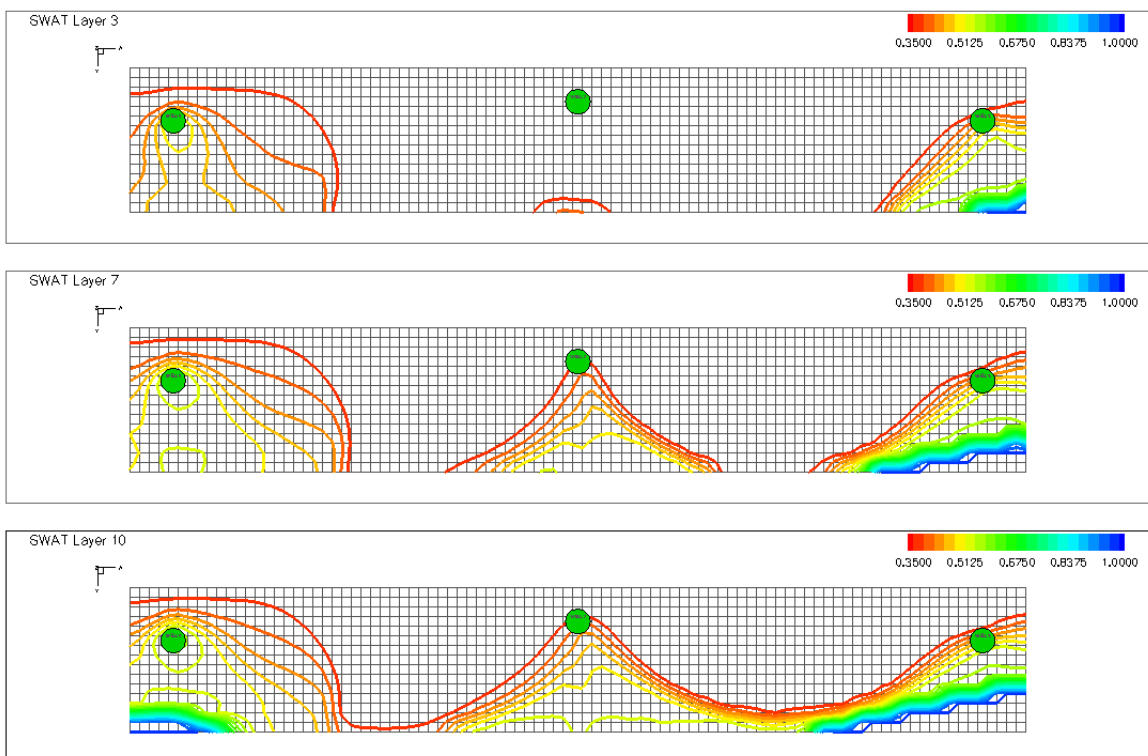


Figure A- 5: Contour map of water saturation for dump flooding via an edge well injector with aquifer/reservoir volume of 0.43rbl/rbl @ day 900

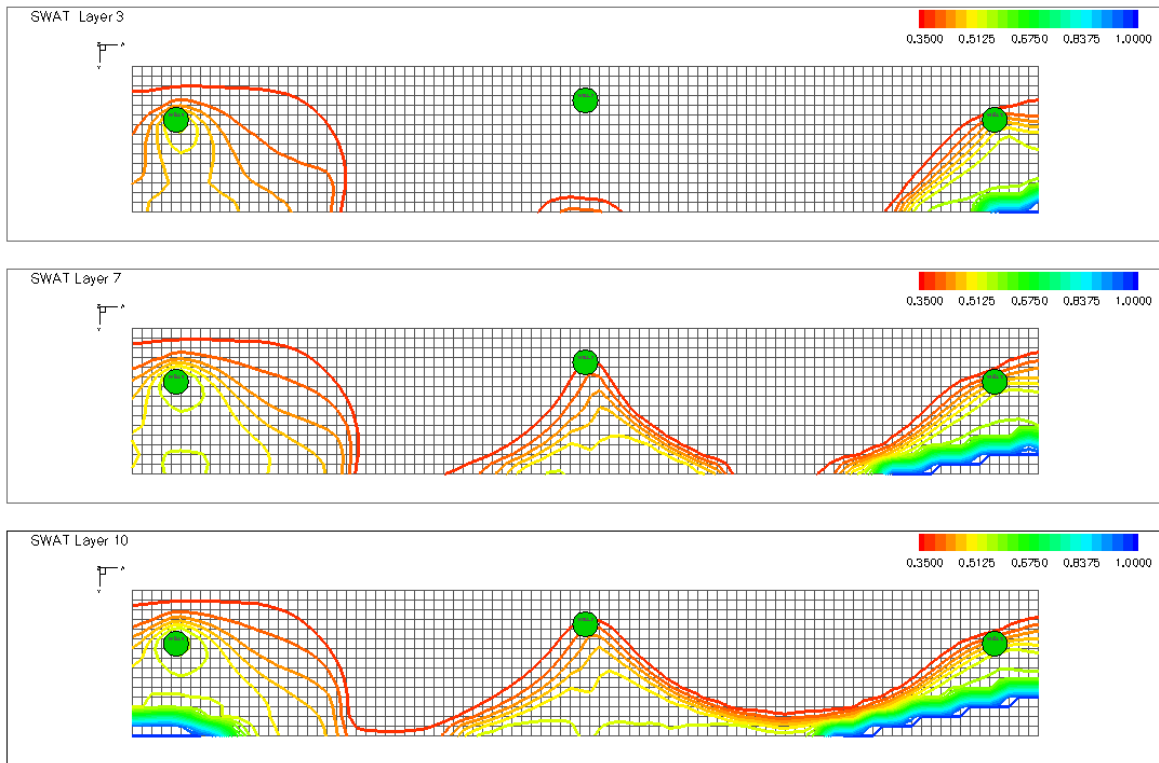


Figure A- 6: Contour map of water saturation for dump flooding via an edge well injector with aquifer/reservoir volume of 0.54rbl/rbl @ day 900

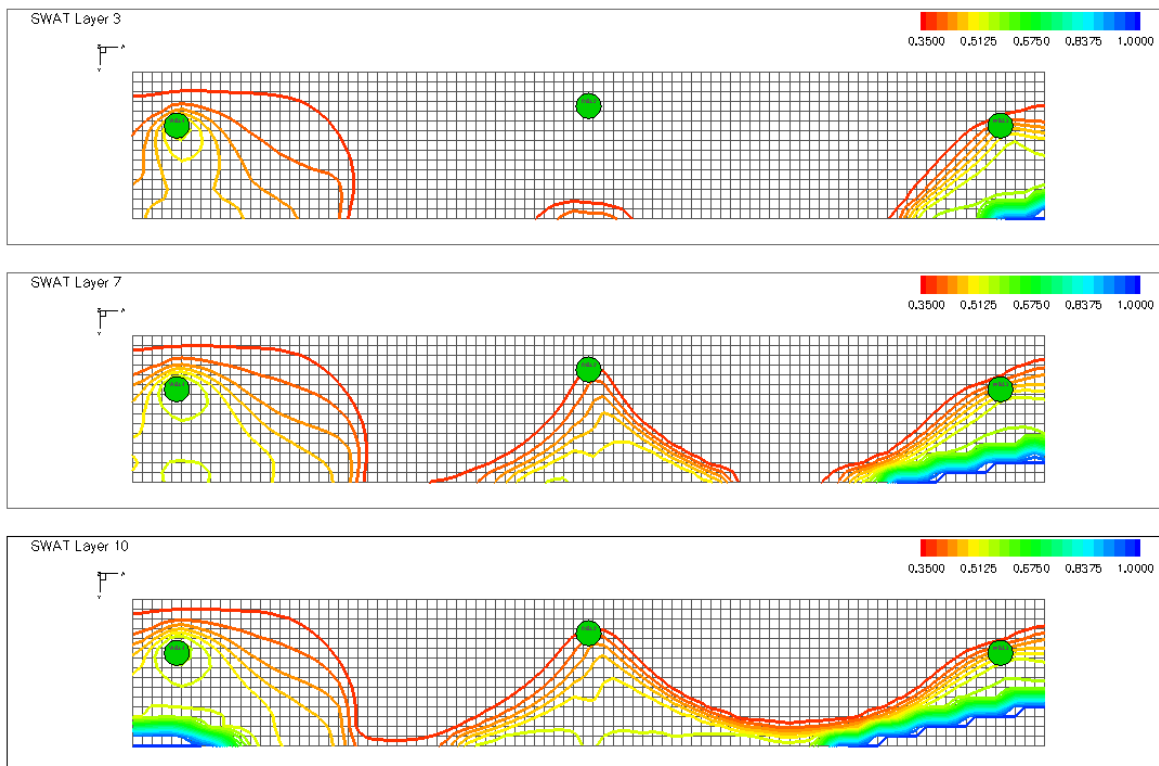


Figure A- 7: Contour map of water saturation for dump flooding via an edge well injector with aquifer/reservoir volume of 0.71rbl/rbl @ day 900

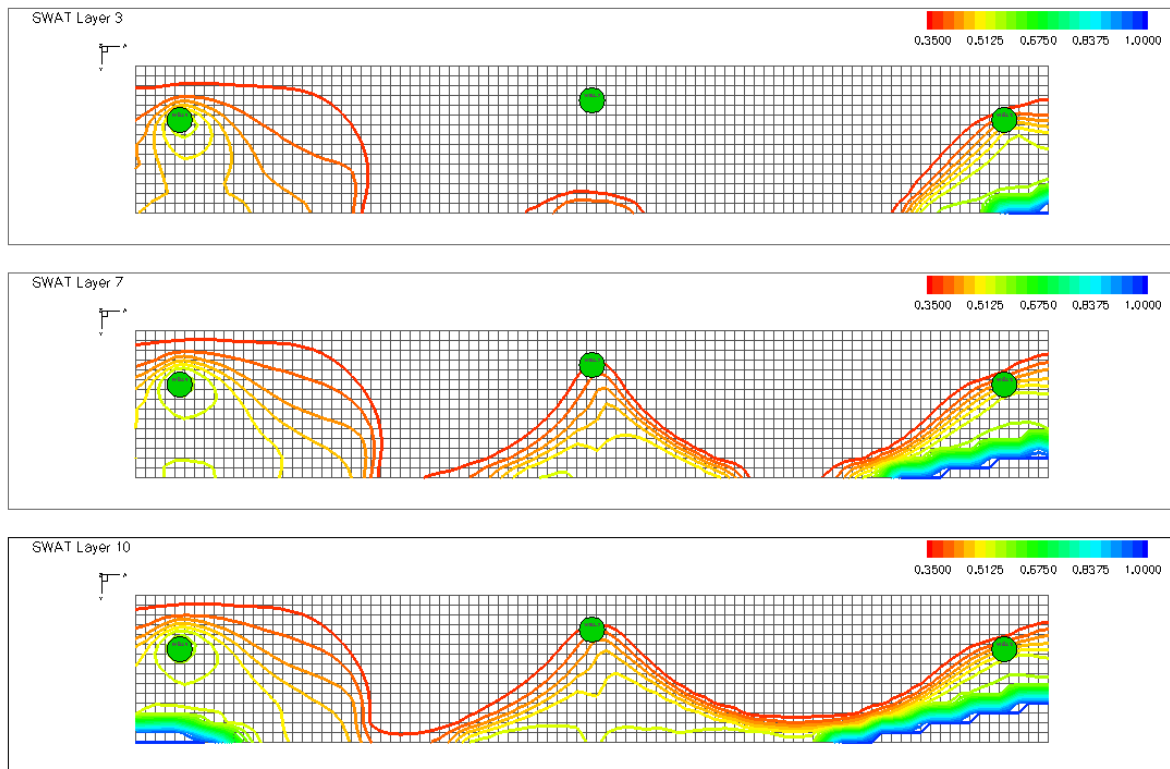


Figure A- 8: Contour map of water saturation for dump flooding via an edge well injector with aquifer/reservoir volume of 1.07rbl/rbl @ day 900

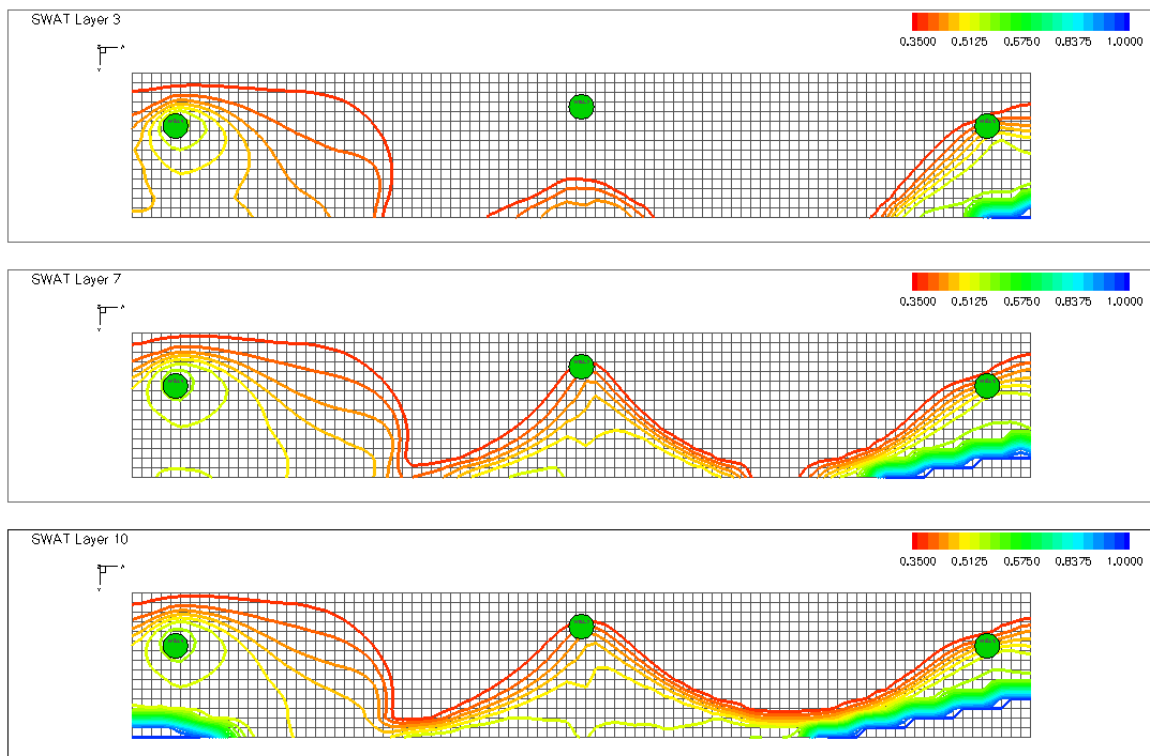


Figure A- 9: Contour map of water saturation for dump flooding via an edge well injector with aquifer/reservoir volume of 2.14rbl/rbl @ day 900

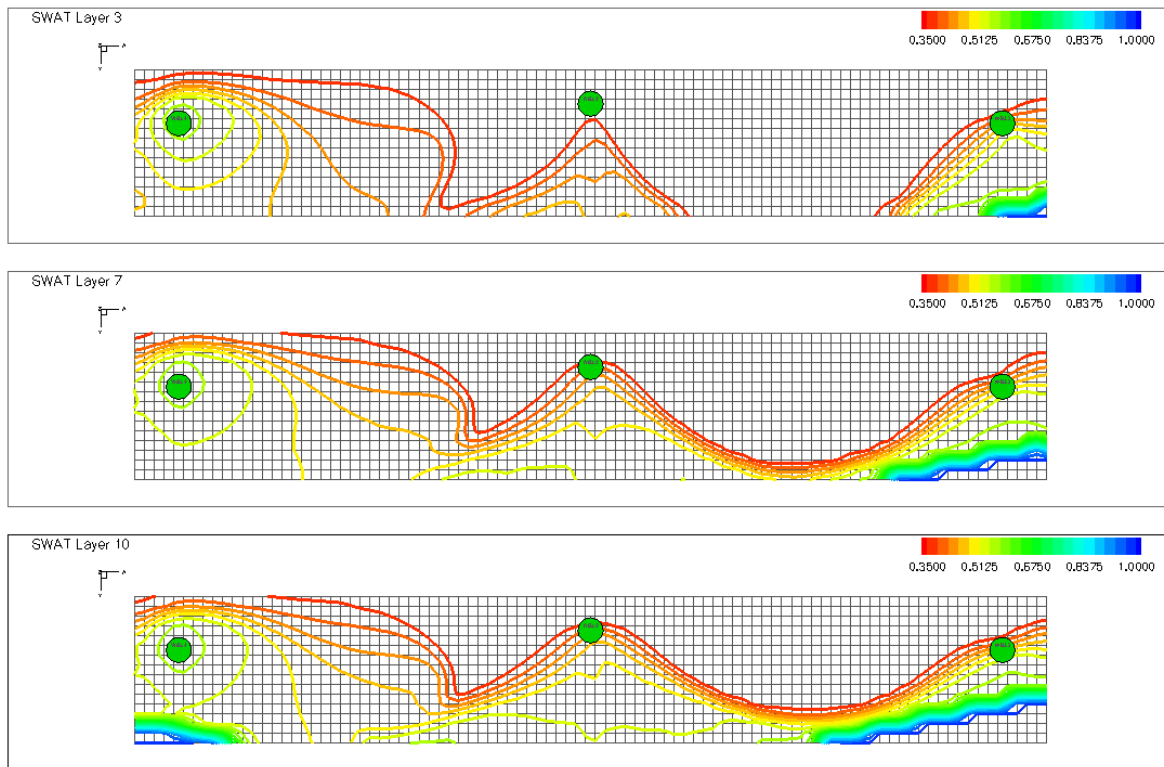


Figure A- 10: Contour map of water saturation for dump flooding via an edge well injector with aquifer/reservoir volume of 4.28rbl/rbl @ day 900

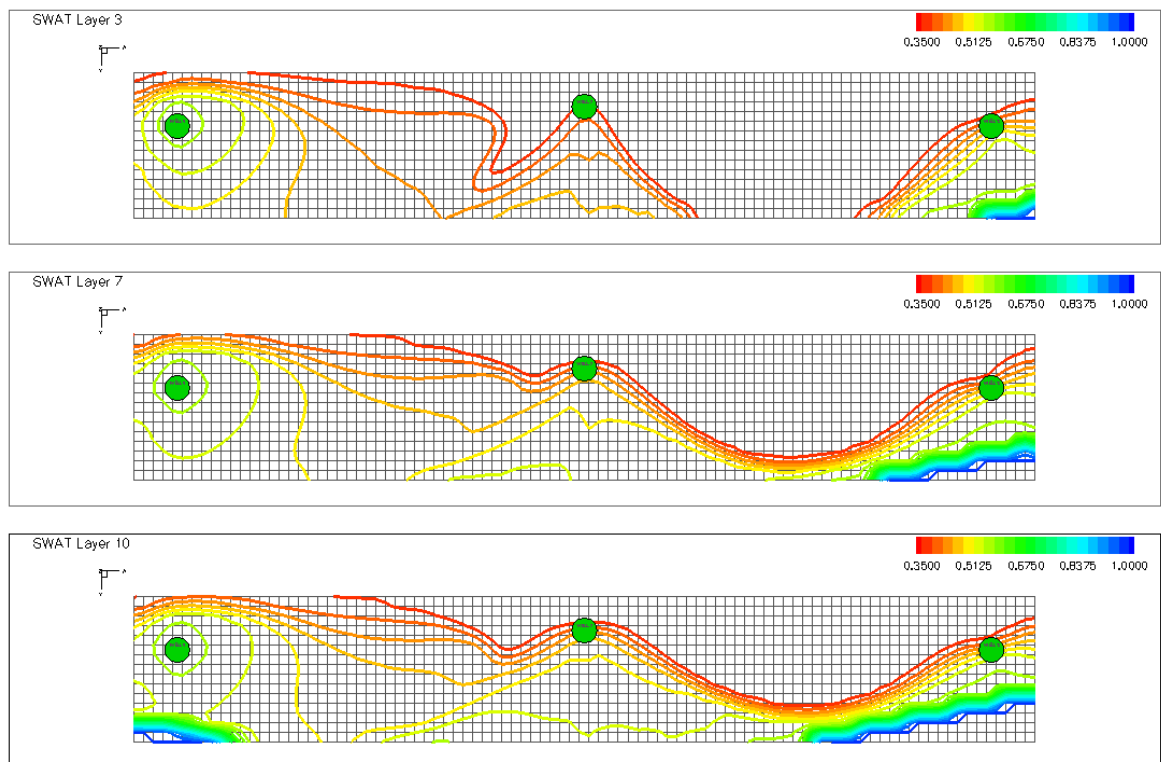


Figure A- 11: Contour map of water saturation for dump flooding via an edge well injector with aquifer/reservoir volume of 6.42rbl/rbl @ day 900

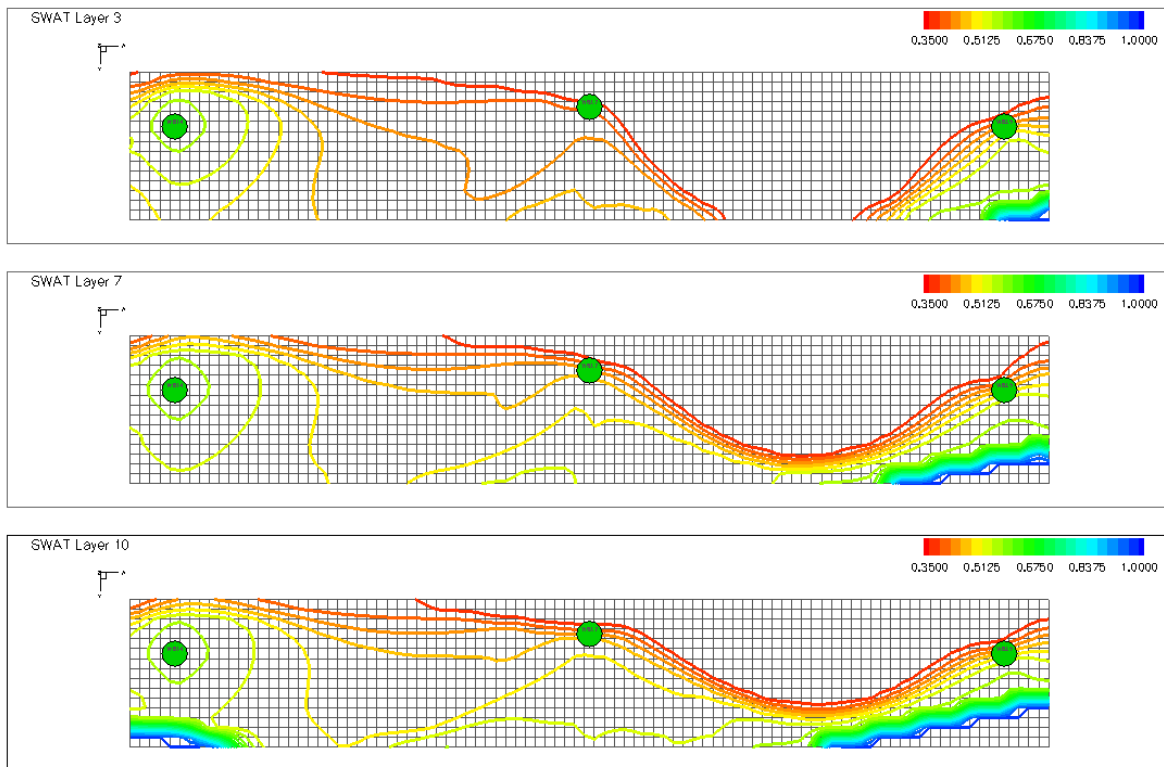


Figure A- 12: Contour map of water saturation for dump flooding via an edge well injector with aquifer/reservoir volume of 8.56rbl/rbl @ day 900

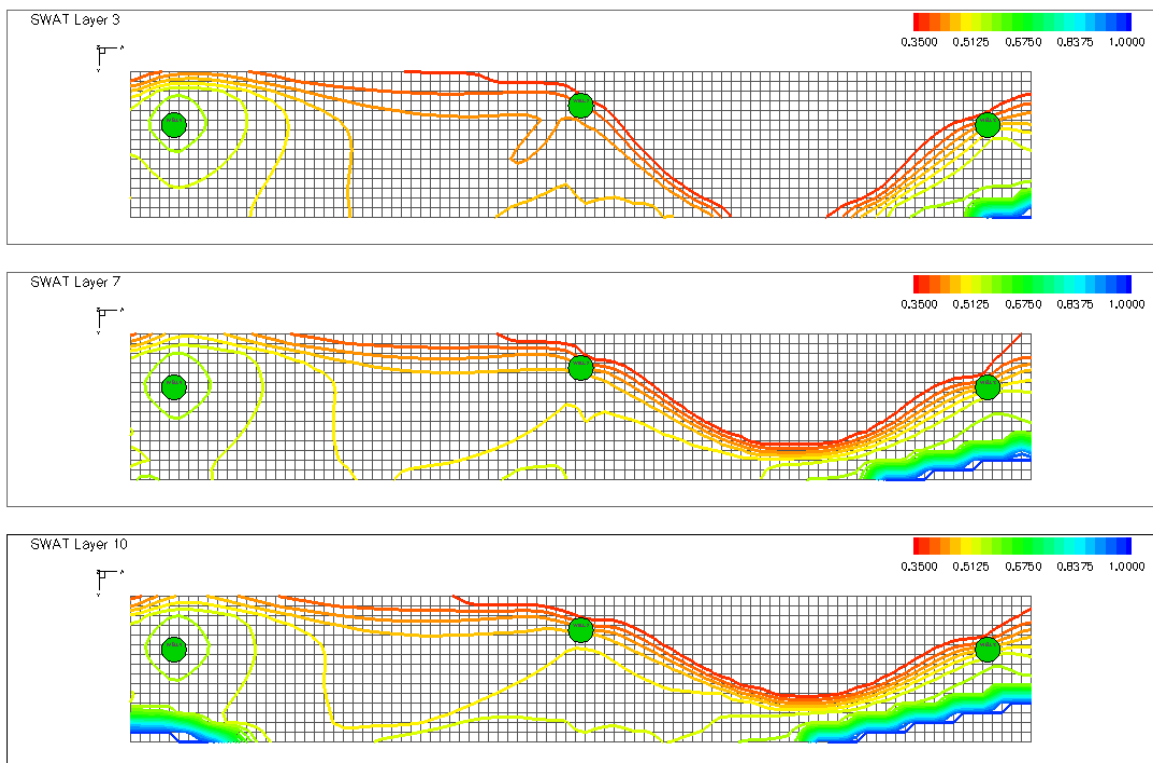


Figure A- 13: Contour map of water saturation for dump flooding via an edge well injector with aquifer/reservoir volume of 10.7rbl/rbl @ day 900

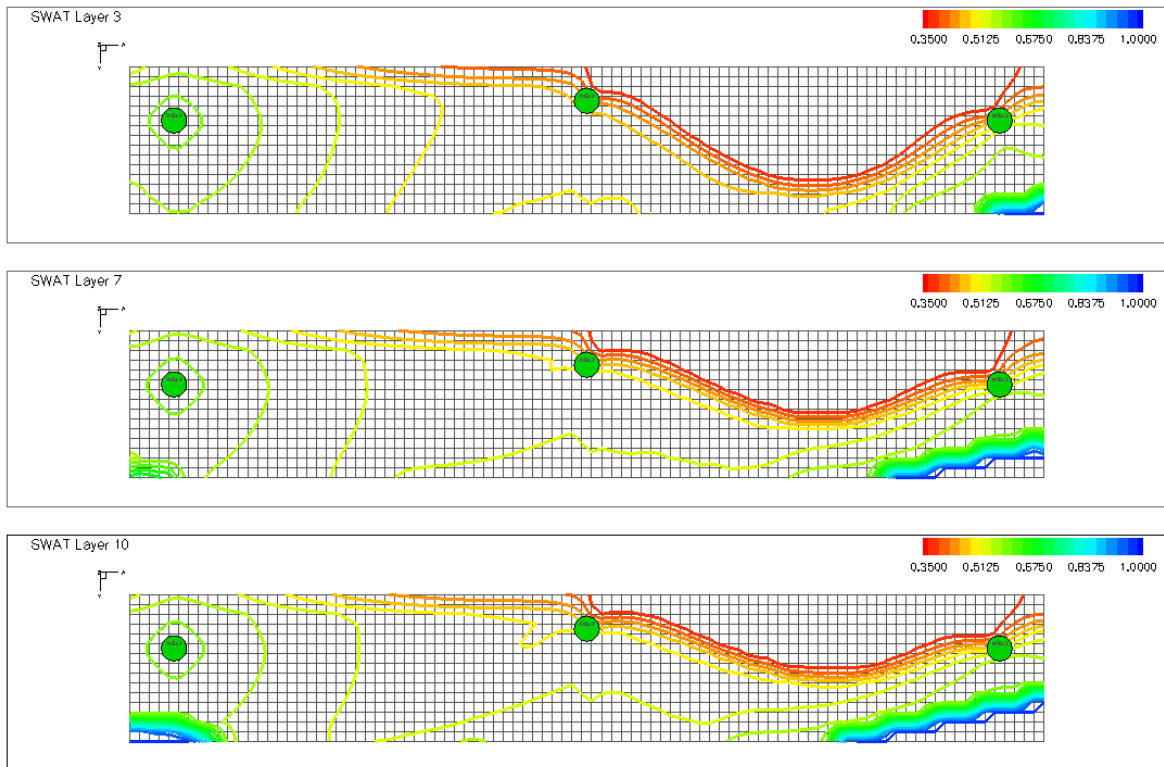


Figure A- 14: Contour map of water saturation for dump flooding via an edge well injector with aquifer/reservoir volume of 21.4rbl/rbl @ day 900

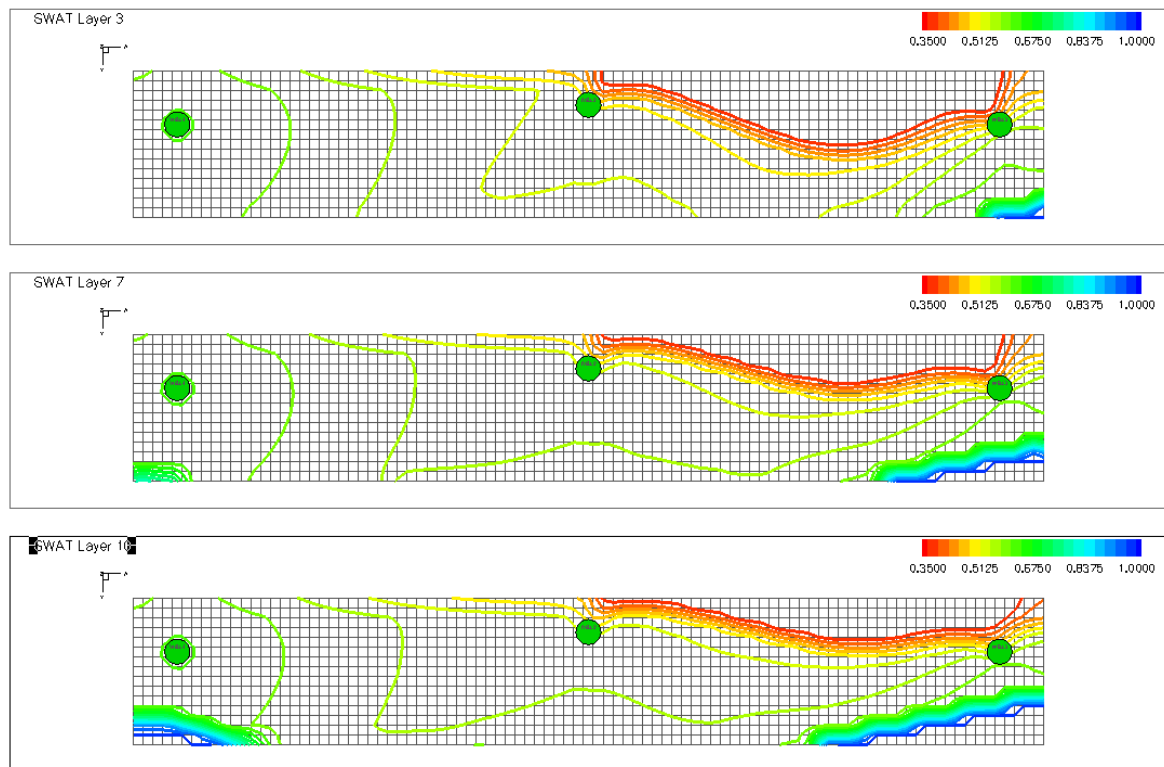


Figure A- 15: Contour map of water saturation for dump flooding via an edge well injector with aquifer/reservoir volume of 42.8rbl/rbl @ day 900

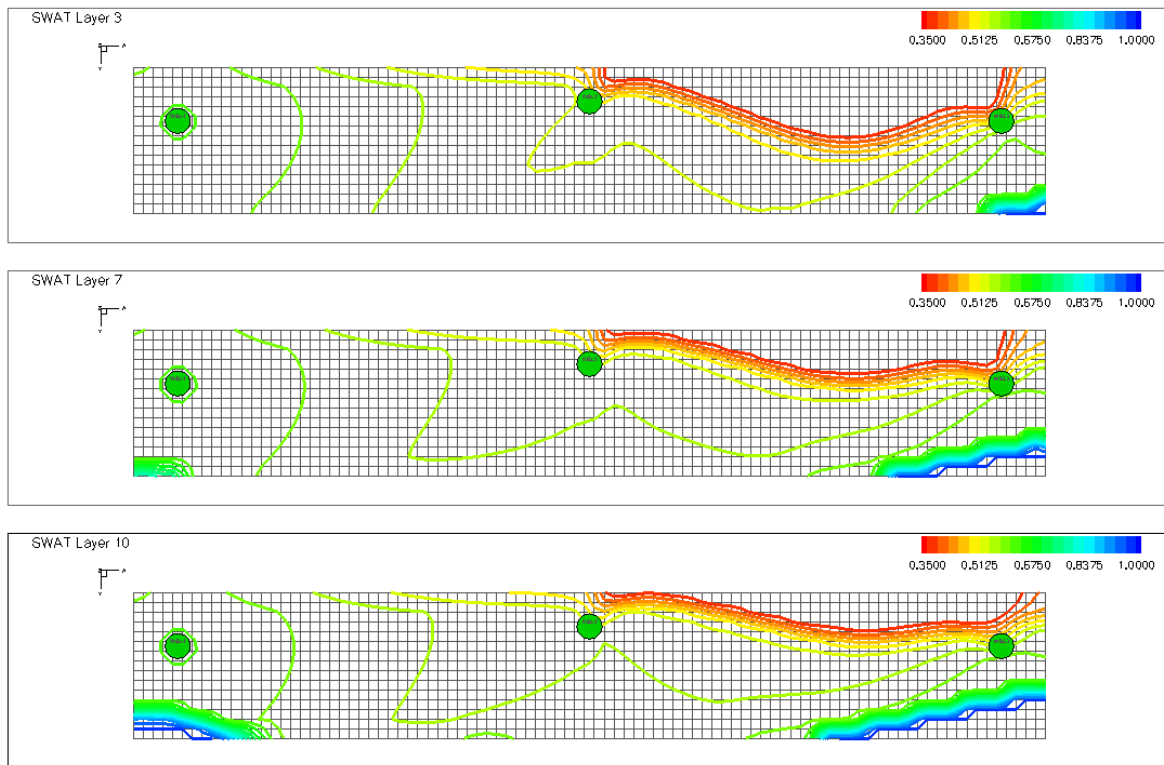


Figure A- 16: Contour map of water saturation for dump flooding via an edge well injector with aquifer/reservoir volume of 64.2rbl/rbl @ day 900

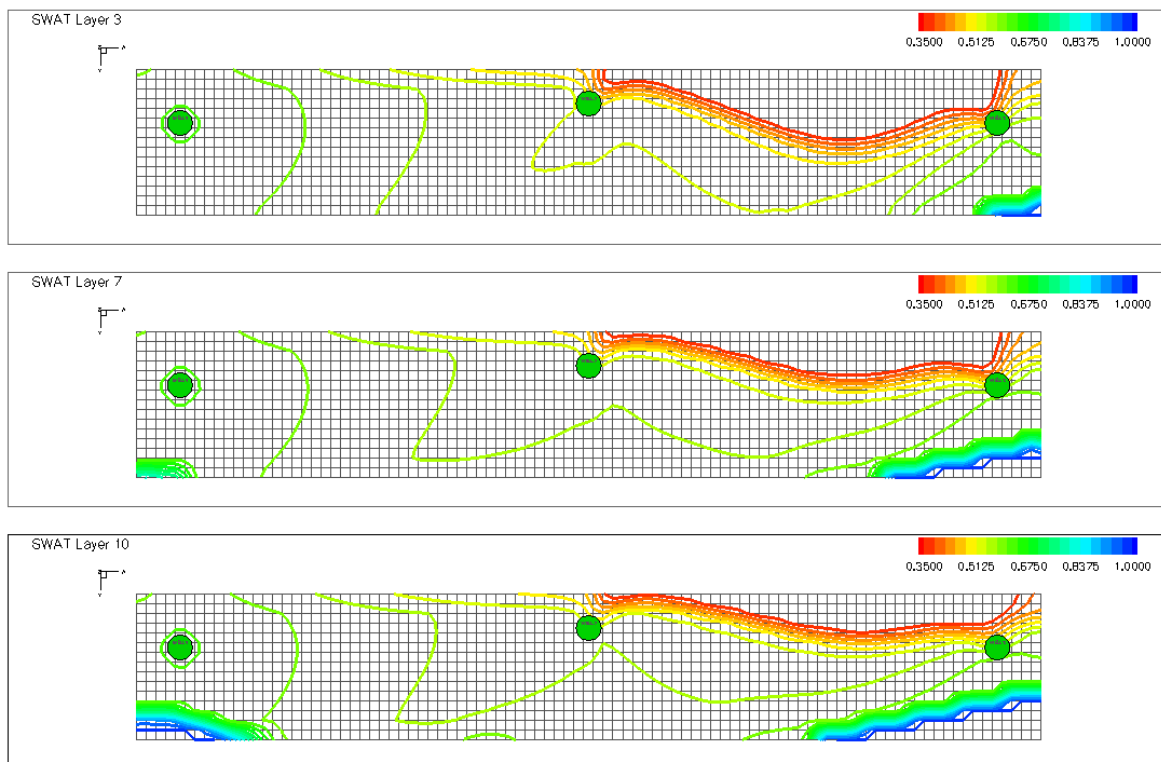


Figure A- 17: Contour map of water saturation for dump flooding via an edge well injector with aquifer/reservoir volume of 85.6rbl/rbl @ day 900

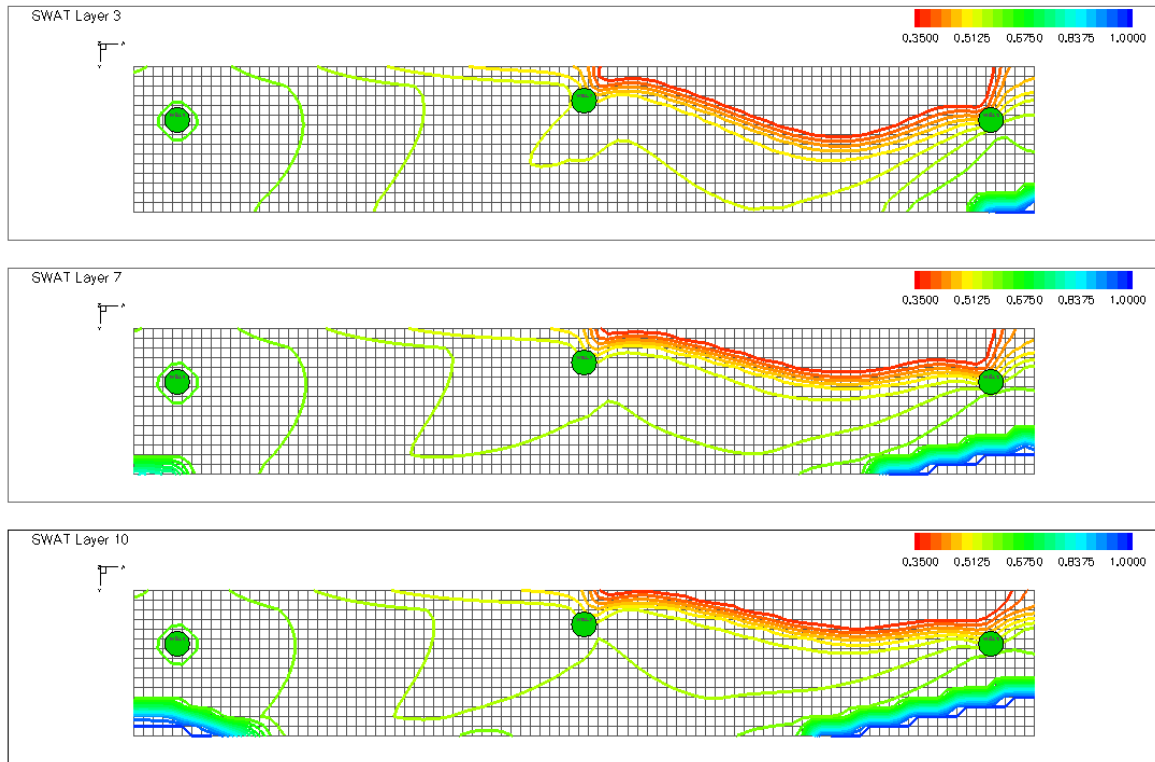


Figure A- 18: Contour map of water saturation for dump flooding via an edge well injector with aquifer/reservoir volume of 107rbl/rbl @ day 900

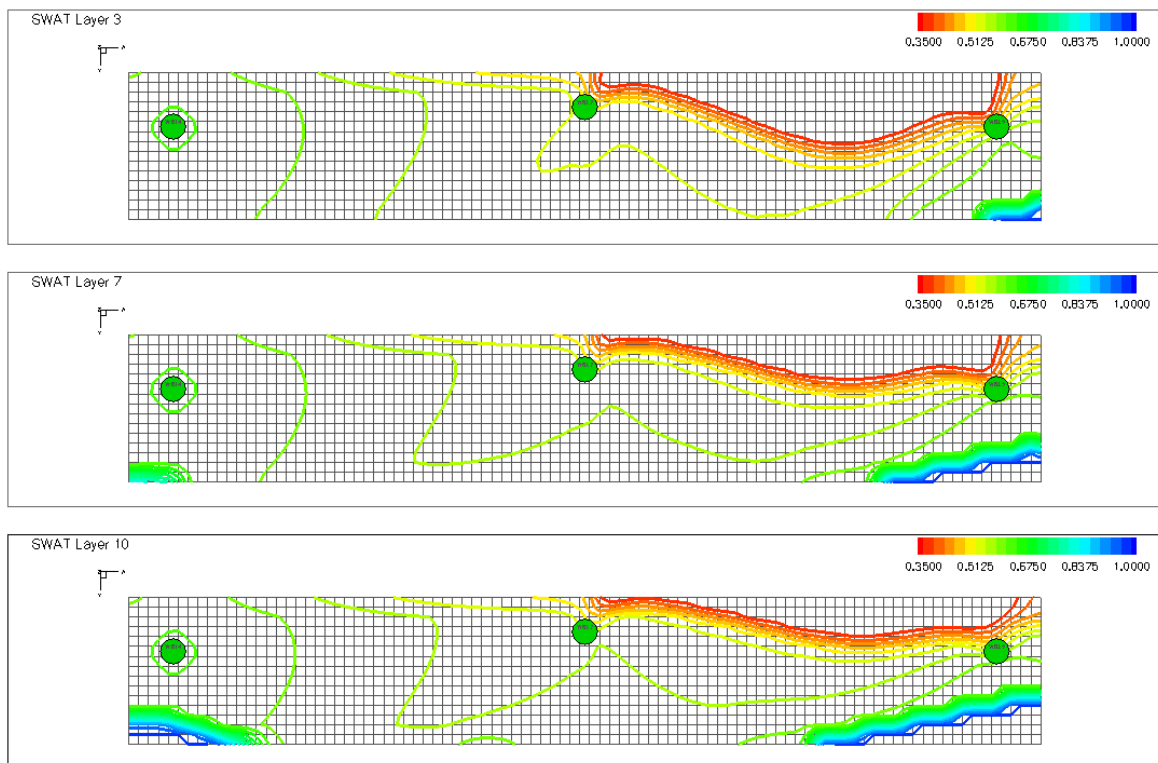


Figure A- 19: Contour map of water saturation for dump flooding via an edge well injector with aquifer/reservoir volume of 214rbl/rbl @ day 900

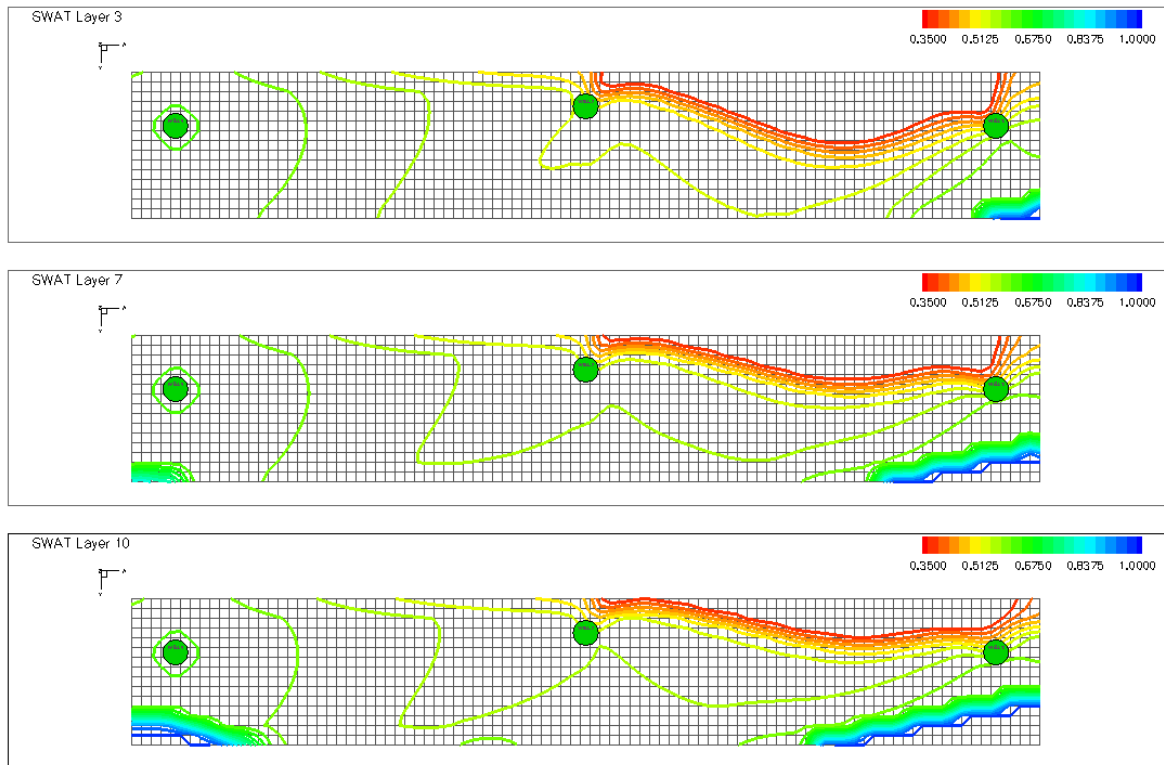


Figure A- 20: Contour map of water saturation for dump flooding via an edge well injector with aquifer/reservoir volume of 321rbl/rbl @ day 900

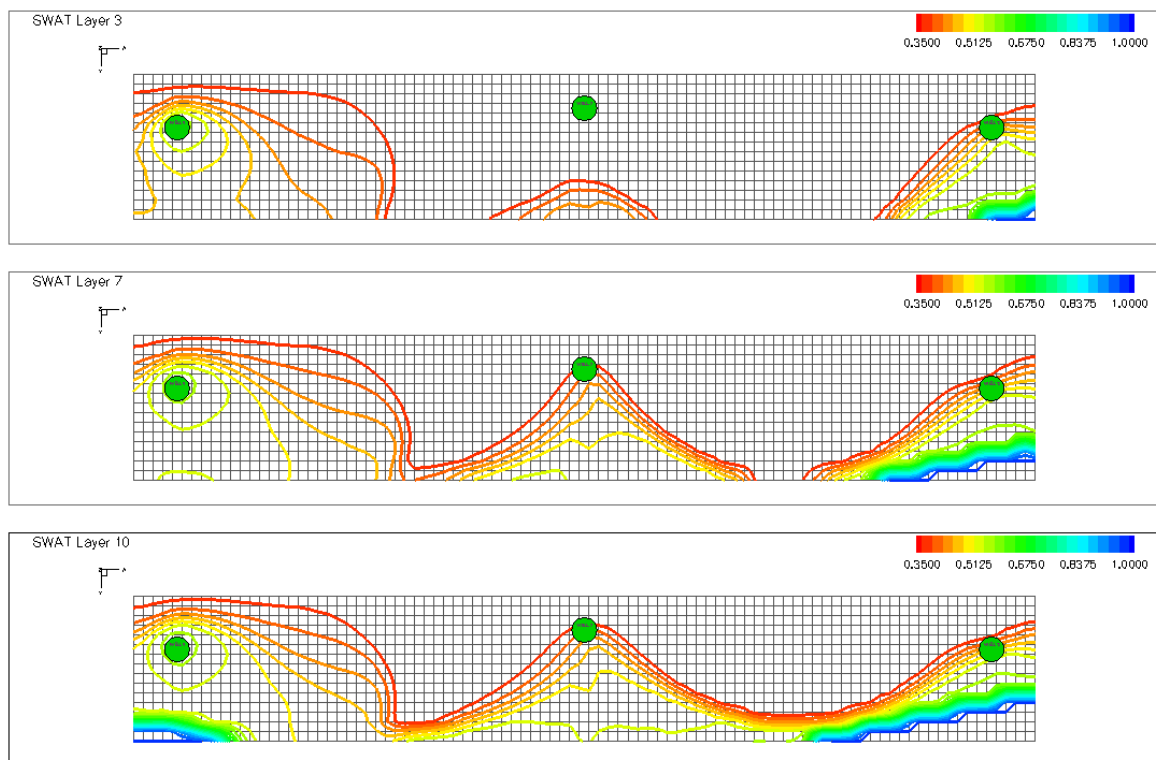


Figure A- 21: Contour map of water saturation for dump flooding via an edge well injector for PI of 28.28stb/day/psi @ day 900

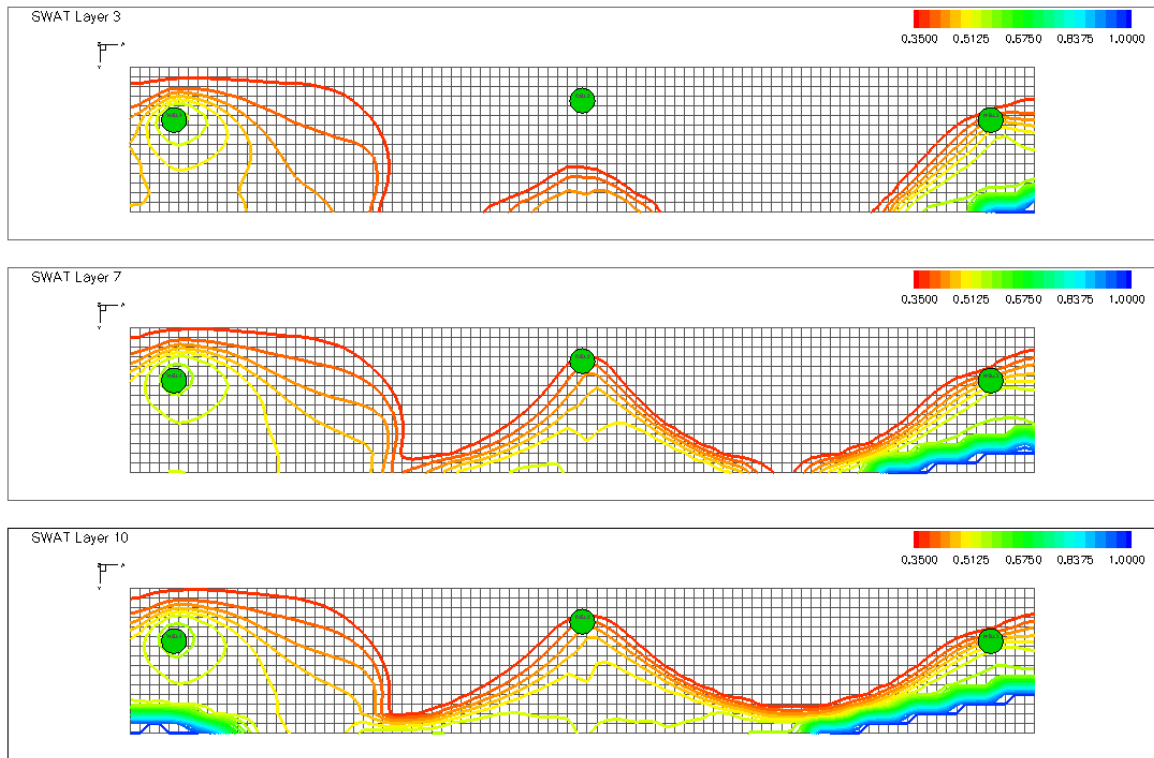


Figure A- 22: Contour map of water saturation for dump flooding via an edge well injector for PI of 14.14stb/day/psi @ day 900

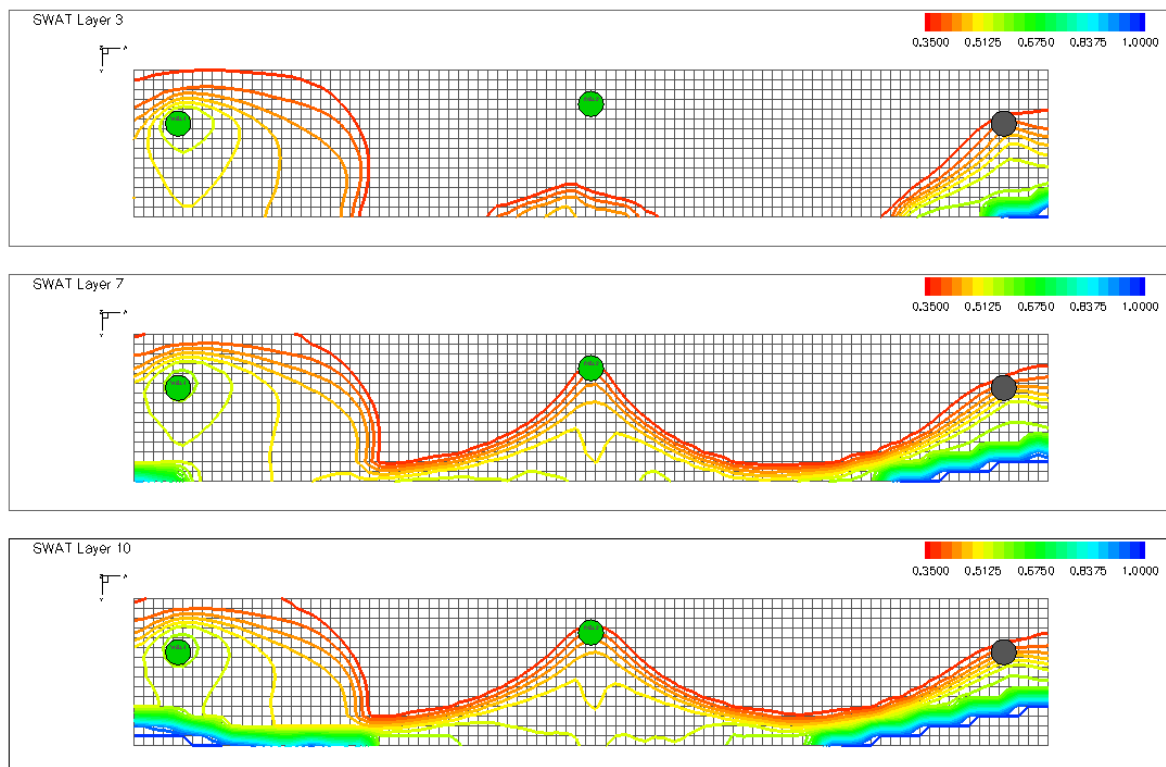


Figure A- 23: Contour map of water saturation for dump flooding via an edge well injector for PI of 2.828stb/day/psi @ day 900

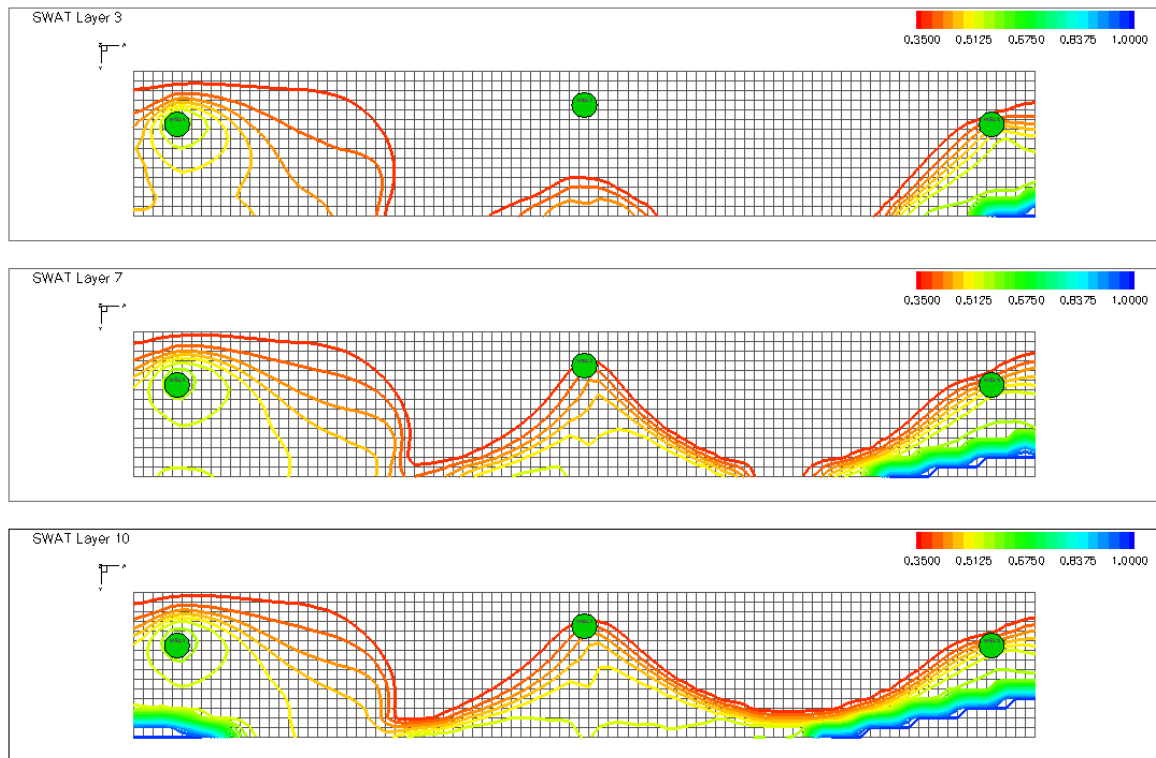


Figure A- 24: Contour map of water saturation for dump flooding via an edge well injector for II of 330stb/day/psi @ day 900

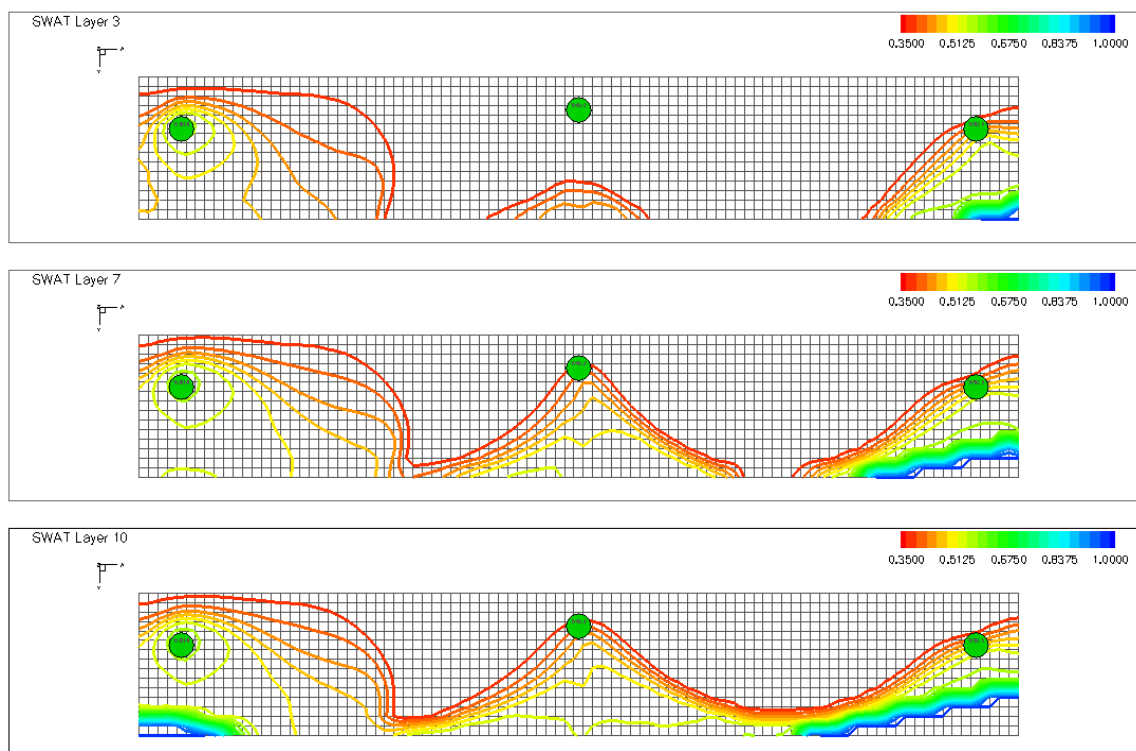


Figure A- 25: Contour map of water saturation for dump flooding via an edge well injector for II of 165stb/day/psi @ day 900

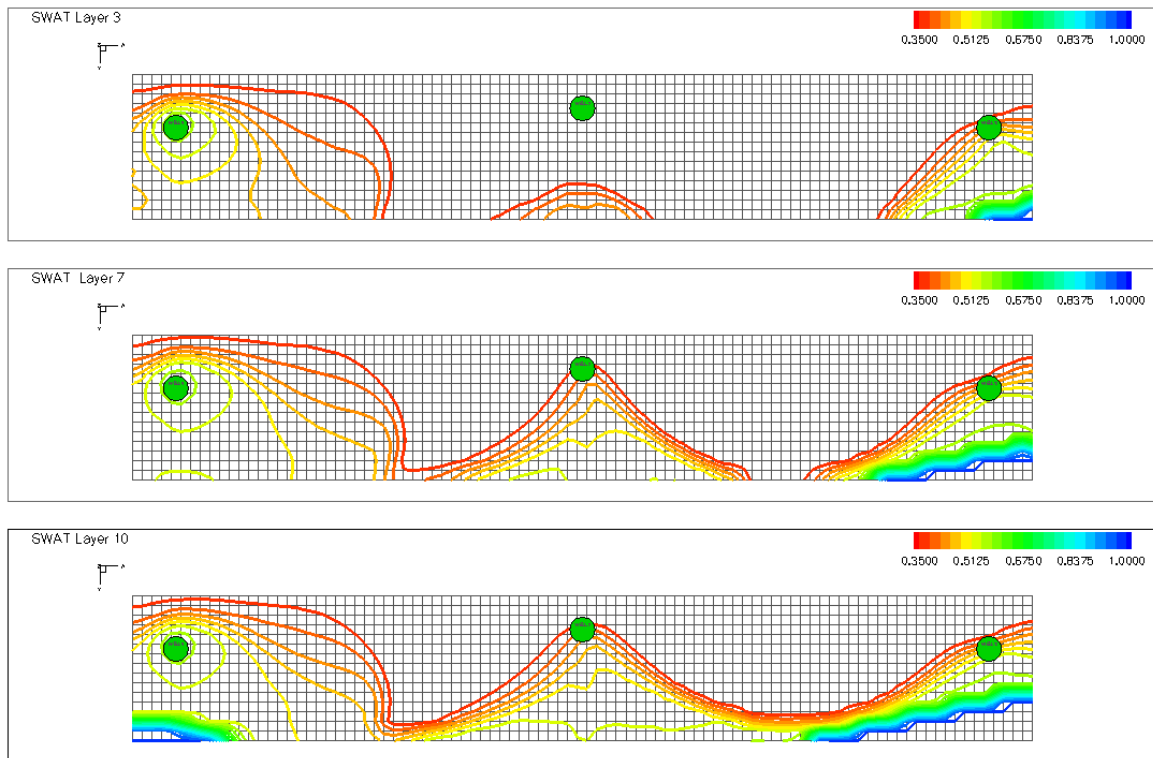


Figure A- 26: Contour map of water saturation for dump flooding via an edge well injector for II of 33stb/day/psi @ day 900

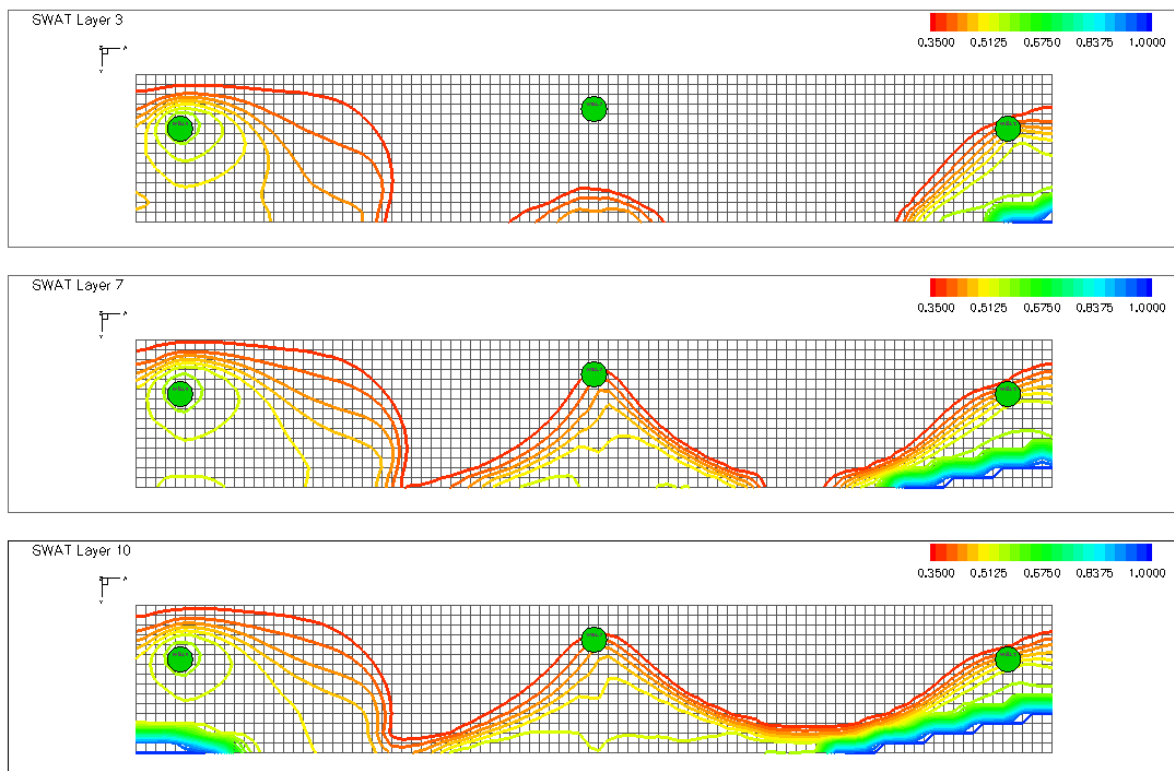


Figure A- 27: Contour map of water saturation for dump flooding via an edge well injector for II of 16.5stb/day/psi @ day 900

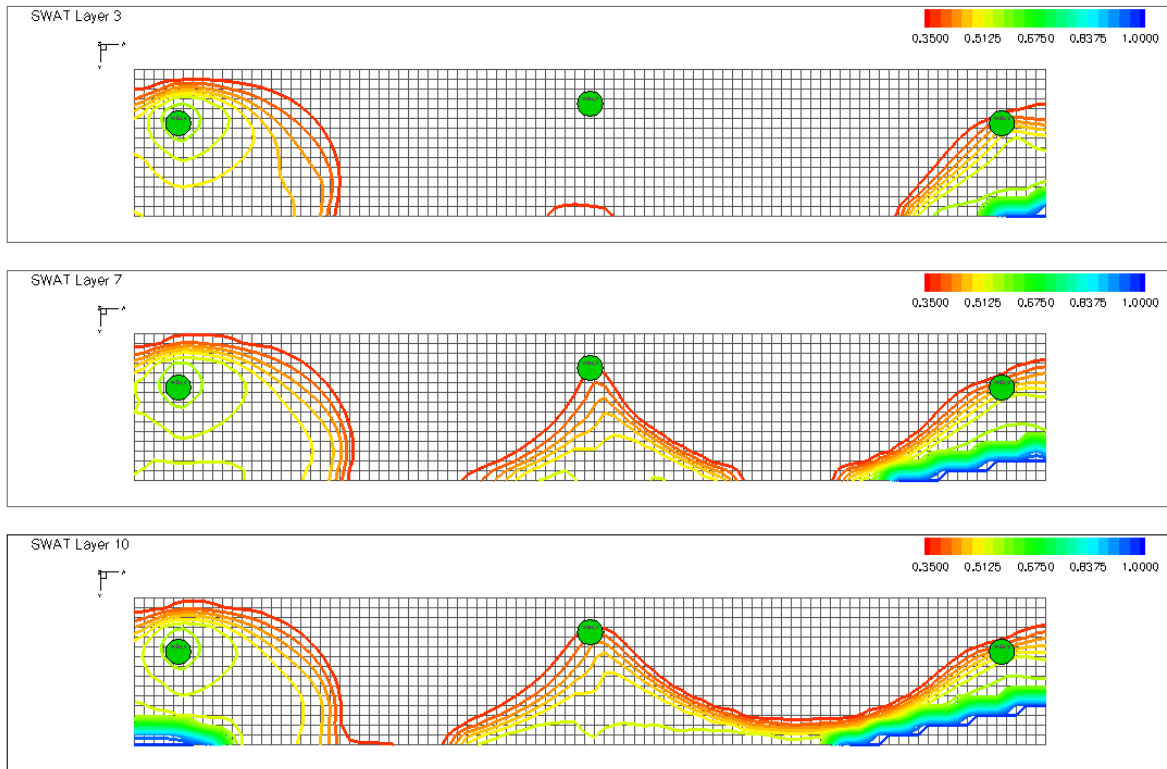


Figure A- 28: Contour map of water saturation for dump flooding via an edge well injector for II of 3.3stb/day/psi @ day 900

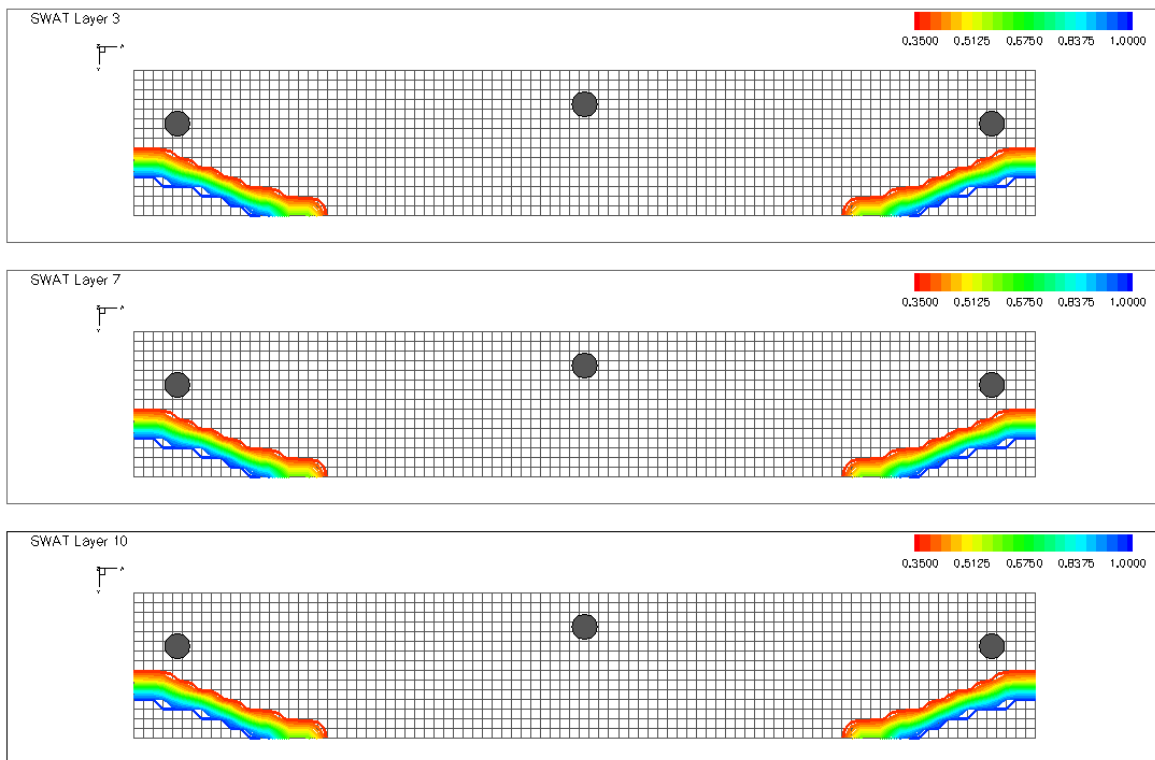


Figure A- 29: Contour map of water saturation at depth 6000 ft for base case @ day 900

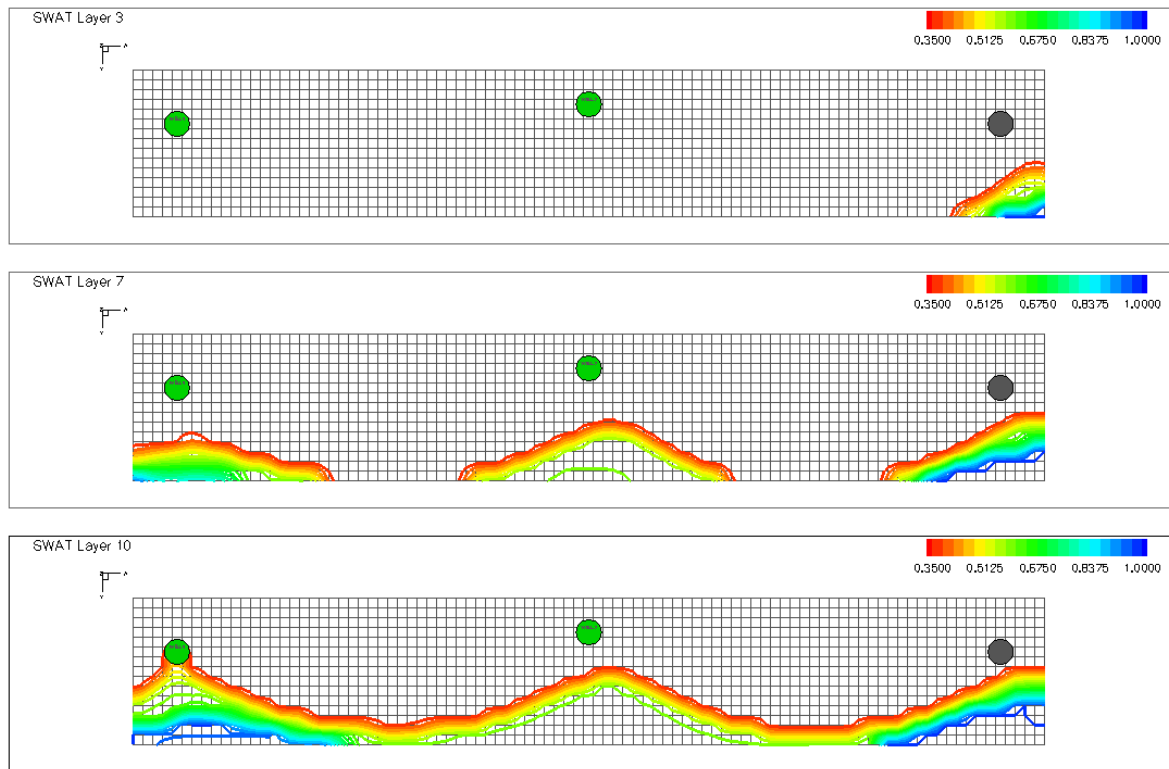


Figure A- 30: Contour map of water saturation of water dump flood at depth 6000 ft for edge well injector @ day 900

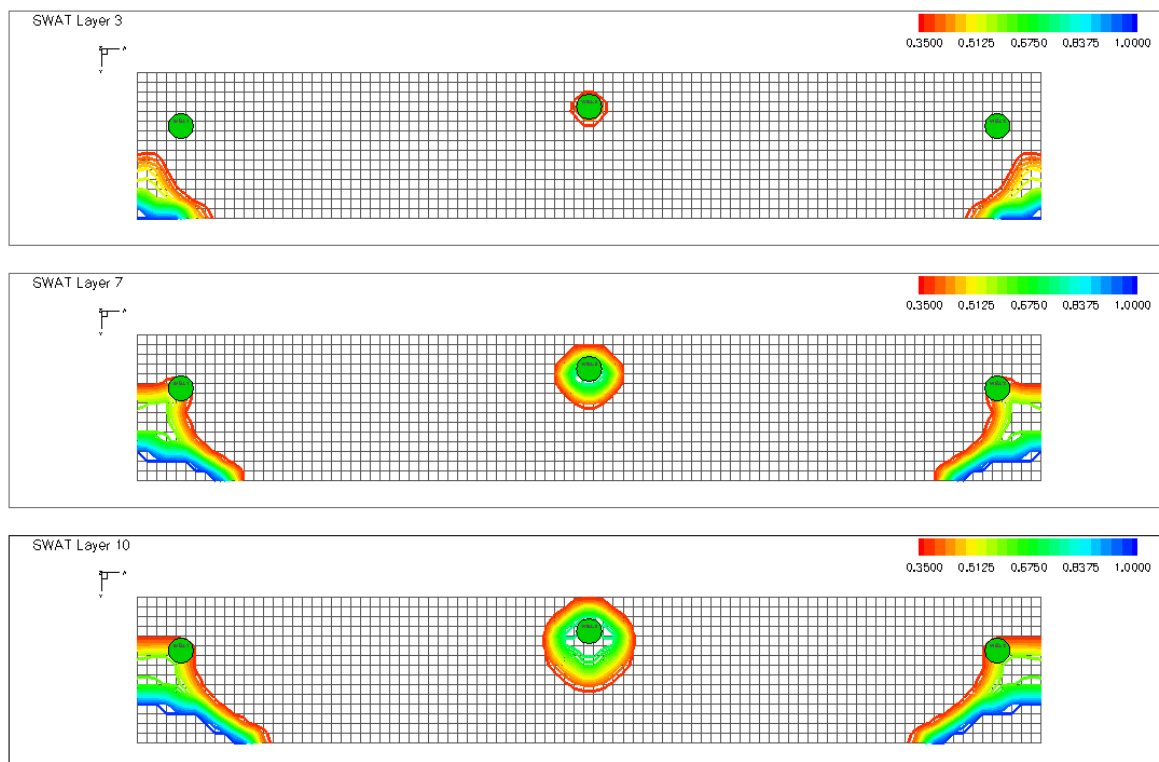


Figure A- 31 : Contour map of water saturation of water dump flood at depth 6000 ft for center well injector @ day 900

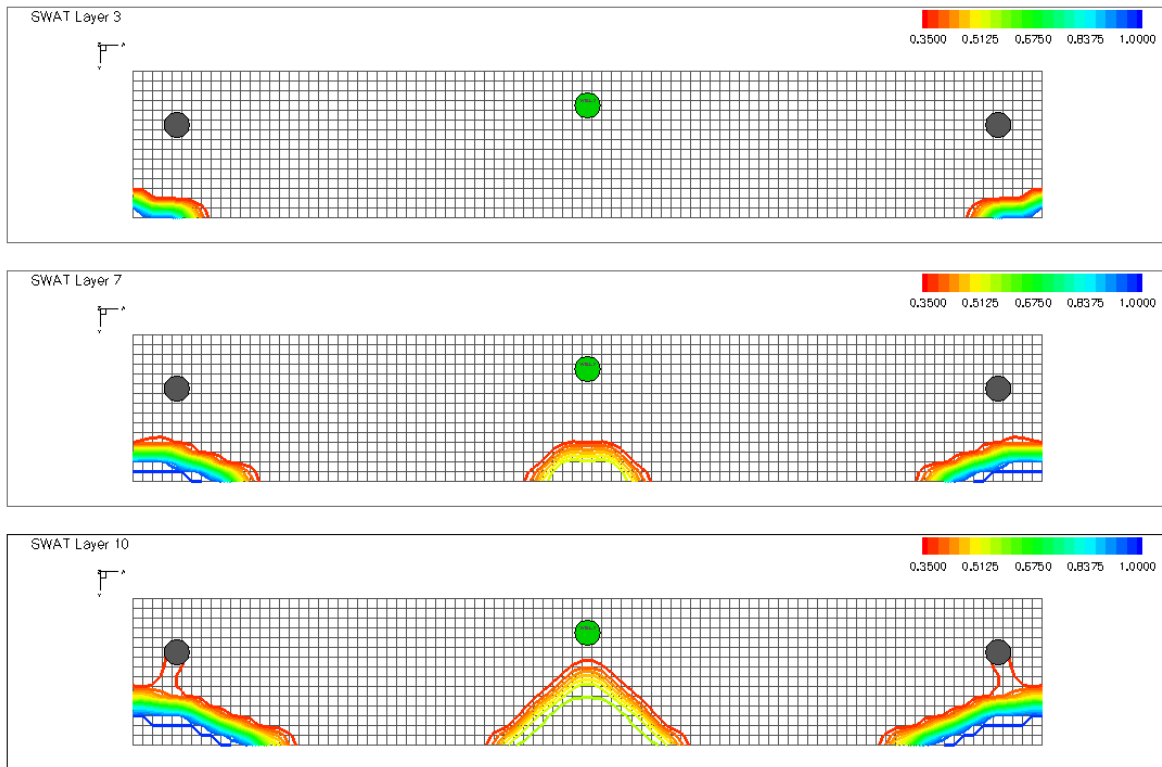


Figure A- 32: Contour map of water saturation at depth 8000 ft for base case @ day 900

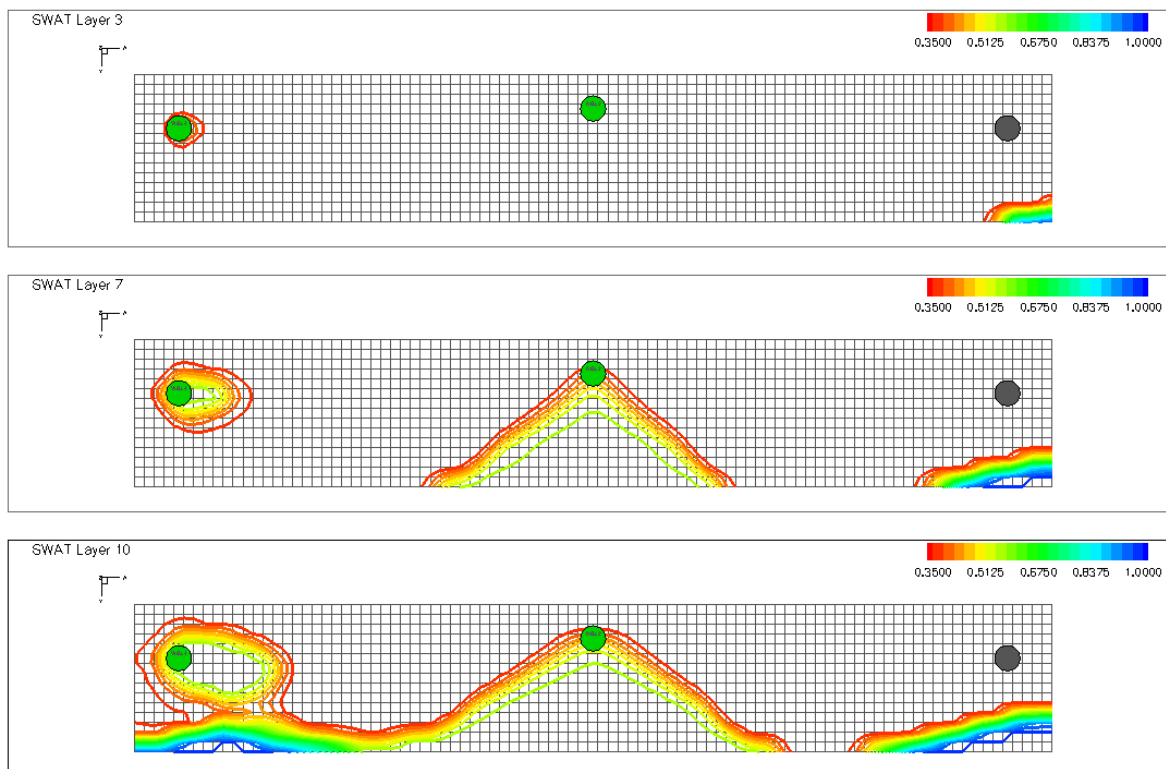


Figure A- 33: Contour map of water saturation of water dump flood at depth 8000 ft for edge well injector @ day 900

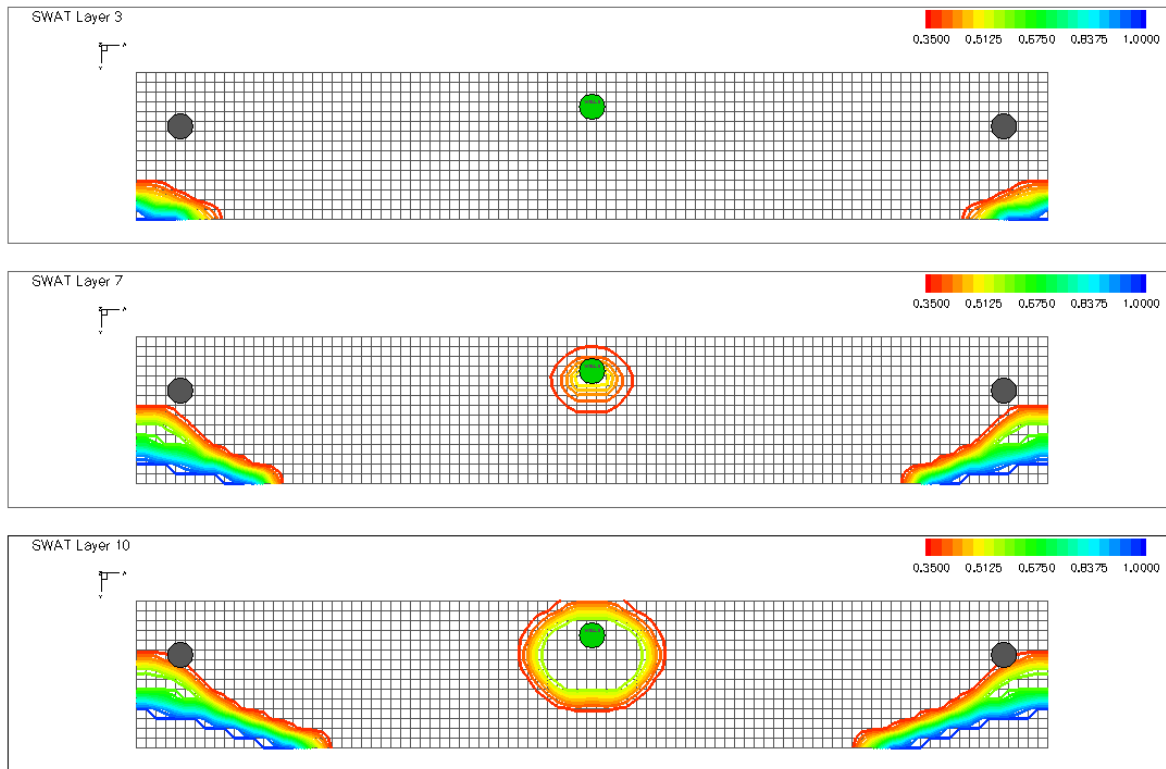


Figure A- 34: Contour map of water saturation of water dump flood at depth 8000 ft for center well injector @ day 900

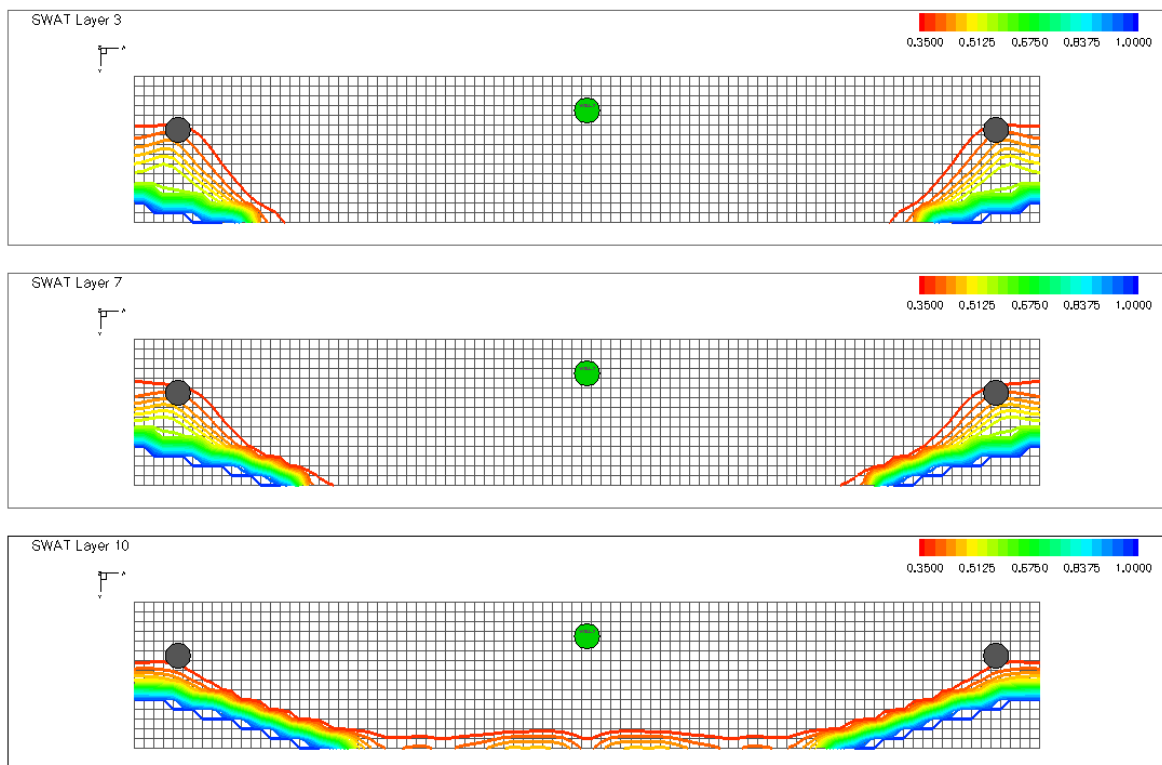


Figure A- 35: Contour map of underlying aquifer for base case @ day 900

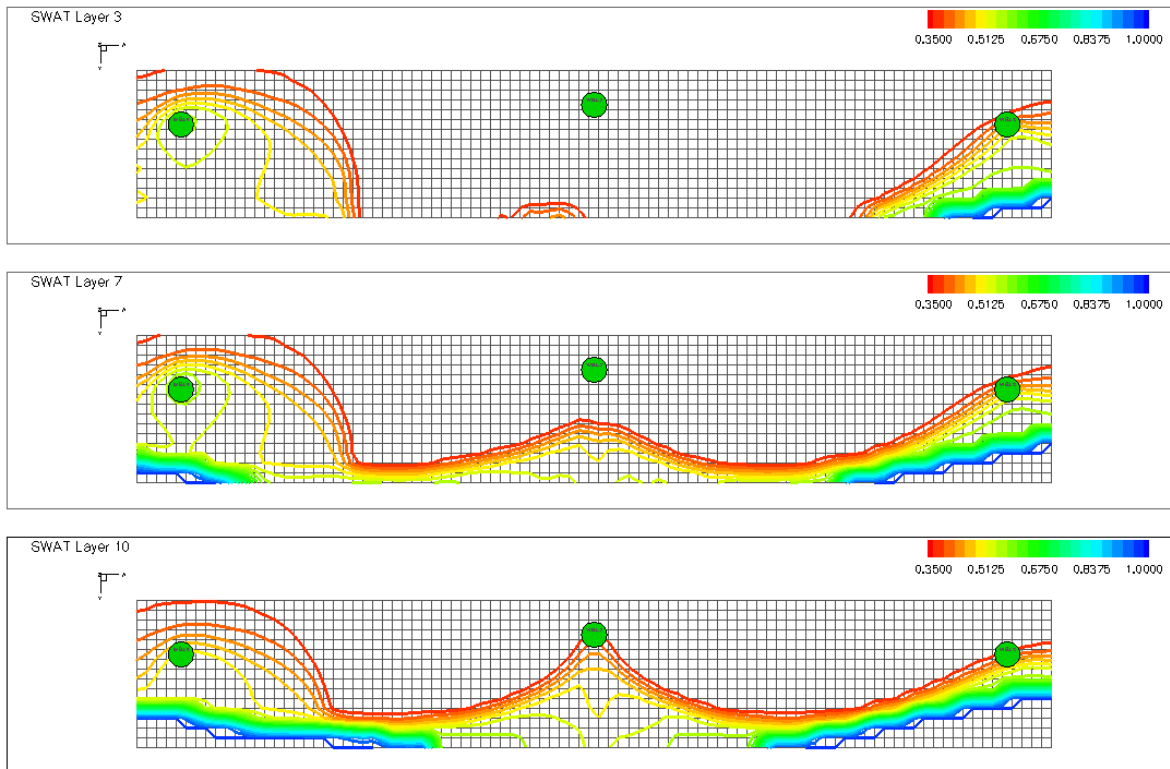


Figure A- 36: Contour map of water saturation of underlying aquifer dump flooding via an edge well injector @ day 900

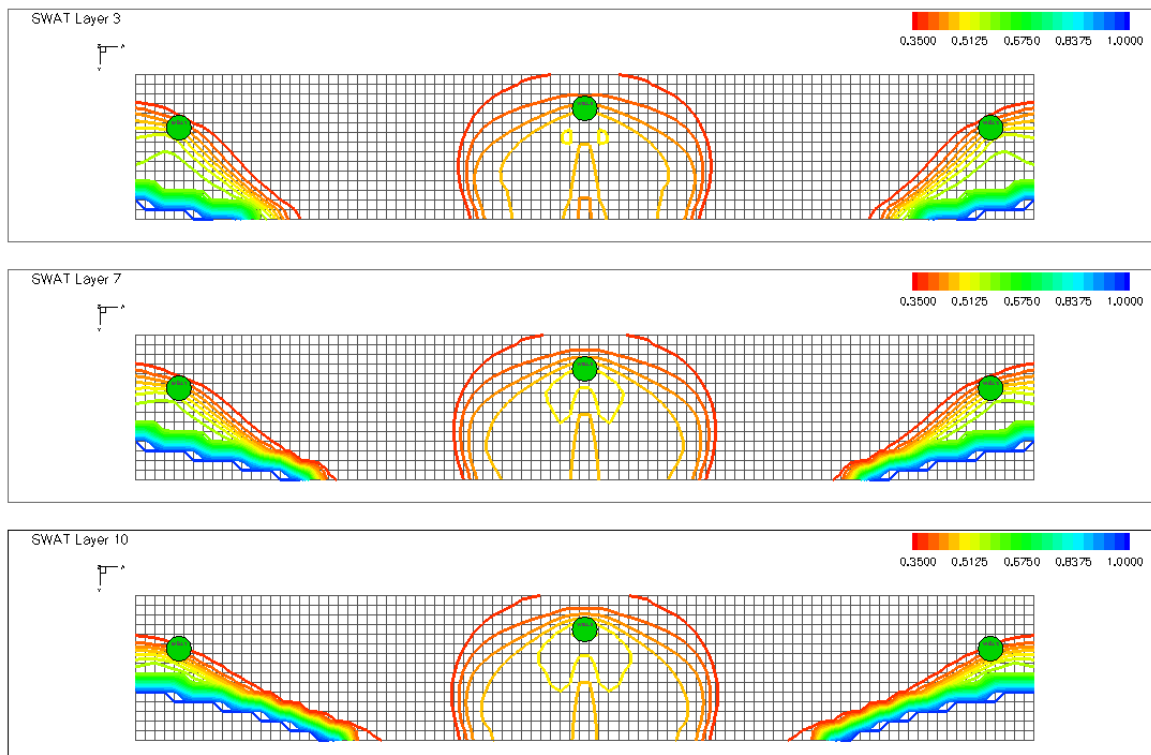


Figure A- 37: Contour map of water saturation of underlying aquifer dump flooding through a center well injector @ day 900

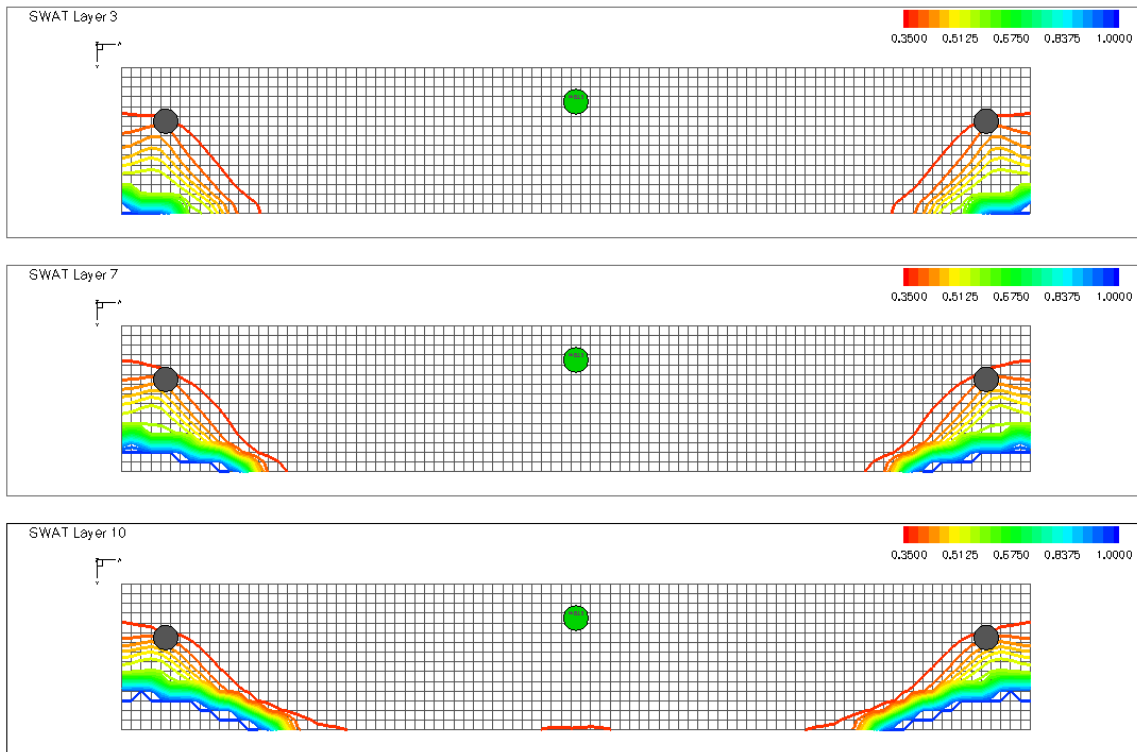


Figure A- 38: Contour map of water saturation for dump flooding on base case for 30API gravity @ day 900

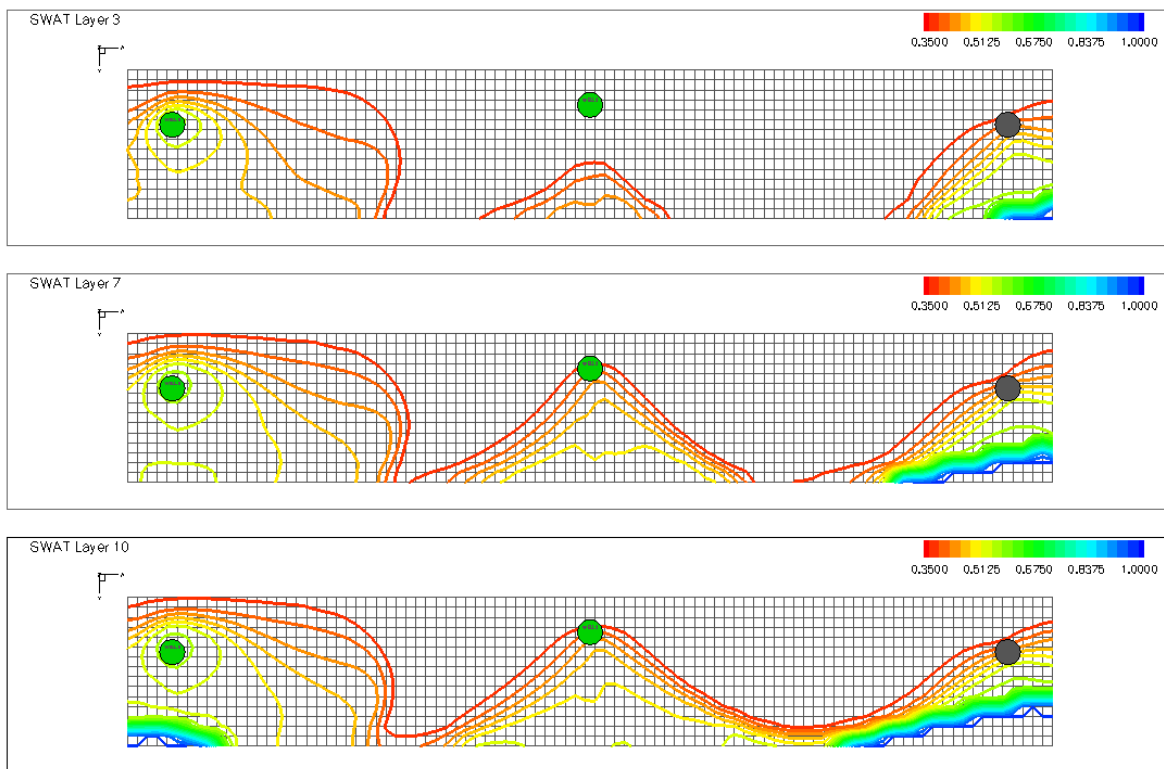


Figure A- 39 Contour map of water saturation for dump flooding via an edge well injector for 30API gravity @ day 900

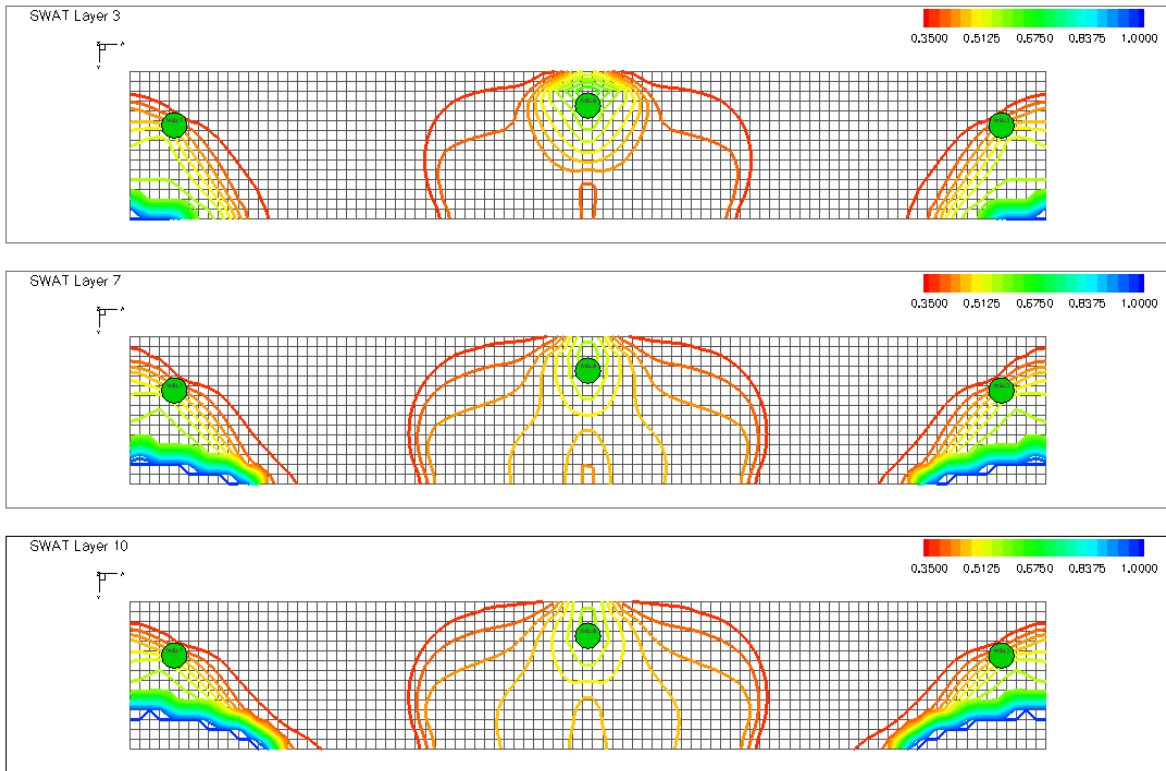


Figure A- 40: Contour map of water saturation for dump flooding through a center well injector for 30API gravity @ day 900

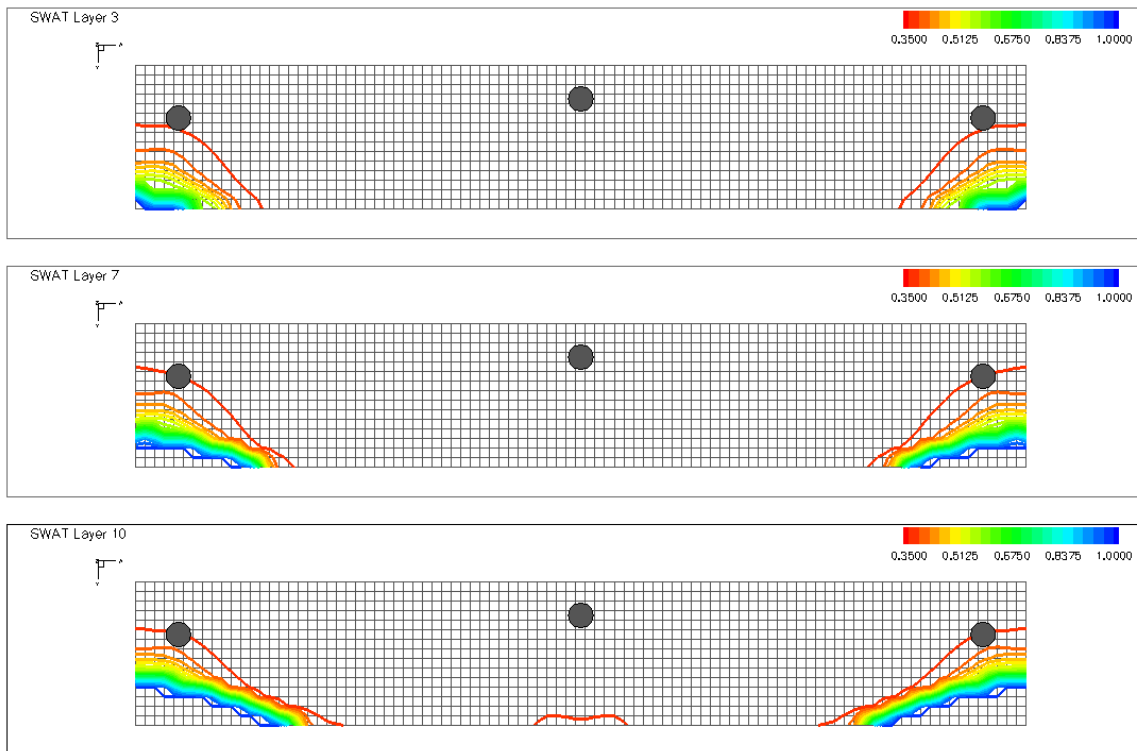


Figure A- 41: Contour map of water saturation for dump flooding on base case for 35API gravity @ day 900

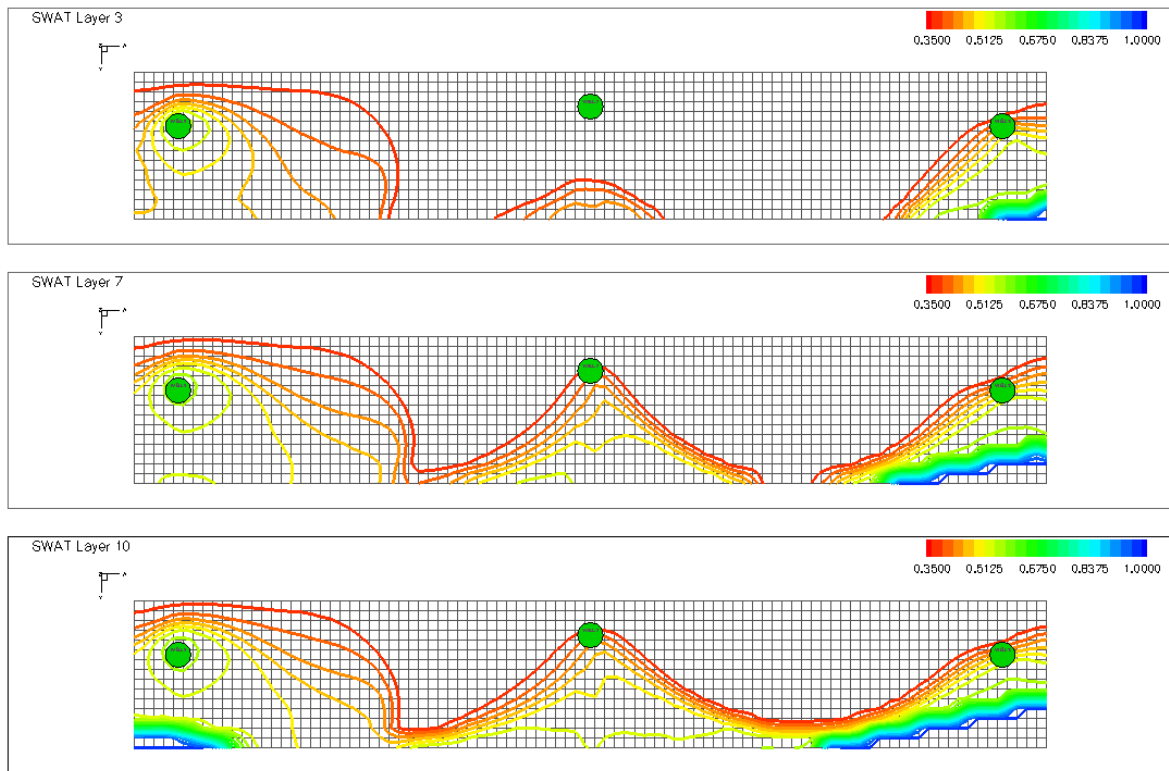


Figure A- 42 Contour map of water saturation for dump flooding via an edge well injector for 35API gravity @ day 900

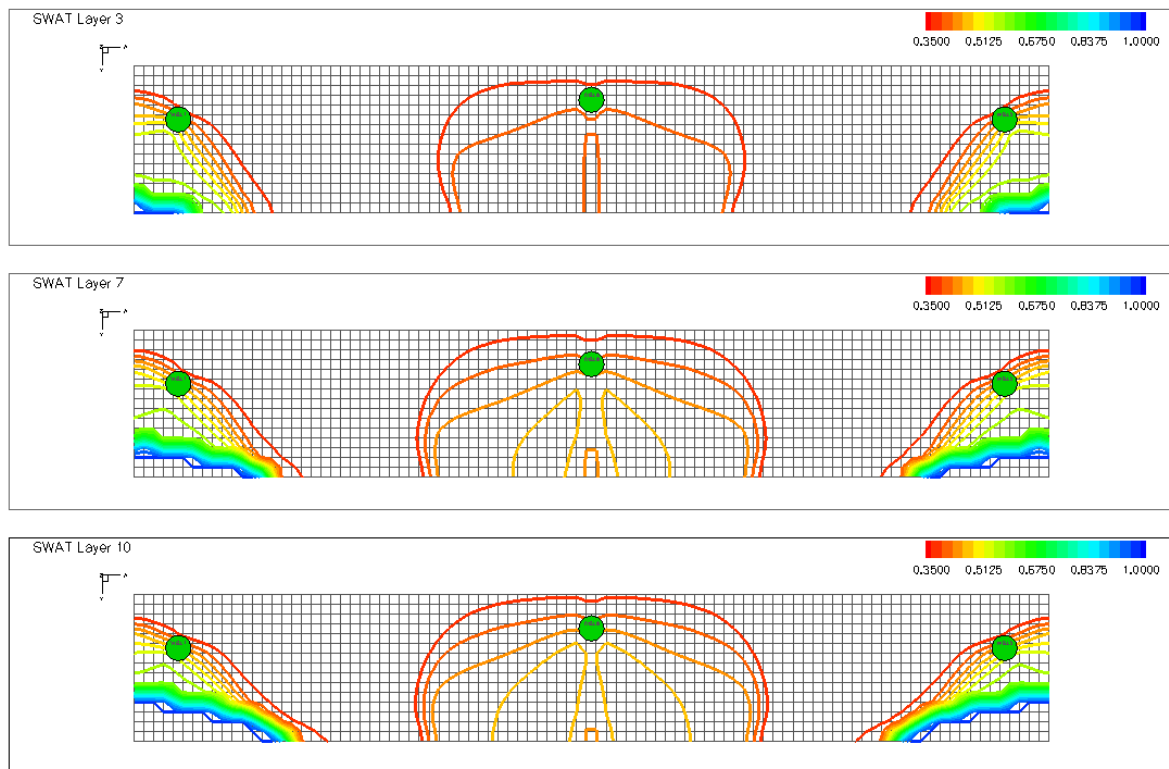


Figure A- 43: Contour map of water saturation for dump flooding through a center well injector for 35API gravity @ day 900

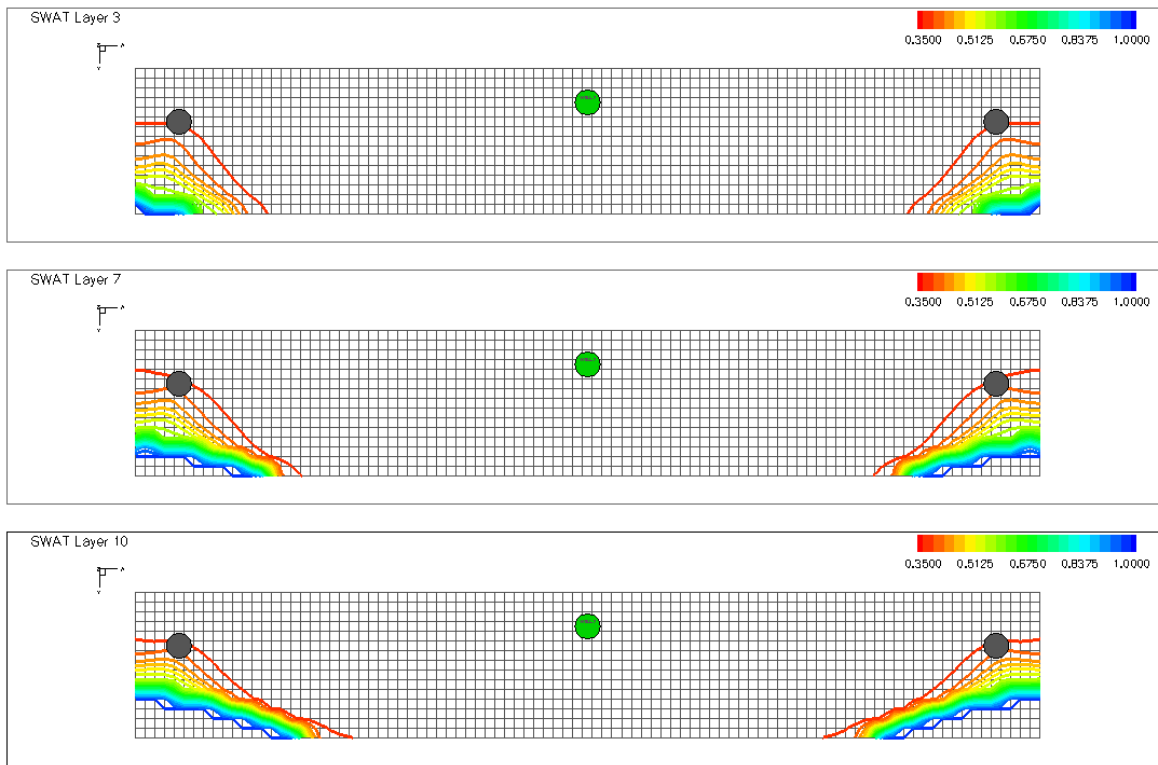


Figure A- 44: Contour map of water saturation for dump flooding on base case for 40API gravity @ day 900

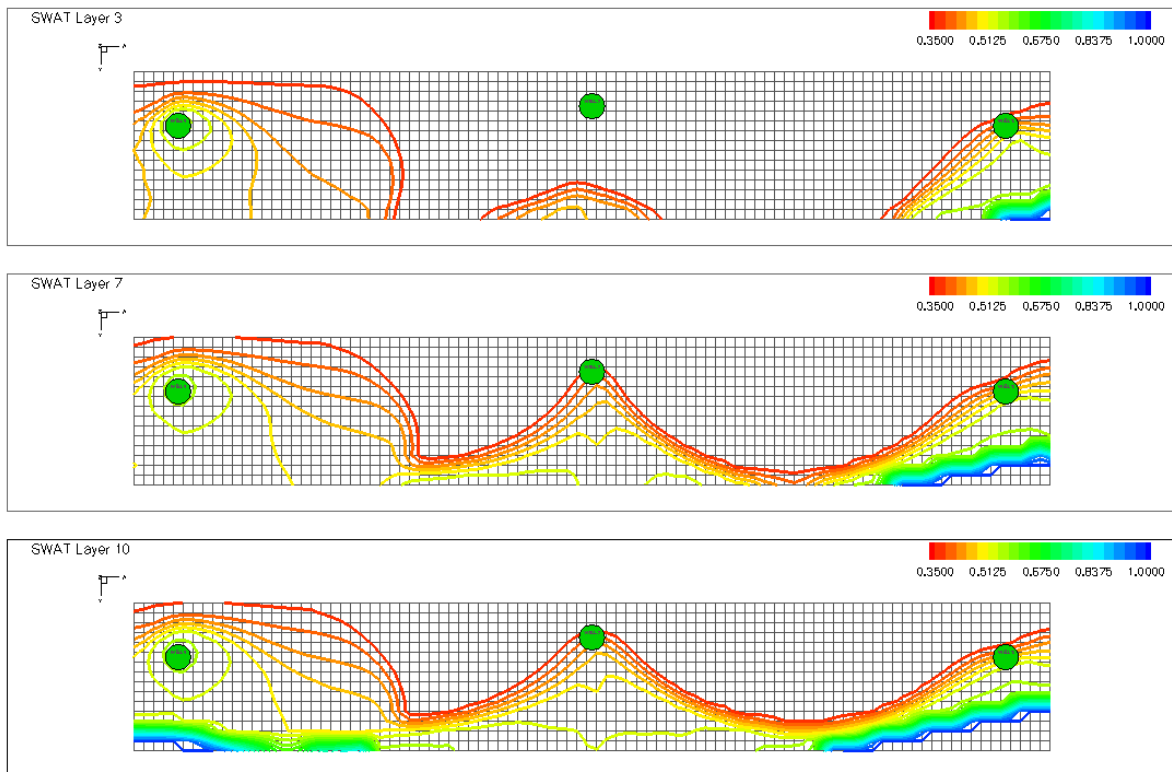


Figure A- 45 Contour map of water saturation for dump flooding via an edge well injector for 40API gravity @ day 900

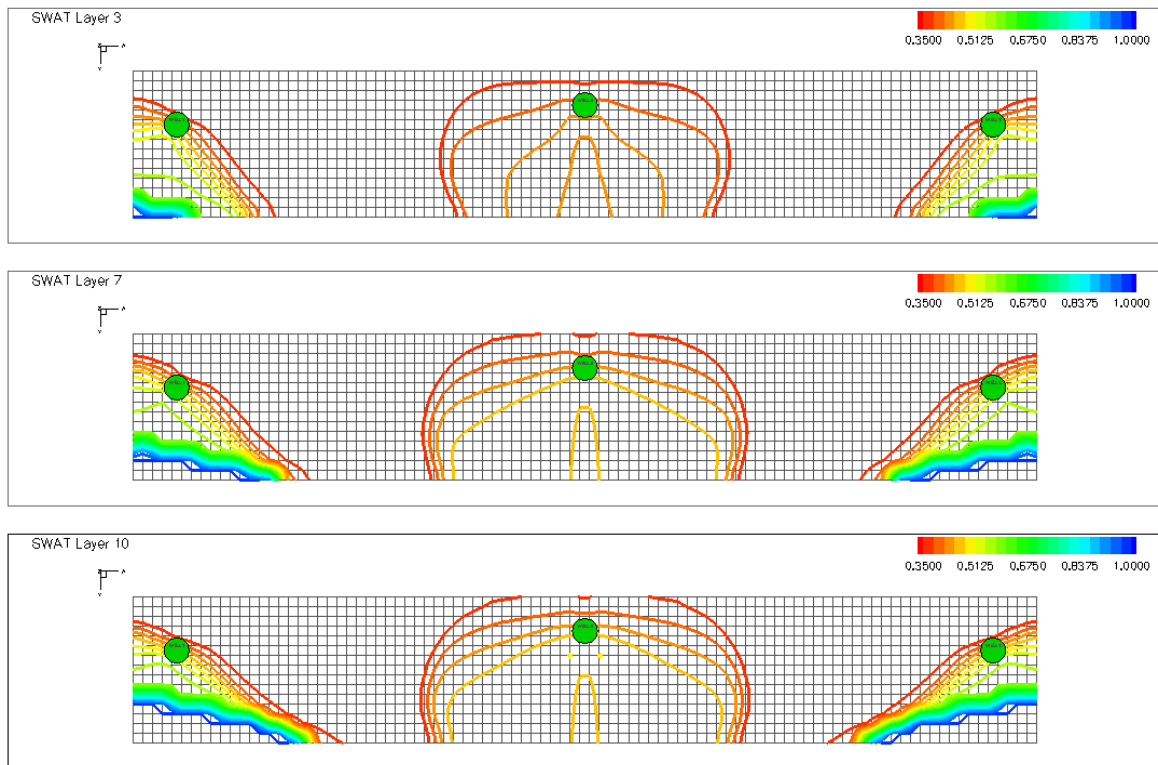


Figure A- 46: Contour map of water saturation for dump flooding through a center well injector for 40API gravity @ day 900

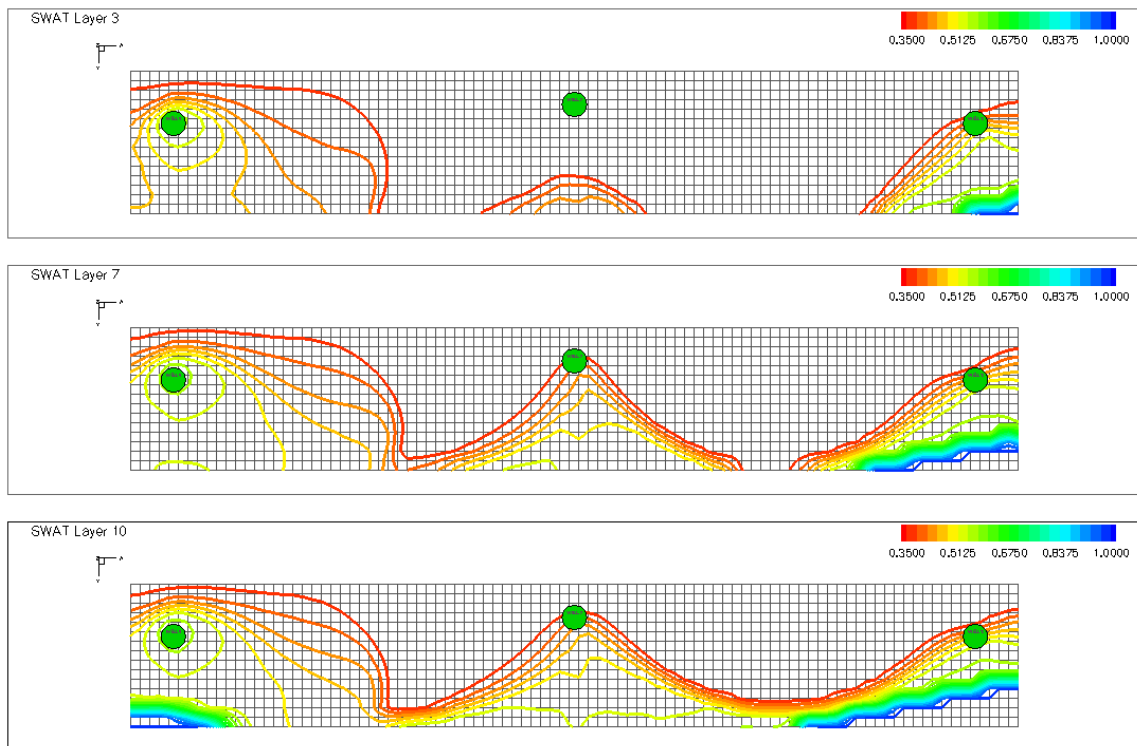


Figure A- 47: Contour map of water saturation of water dump flood via an edge well injector at day 1 @ day 900

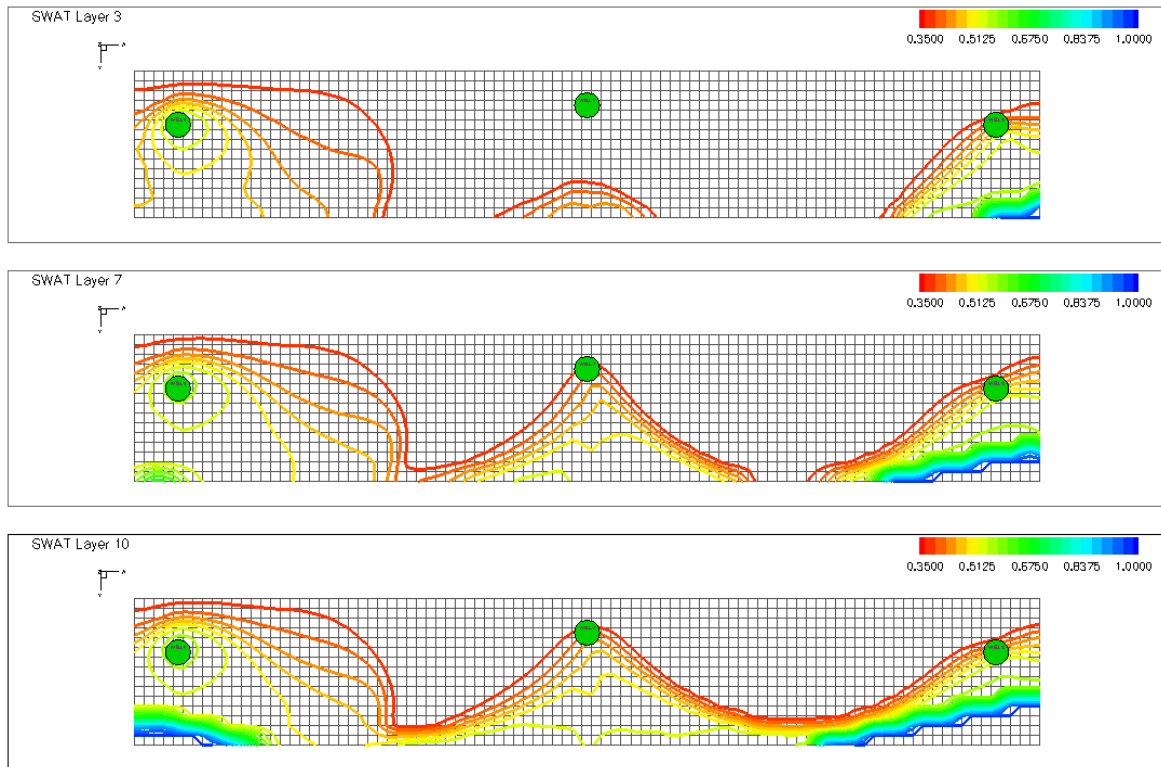


Figure A- 48: Contour map of water saturation of water dump flood via an edge well injector at day 15 @ day 900

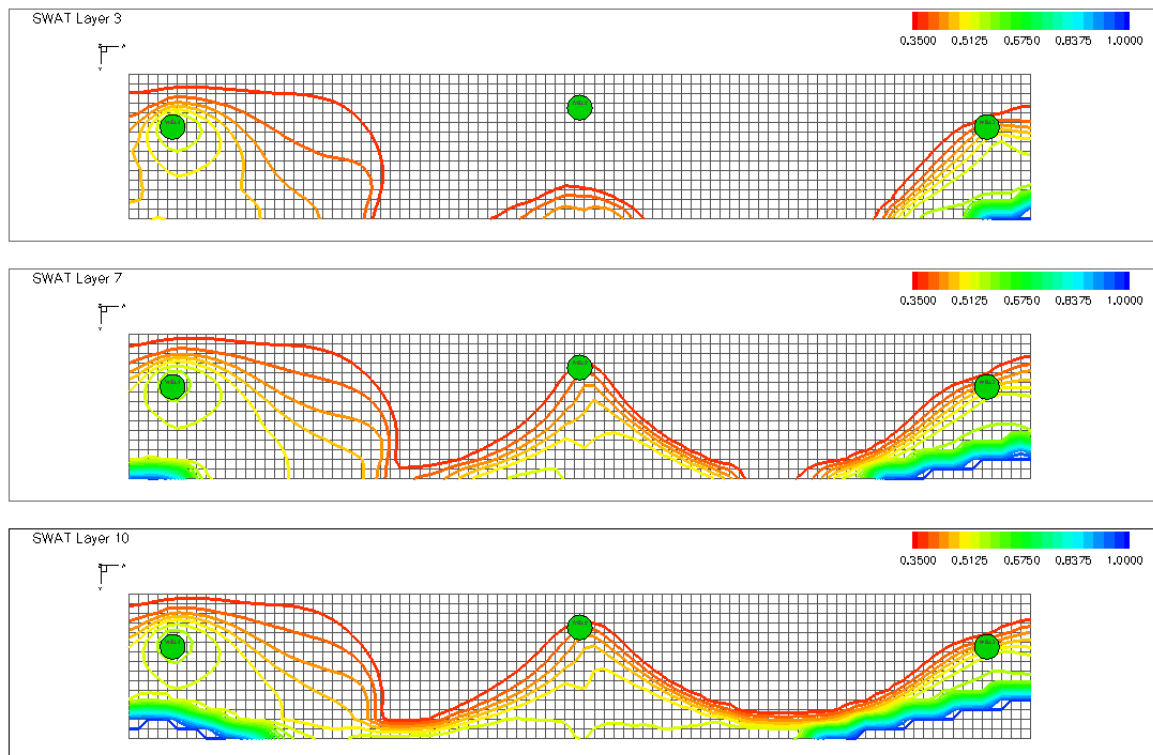


Figure A- 49: Contour map of water saturation of water dump flood via an edge well injector at day 30 @ day 900

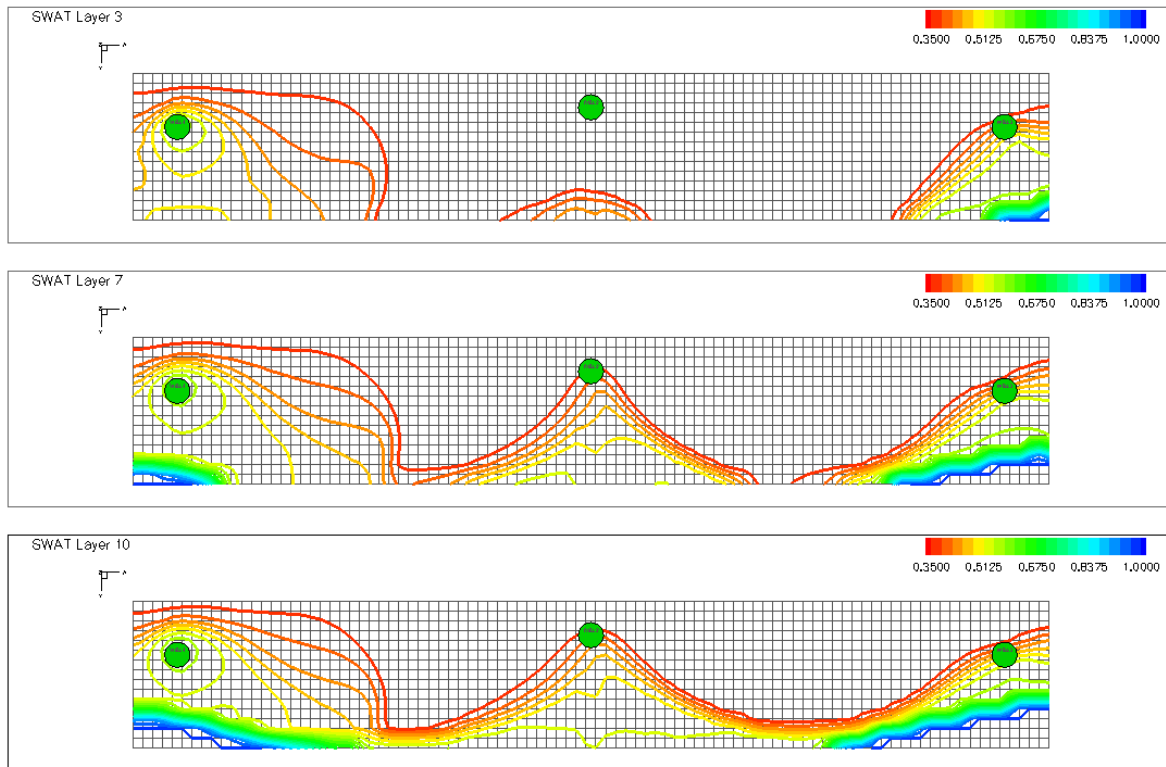


Figure A- 50: Contour map of water saturation of water dump flood via an edge well injector at day 60 @ day 900

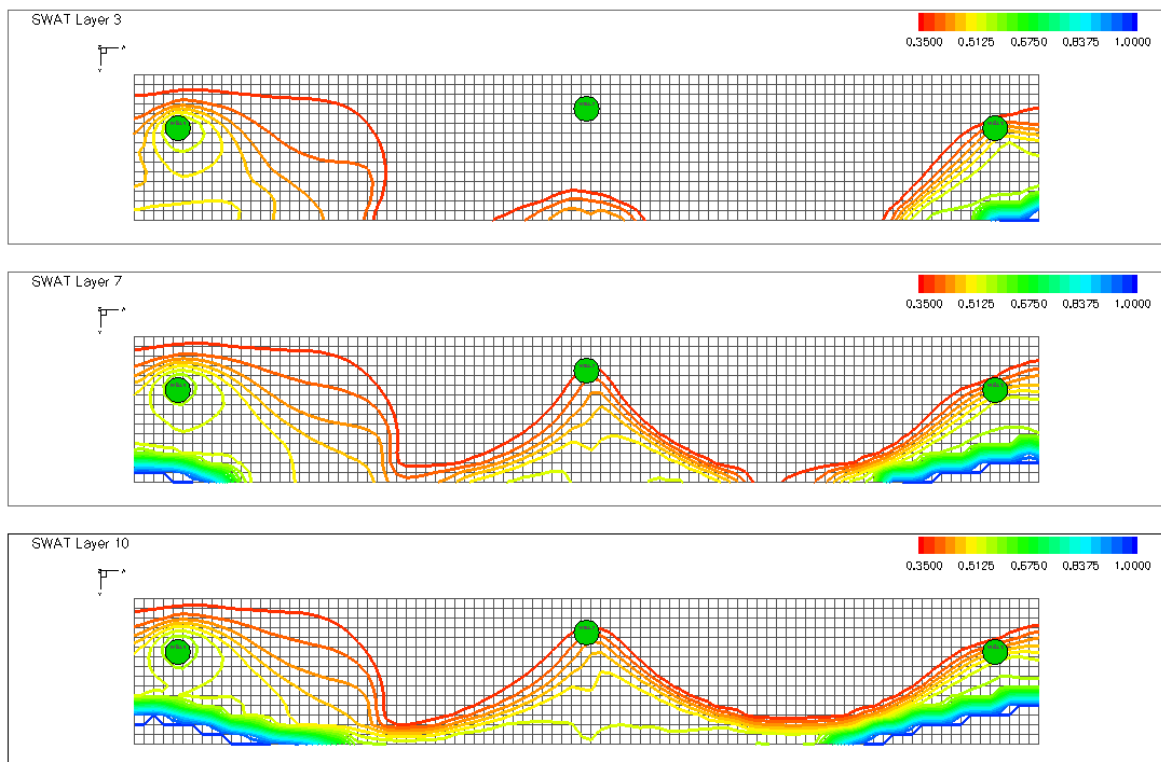


Figure A- 51: Contour map of water saturation of water dump flood via an edge well injector at day 90 @ day 900

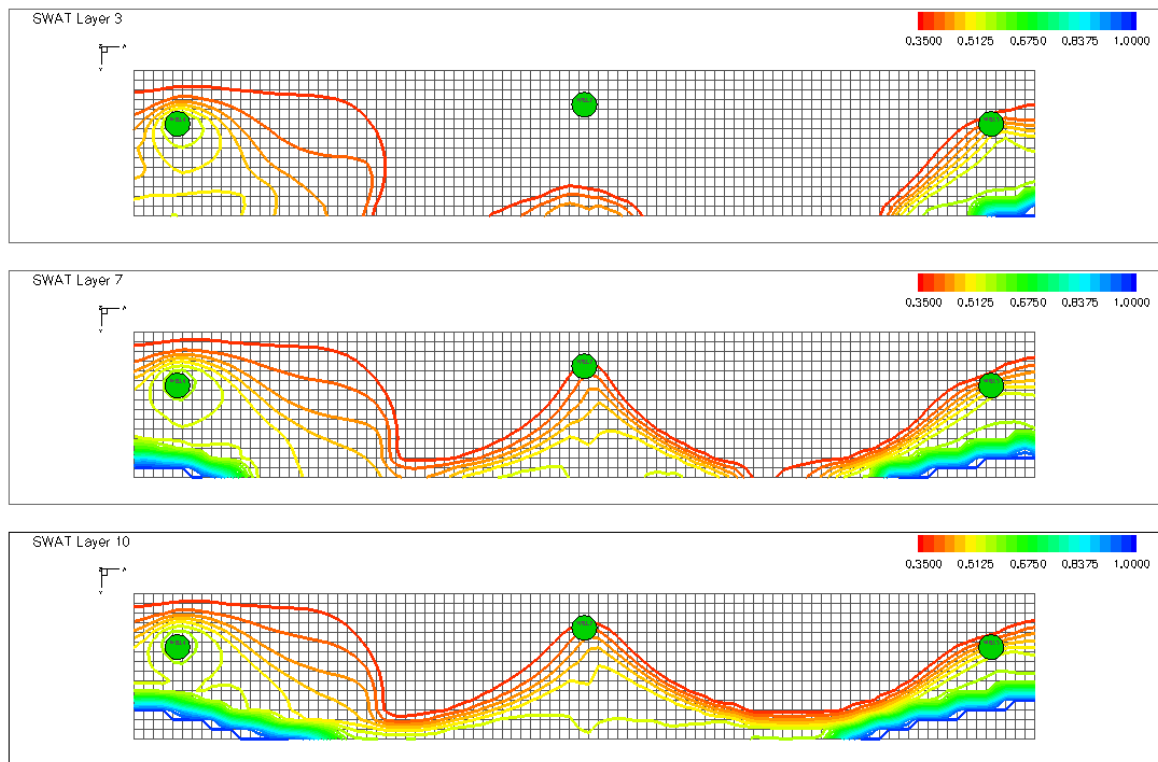


Figure A- 52: Contour map of water saturation of water dump flood via an edge well injector at day 120 @ day 900

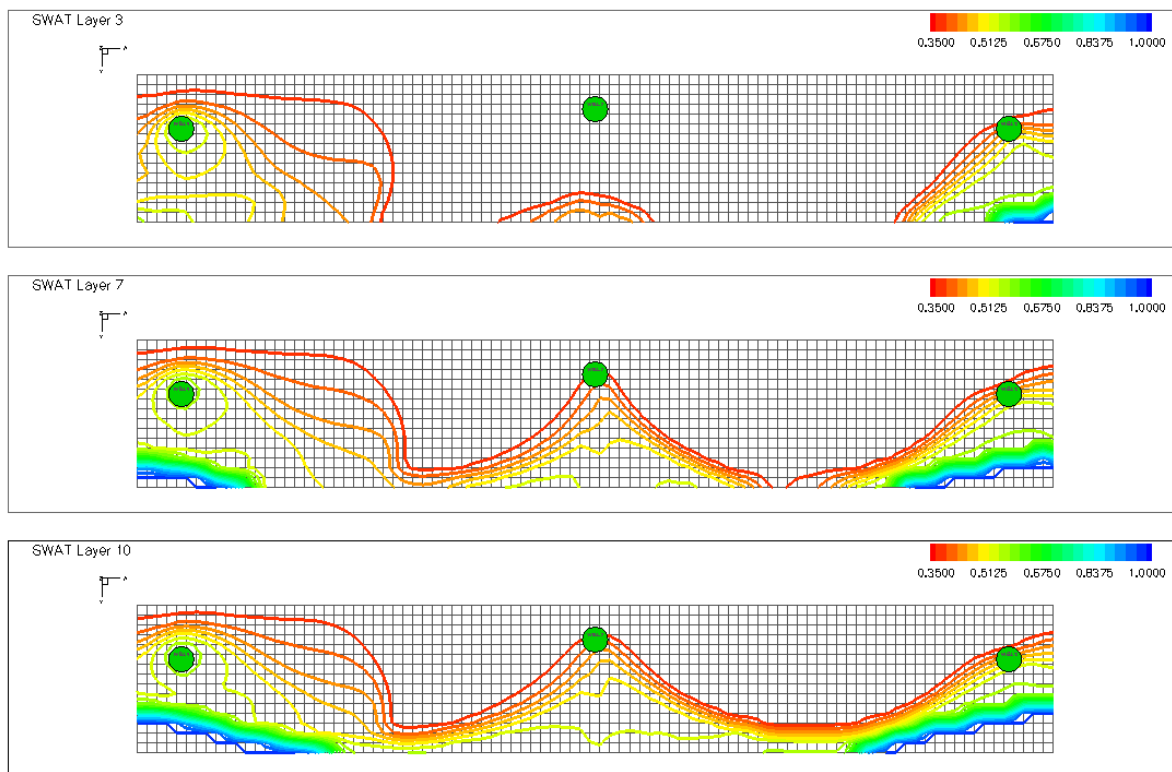


Figure A- 53: Contour map of water saturation of water dump flood via an edge well injector at day 150 @ day 900

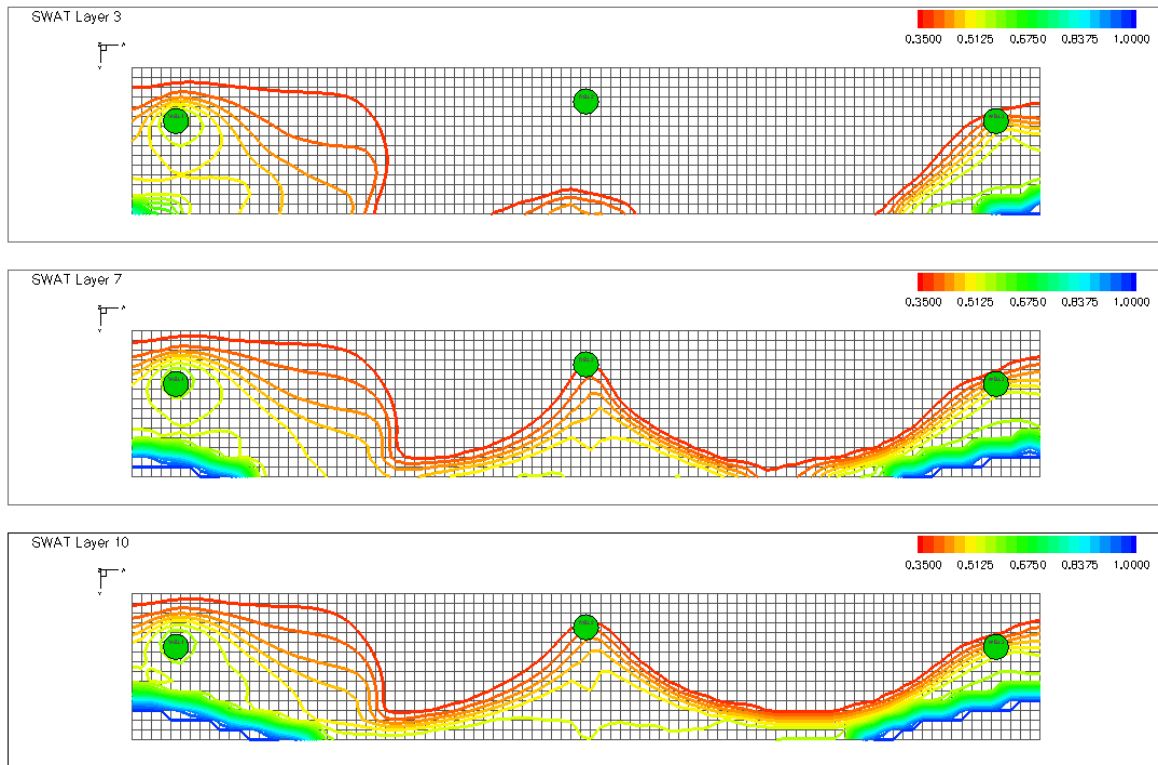


Figure A- 54: Contour map of water saturation of water dump flood via an edge well injector at day 240 @ day 900

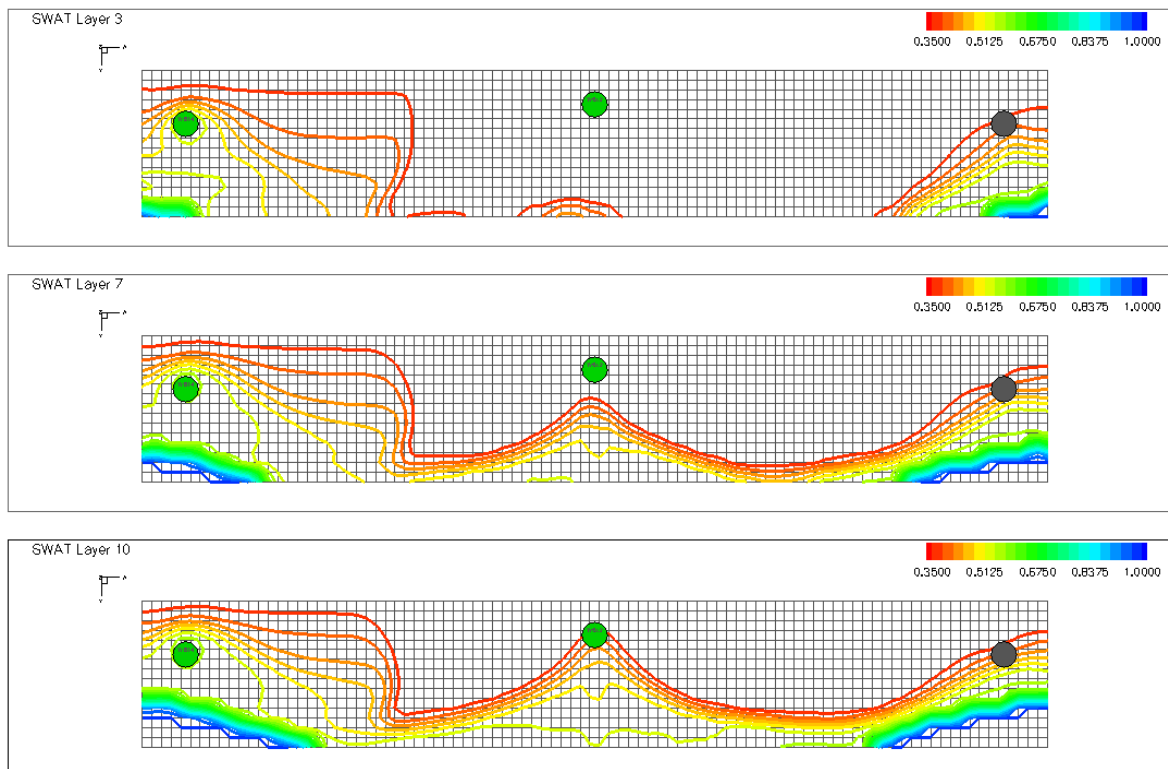


Figure A- 55: Contour map of water saturation of water dump flood via an edge well injector at day 330 @ day 900

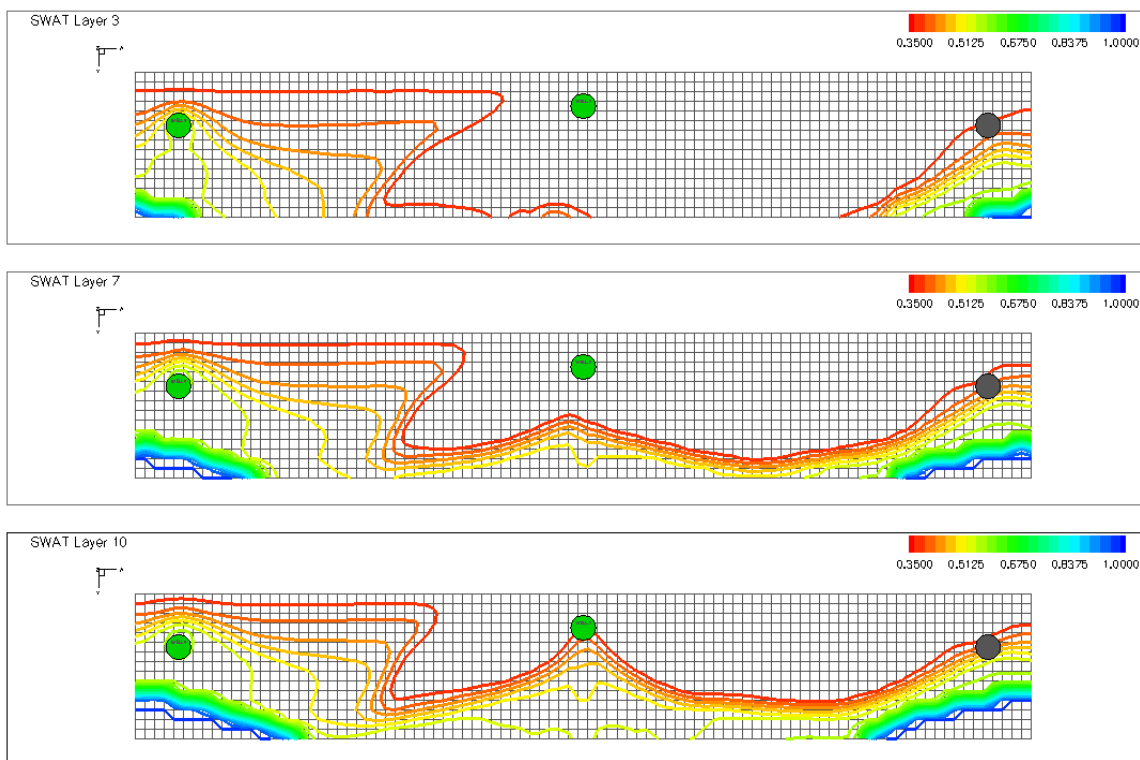


Figure A- 56: Contour map of water saturation of water dump flood via an edge well injector at day 420 @ day 900

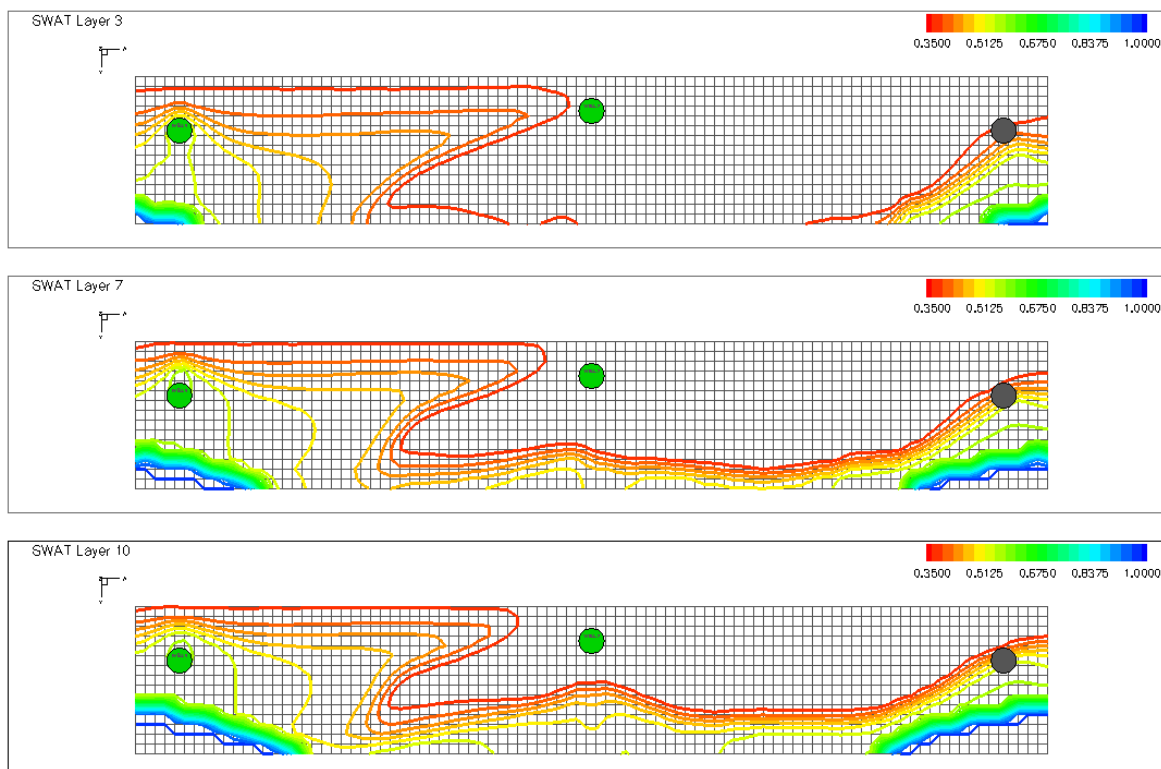


Figure A- 57: Contour map of water saturation of water dump flood via an edge well injector at day 510 @ day 900

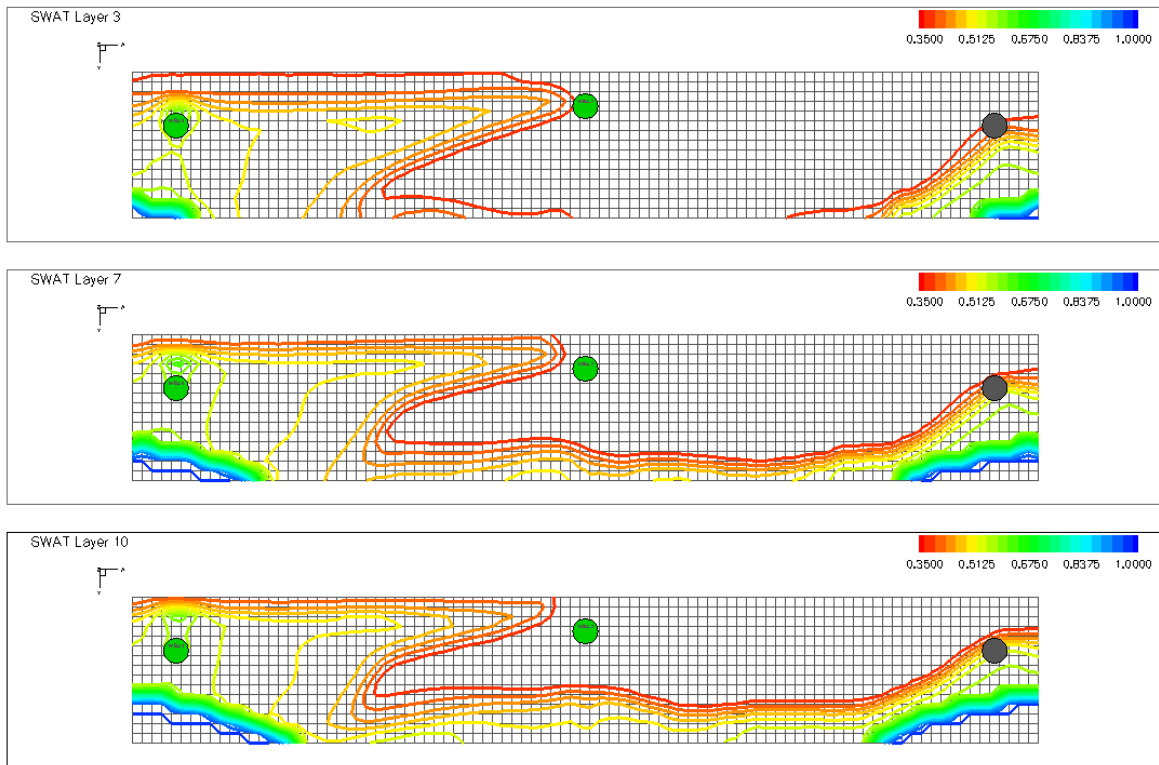


Figure A- 58: Contour map of water saturation of water dump flood via an edge well injector at day 600 @ day 900

APPENDIX B

B -1) Water dump flood through a center injector in case of decrease in aquifer size.

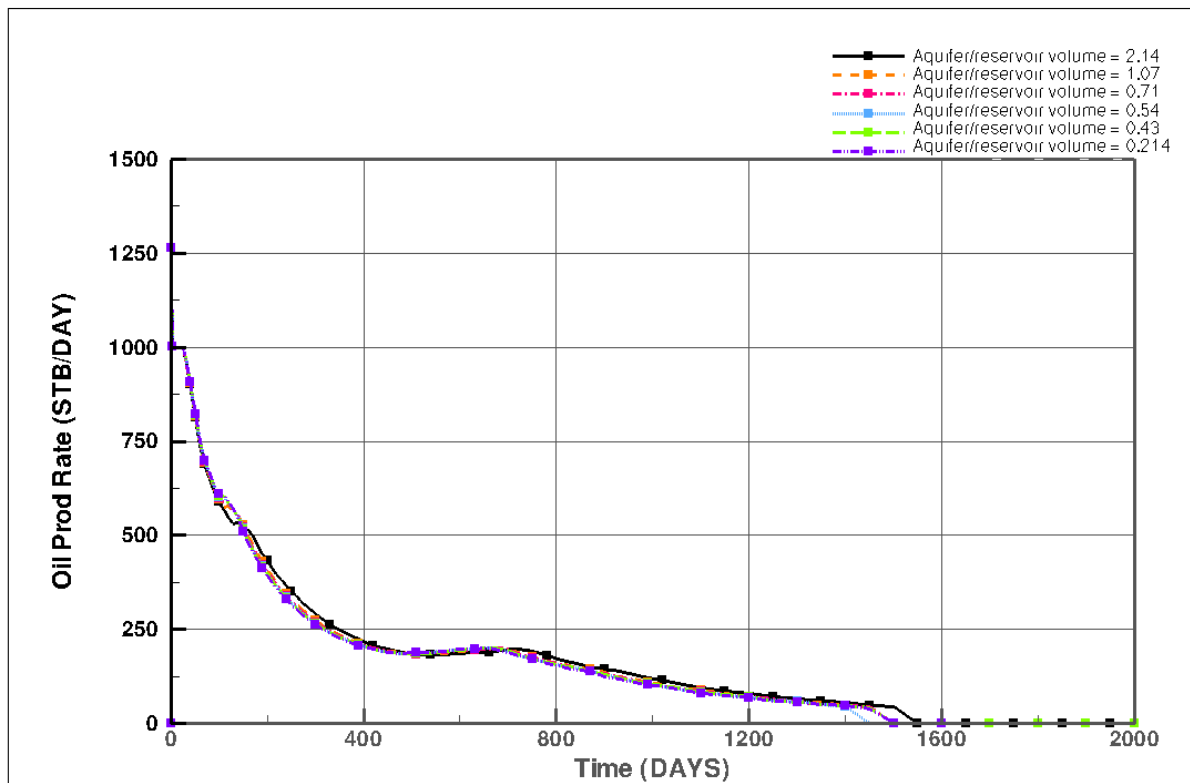


Figure B- 1: Oil production rate through a center injector with decreased in aquifer sizes

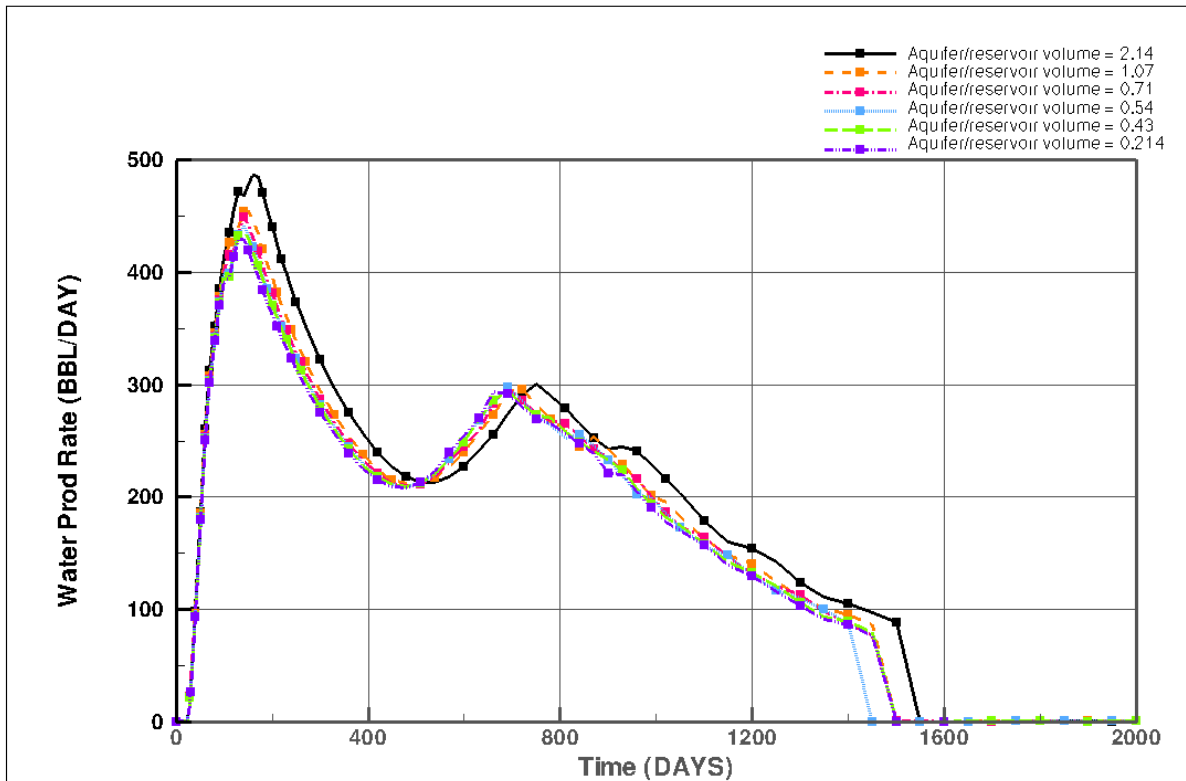


Figure B- 2: Water production rate through a center injector with decreased in aquifer sizes

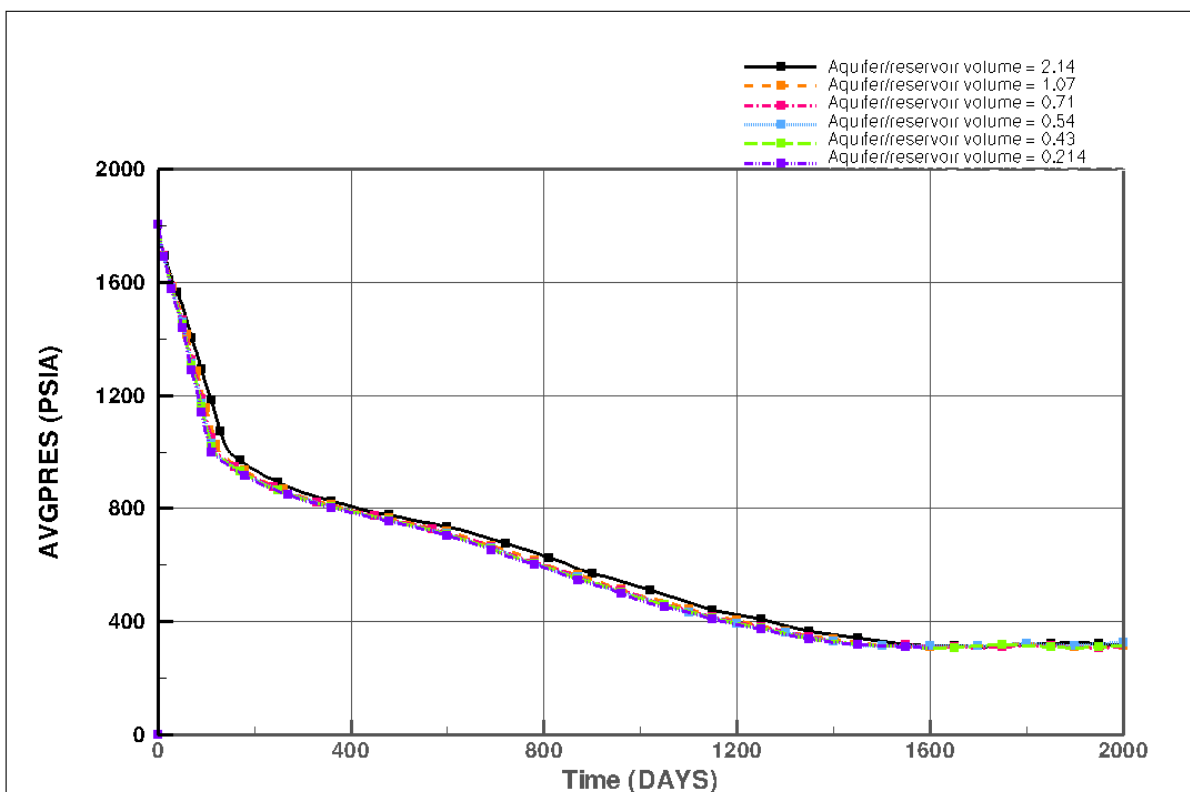


Figure B- 3: Average reservoir pressure through a center injector with decreased in aquifer

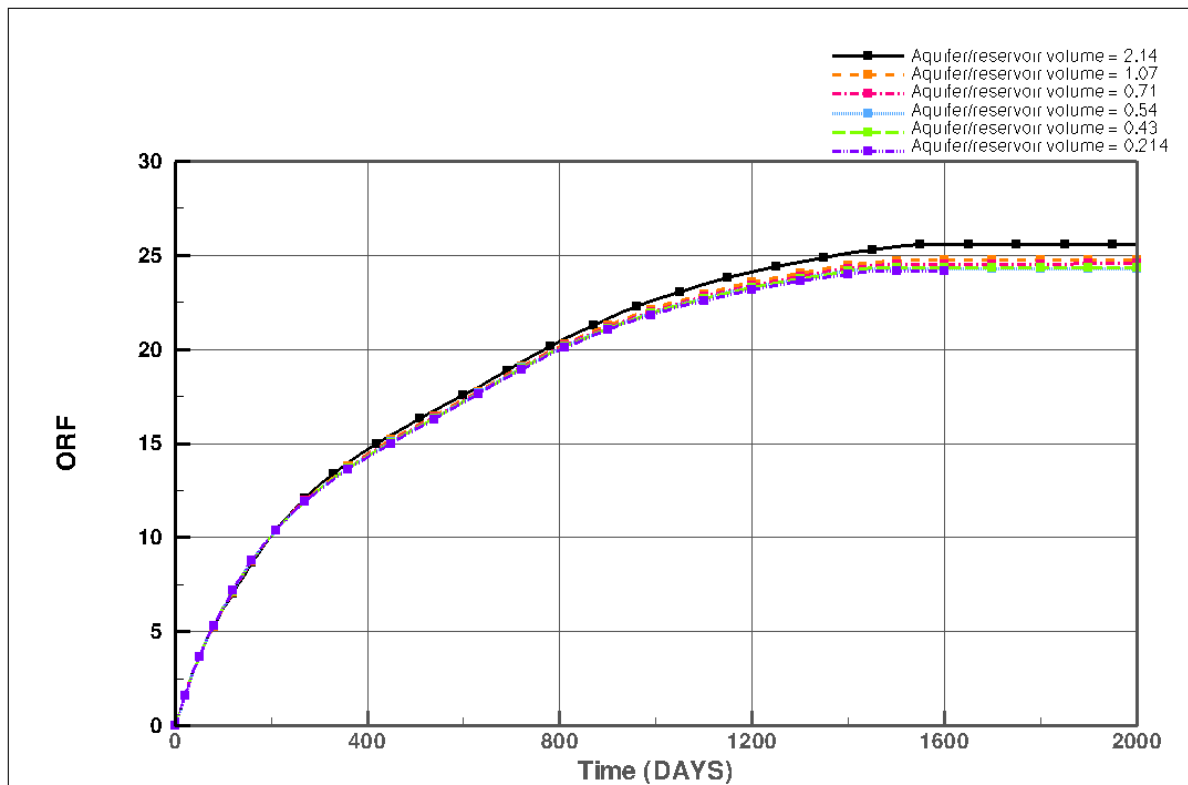


Figure B- 4: recovery factor through a center injector with decreased in aquifer sizes

Table B- 1: Oil recovery through a center injector with decreased in aquifer sizes

Aquifer/Reservoir ratio (RBL/RBL)	Aquifer size	RF (%)
2.60	1	25.56
1.30	÷ 2	24.73
0.87	÷ 3	24.54
0.65	÷ 4	24.34
0.52	÷ 5	24.29
0.26	÷ 10	24.17

B -2) Water dump flood through a center injector in case of increasing in aquifer size.

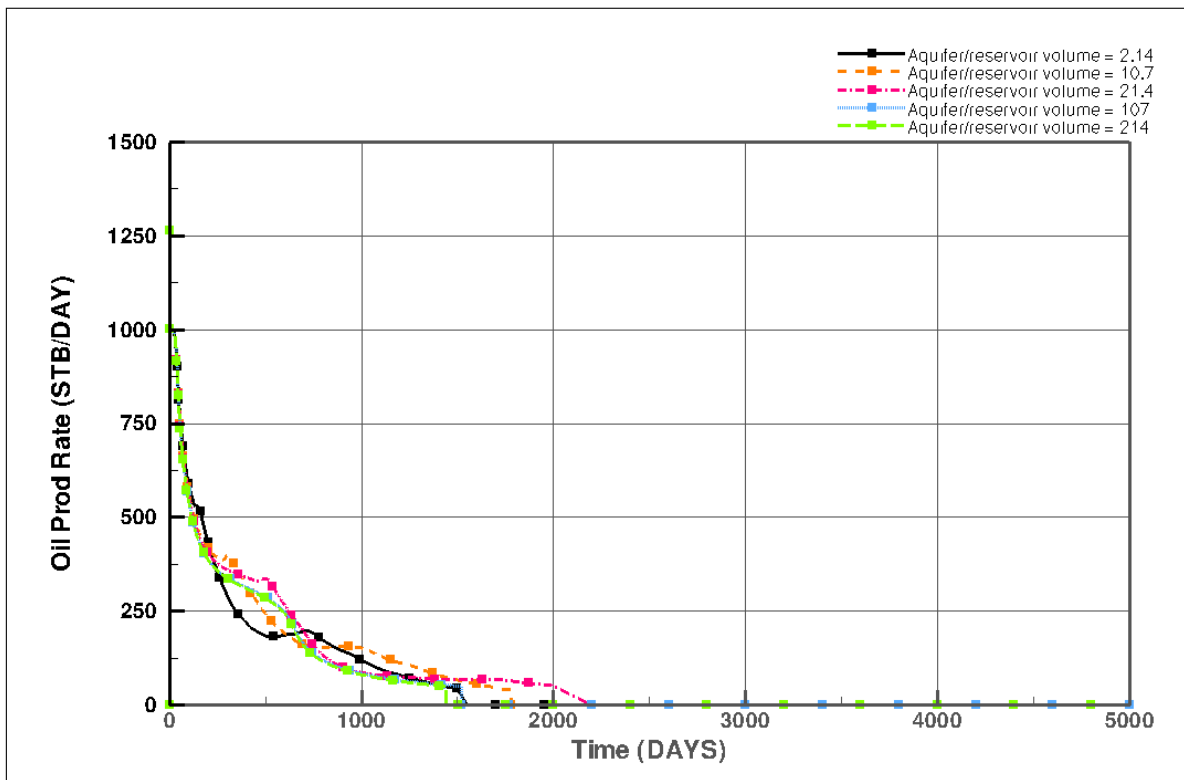


Figure B- 5: Oil production rate through a center injector with increase in aquifer sizes

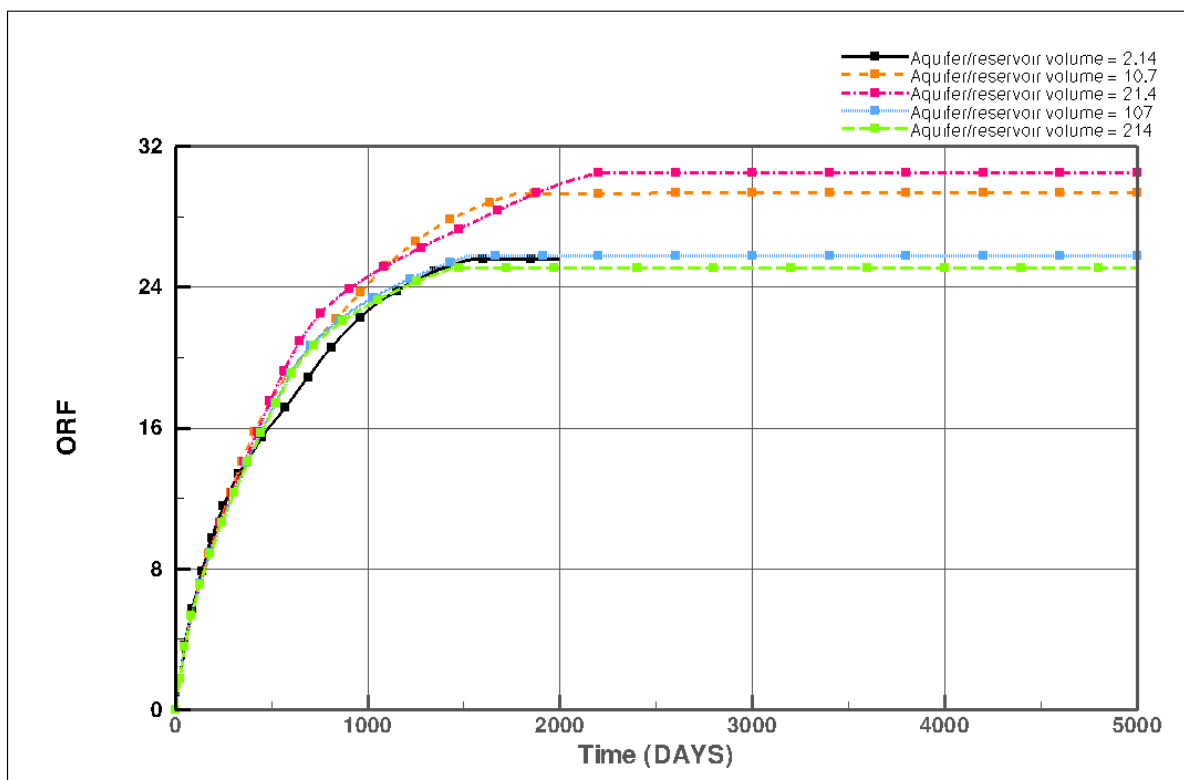


Figure B- 6: Oil recovery factor through a center injector with increase in aquifer sizes

Table B- 2: Oil recovery through a center injector with increase in aquifer sizes

Aquifer/Rsvr ratio (RBL/RBL)	Aquifer size	RF (%)
2.14	1	25.56
4.28	x 2	26.50
6.42	x 3	27.60
8.56	x 4	28.74
10.7	x 5	29.34
21.4	x 10	30.50
42.8	x 20	28.76
64.2	x 30	27.81
85.6	x 40	26.15
107	x 50	25.78
124	x 100	25.07
321	x 150	24.85

VITAE

Apirudee Anansupak was born on July 28, 1983 in Bangkok, Thailand. She received her B.Eng. in Chemical Engineering from the Faculty of Engineering, King Mongkut's Institute of Technology North Bangkok in 2005. After graduating, she had worked in construction industry for one year then started her career in petroleum industry by working with Chevron Thailand Exploration and Production, Ltd. as a Technologist. In year 2009, she continued her study in Master of Petroleum Engineering program at Department of Mining and Petroleum Engineering, Faculty of Engineering, Chulalongkorn University.